Modeling seasonal hydrologic response to forest harvesting and road construction: The role of drainage organization

by

Christina Tague

A thesis submitted in conformity with the requirements for the degree of Doctor of Philosophy

Graduate Department of Geography
University of Toronto

Modeling seasonal hydrologic response to forest harvesting and road construction: The role of drainage organization, Christina Lee Tague, 2000

Abstract

This study addresses several challenges in the application of hydro-ecological models as tools for studying the spatially distributed pattern of soil moisture and runoff production in the context of land use change. This research is comprised of two components: a) The development and assessment of a methodology used to model hillslope drainage organization at the small basin scale and b) application of this methodology for assessing forest harvesting and road construction effects on hydrologic response.

This investigation focuses specifically on the Pacific Northwest region where the impact of forest harvesting on hydrologic response is an important and controversial issue. This work presents modifications to the Regional Hydro-Ecological Simulation System (RHESSys) modeling framework and discusses specific issues related to modeling landscape drainage organization in hydro-ecological models. Within RHESSys, tradeoffs between using a spatially explicit routing approach versus a less detailed statistical approach to modeling distributed hydrology are explored. Results from this study illustrate the limitations of using a statistical approach in modeling drainage organization and the sensitivity of both routing methods to calibration and errors in topographic and soil input data. Different strategies for landscape representation are also compared. Results highlight the significant role played by fine scale topographic variability in areas adjacent to streams, and the importance of these local areas in controlling watershed hydrologic response.

Application of the RHESSys modeling tool is further developed by incorporating a conceptual model of forest harvesting and road construction effects on hydrology. Comparing simulations with observed streamflow for a study catchment in the Pacific Northwest provides an illustration of forest harvesting and road construction effects on hydrologic response. The model illustrates how the effects of these disturbances are dependent upon road construction characteristics and the spatial distribution of vegetation

and its water use. Road construction characteristics include both culvert drainage topology and the position of the road relative to hillslope drainage organization. Effects on downslope soil moisture and the spatial and temporal dynamics of seasonal runoff production illustrate the potential ecological significance of different disturbance scenarios.

Acknowledgements

I gratefully acknowledge the support that I have received from both friends and colleagues in the development of this thesis. I wish to thank the "Bandits" group and others in the Physical Geography 3rd floor lab who were always part of the day to day pleasures and frustration of doing research. In particular, I wish to thank Irena Creed for her support, both as a friend and as a colleague and Richard Fernandes for his collaboration in RHESSys development and his many insights into some of the trickier modeling and research problems associated with this work. I am grateful also to my committee members, Ferko Csillag, Tony Price, Joe Desloges, Scott Munro and Brian Branfireum for their review of and comments on this thesis. I also appreciate greatly the thoughtful and supportive comments of my external reviewer, Jeff McDonnell. At the H.J.Andrews Experimental Forest, I thank the staff who have provided me with much of the data used in this work. In particular, I thank Gordon Grant and Beverly Wemple for their supportive ideas and many interesting discussions.

Finally, I wish to thank my advisor Larry Band. Working with Larry has been both inspiring and very often fun. In the past few years, I feel that I have benefited greatly from being his student. His approach to doing research and his insight into the questions that we ask as scientists has provided a strong foundation for the work presented here and hopefully, for its continuation in the future.

Table of Contents

List of Figures

Figure 2.3: Landscape Partitioning Strategies including 30m pixels, contiguous patches based on a combination of a wetness index image and a DEM, 90m pixels and non-contiguous patches based on a wetness index.

Figure 2.4: Watershed 2 Outflow, Comparison between simulations using TOPMODEL (implicit routing), explicit routing and observed outflow for 1986-1988.

Figure 2.5: Soil Moisture Distribution for January 10, 1998 - Comparison between different routing approaches.

Figure 2.6: Soil Moisture Distribution for August 20, 1998 - Comparison between different routing approaches

Figure 2.7 Saturation deficit along a single flow path - from stream to ridge. Comparison between TOPMODEL and explicit routing for January (wet period) and August (dry period).

Figure 2.8: Spatially Distributed Mean Monthly Saturation Deficits for a small sub-hillslope in Watershed 2: Comparison between different routing methods

Figure 2.9: Sensitivity to simulated outflow to error (Gaussian noise) in input DEM and in the spatial pattern of soil hydraulic conductivity, K_{sat}; Comparison between TOPMODEL and the explicit routing approach (PR). Random Gaussian noise (μ=0; σ= 5m) is applied to the DEM; Two scenarios of Gaussian noise are applied to the Ksat image: low (μ=0; σ= 8m/day) and high (μ=0; σ= 40m/day) noise scenarios

Figure 2.10: The Effect of Gaussian noise in DEM and Ksat input information on the distribution of TOPMODEL wetness index. Random Gaussian noise (μ=0; σ= 5m) is applied to the DEM; Two scenarios of Gaussian noise are applied to the Ksat image: low (μ=0; σ= 8m/day) and high (μ=0; σ= 40m/day) noise scenarios

Figure 4.5: Cumulative outflow difference for simulations with roads and base line (no road) scenarios using a low 0.5 m road cut depth for three road - culvert drainage scenarios a) road culverts route water directly to the stream b) road culverts concentrate the flow in relatively wet areas i.e. high wetness index, WI or c) road culverts concentrate flow in relatively dry areas i.e. low wetness index.

Figure 4.6: Cumulative outflow difference for simulations with roads and base line (no road) scenarios using a moderate 5 m road cut depth for three road - culvert drainage scenarios a) road culverts route water directly to the stream b) road culverts concentrate the flow in relatively wet areas i.e. high wetness index, WI or c) road culverts concentrate flow in relatively dry areas i.e. low wetness index.

Figure 4.7: Cumulative outflow difference for simulations with roads and base line (no road) scenarios- 5 m road cut depth for fine (30m) and coarse (90-120m) culvert spacing.

Figure 4.8: Spatial distribution of differences in saturation deficit and evapotranspiration below the road due to road construction effects; for July 22, 1959.

Figure 4.9: Spatial and temporal persistence of road construction effects on downslope soil moisture and evapotranspiration; mean and variance for 1959 a) saturation deficit difference by distance from road b) daily saturation difference c) evapotranspiration difference by distance from road d) daily evapotranspiration difference.

Figure 4.10: Annual outflow difference due to roads for Watershed 3 a) residuals (observed - predicted) for empirical relationship based on Watershed 2 and Watershed 3 b) simulated differences (simulations with roads (5m cut depth; routing to the stream) and forest harvesting - baseline unharvested simulation)

Figure 4.11: Annual outflow difference due to roads for Watershed 3 a) residuals (observed - predicted) for empirical relationship based on Watershed 2 and Watershed 3 b) simulated differences (simulations with roads (5m cut depth; routing to lowest wetness index) and forest harvesting - baseline unharvested simulation)

Figure 4.12: Empirically derived cumulative outflow residuals (observed - predicted) for pre-road construction years (1956-1957) and post road construction years (1960-1961).

Figure A.1: Alternative routing for patches containing roads where patches containing roads route water to a stream patch, a relatively wet patch or a relatively dry patch.

List of Tables

List of Symbols

Age_{snow}	snowpack age
b	pore size index
c	soil parameter
cf	cloud fraction
Cmin, Cmax	min and max soil/strata heat capacity
co	cloud opacity
c_{water}	specific heat of water
D	water equivalent depth at the maximum soil depth
Day	daylength (sunlight)
e_a	atmospheric vapor pressure.
E_{dry}	evaporation during dry periods
E_{rain}	evaporation during rainy periods
E_{sat}	saturation vapour pressure
ess_{atm}	atmospheric emissivity
F	fractional canopy cover
f_{stm}	stomatal fraction
gap	gap fraction
gs	stomatal conductance
g_{surf}	surface conductance
G_{surf}	surface heat flux
k	Beer's Law extinction coefficient
$K_{clear\_sky\_diffuse}$	incoming diffuse radiation (with no cloud cover attenuation)
$K_{clear\_sky\_direct}$	incoming direct radiation (with no cloud cover attenuation)
$K_{diffuse}$	diffuse radiation
K_{direct}	direct radiation
K_{sat}	saturated zone hydraulic conductivity
K_{sat0}	saturated zone hydraulic conductivity at surface
K_{unsat}	unsaturated zone hydraulic conductivity
L	longwave radiation

LAI	leaf area index
LWP_{min_spring}	minimum leaf water potential for full stomatal open
$LWP_{predawn}$	pre-dawn leaf water potential
LWP_{sc}	leaf water potential at stomatal closure
M_{rad}	snowpack radiation melt
m_s	decay rate of soil hydraulic conductivity with soil moisture deficit
M_T	snowpack temperature melt
MT_{coef}	temperature snowmelt coefficient
M_V	snowpack melt due to advection
m_z	decay rate of soil hydraulic conductivity with depth
P	precipitation
P_{dur}	precipitation duration
p	porosity decay rate
PAI	plant area index
q_{base}	baseflow
q_{cap}	capillary rise
q_{drain}	drainage from unsaturated zone
q_{patch}	flow from patch
q_{pot_exfil}	potential soil exfiltration
$q_{potential\_drainage}$	drainage to field capacity
q_{road}	flow from road cut interception
Q_{snow}	snowpack energy deficit
R_{net}	net radiation
Rh	relative humidity
S	relative soil moisture storage
s	saturation deficit (water)
$s_{active\_soil\_depth}$	depth over which soil exfiltration can occur
S_{fc}	soil moisture at field capacity
s_{road_cut}	water equivalent depth of road cut
T	soil transmissivity
T_{air}	air temperature

T_{avg}	average daily temperature
T_{min}	minimum daily air temperature
$T_{nightmax}$	maximum night-time air temperature
Tr	transpiration
Tr_{sat}	transpiration from saturated zone
Tr_{unsat}	transpiration from unsaturated zone
T_{sat}	transpiration from the saturated zone
T_{soil}	soil temperature
T_{unsat}	transpiration from the unsaturated zone
v	wind speed
vpd	vapour pressure deficit
z	depth
z_{root}	rooting depth
z_s	depth to saturation
α	albedo
β	slope
γ	psychrometric constant
φ	porosity
Ψ_{ae}	soil air entry pressure
$\Psi_.$	soil moisture tension
λ_f	latent heat of fusion
λ_s	latent heat of sublimation
λ	mean hillslope wetness index value
ρ_{snow}	density of snow
ρ_{water}	density of water
σ	Stefan-Boltzmann constant
Θ_{cap}	specific interception storage capacity
Θ_{fc}	soil moisture at field capacity
Θ_{int}	interception storage
Θnoon	solar angle at noon

Θ_{unsat}	unsaturated zone soil moisture
ω	flow width

Introduction

This study addresses several challenges in the application of hydro-ecological models as tools for studying the spatially distributed pattern of soil moisture and runoff production and how forest harvesting activity can alter this pattern. Specifically, I address a number of issues related to modeling hillslope drainage organization and its role in controlling subsurface and surface runoff production, soil moisture and forest ecological processes at the small basin scale. I also illustrate how drainage organization plays a key role in assessing forest harvesting effects, particularly those related to road construction. The first part of this document focuses on providing an adequate model of drainage organization given the goal of assessing forest harvesting effects. The second part of this document then explores the potential for forest harvesting to modify drainage organization via road construction and presents a modeling study of the effects of forest roads on hydrologic response for a catchment in the Pacific Northwest.

The impact of forest harvesting on hydrologic response involves complex interactions between forest water use through interception and evaporation, hillslope drainage patterns and climate. Hillslope drainage patterns are in turn controlled by topography and soil within particular climate regimes. Given the complexity of these interactions and their spatial and temporal variability, computer-based hydro-ecological modeling linked with geographic information systems provides one method to gain insight into the effects of forest harvesting across a range of different ecological conditions. Ideally, this modeling approach provides a tool that can be used to generalize information from intensive plot studies to the broader regions over which management initiatives and decision-making must be applied.

Historically, we have learned much from plot level studies of the effects of forest harvesting on hydrologic response. There is also a strong and growing body of knowledge pertaining to the modeling of forest hydrology and of the effect of forest harvesting. Summaries of the effects of forest harvesting on annual water yield generally show an initial increase in outflow, as a function of percent catchment harvested, followed by several decades of recovery (Stednick, 1996; and Bosch and Hewlett, 1982). From these studies, Stednick (1996) estimates a 50mm linear increase in annual water yield on average per 10% percent

catchment harvested area for the Pacific Coastal region. He notes, however, that considerable variability in annual response to harvesting exists across sites within a given region. Variability in hydrologic response to harvesting has been related to catchment position, vegetation type and distribution and climate. (Stednick, 1996; Sahin and Hall, 1996)

In the Pacific Northwest, the greatest net effects of logging occur at the onset of the rainy season. Relative effects, however, are often larger during the summer season (Harr, 1983). Changes in summer low flow can have significant ecological consequences including effects on water supply, water quality and aquatic habitat (Johnson, 1998; Hicks et al., 1991). Johnson (1998) summarizes catchment studies that focus on low flow response and recovery to disturbance. These studies also show considerable variability in response that is related to climate, topography, vegetation and soil characteristics. Typically summer low flow volumes and the number of low flow days increase as a function of the percent area cut. In addition to changes in outflow, significant decreases/increases in soil moisture following disturbances during summer dry periods can increase/decrease vegetation water stress and ultimately plant productivity and the rate of re-growth in harvested areas. Adams et al (1991), for example, observe an eventual decrease in soil moisture deficits during recovery from forest harvest in a small catchment in the western Oregon Cascades and they note the potential for these deficits to influence forest recovery. Ultimately, differences in soil moisture patterns can influence the distribution of species if natural recovery occurs following harvest.

At sub-daily time scales, observed hydrologic responses to cutting include both increases and decreases in peak flow storm response (Jones and Grant 1996, Wright et al., 1990). In general, studies of peak flow response link an initial (within 5 years after harvest) increase in peak flow with a decrease in evapotranspiration and interception by vegetation removal. In some cases, an initial *decrease* in outflow has been observed and explained as a reduction in moisture input due to fog drip by pre-harvested vegetation (Harr, 1983). In regions where snowfall is significant, forest harvesting has been shown to also increase peak flow by facilitating high snow accumulation and more rapid melt (Berris and Harr, 1987). Greater snowpack accumulation occurs due to the reduction in snow interception by the canopy and subsequent sublimation. More rapid melt has been shown to occur in cleared areas due to the increase in turbulent transfer.

The initial increase (or decrease) in peak, low and annual flow is followed by a recovery period as vegetation regrows. Recovery typically requires several decades as replacement vegetation recovers evapotranspiration and interception characteristics of the previous forest. In some cases there is an initial augmentation in water use (and therefore lower outflow) by young high consumptive vegetation in comparison with pre-cut mature forest (i.e. Hicks et al., 1991). Alternatively, if replacement species differ from pre-cut forest, differences in water use may be permanent (Hornbeck et al., 1993). Variability in the magnitude and timing of recovery has again been related to climate, topographic and vegetation characteristics of the landscape (Stednick, 1996; Hornbeck et al., 1993).

In addition to evidence of the effects on vegetation removal, there is also evidence that road construction can alter hydrologic response. Plot level studies indicate two mechanisms through which forest roads can influence hydrologic response. Luce and Cundy (1994) illustrate responses due to increased overland flow resulting from the decreased infiltration capacity associated with road surfaces. Other researchers have illustrated the potential for roads to increase overland flow generation by cut bank interception of subsurface throughflow (Wemple et al., 1996). The connectivity of road ditches and culverts with the stream network facilitate the impact of this increase in overland flow on peak flow. Chapter 4 discusses this effect in more detail.

Field studies have indicated that some of the variability in hydrologic response may be due to the construction of roads. Jones and Grant (1996) found increases in the magnitude and timing of peak flow responses during a 4-year pre-cut period in which road construction occurred for a small watershed in the Pacific Northwest. They found that peak flow increases were greater for winter and spring versus fall events and for intermediate storm sizes, following road construction. Peak flow increases during the period following harvesting were also greater than what would have been expected given the 25% cutting and regrowth. Thomas and Megahan (1998), however, present a critique of this analysis which suggest that results may not be significant across all storm sizes. Alternatively, Wright et al. (1990) in a paired catchment study at Caspar Creek in northwest California found that, in an initial road construction period prior to harvesting, roads increased peak flows only for small storm events. They note, however, that roads in the harvested catchment at Caspar Creek

were concentrated near to the stream (88% within 61m of main channel) and thus may not have contributed significantly to runoff efficiency. Other studies, Harr et al. (1975) and King and Tennyson (1984) also present significant but highly variable increases in peak flow associated with road construction. In summary, roads can have effects on peak flow but these effects vary significantly across sites, for different road construction patterns (i.e. roads located near to the stream vs. upslope or midslope locations), and across different magnitudes and frequencies of storm events. The exploration of the effect of roads has centered on the effects on peak flow response. Peak flow response, however, occurs within the context of a seasonal flow regime and the exploration of the seasonal effects of roads has received less attention.

The above discussion illustrates that there is considerable spatial and temporal variability in hydrologic response to both road construction and forest harvesting. Modeling provides one method to integrate the variety of controls on hydrologic response to try to understand this variability. Spatially distributed models can illustrate the degree to which differences in hydrologic response are due to a difference in drainage organization and how disturbances are organized relative to this drainage pattern. Variability in response from road construction, given the mechanism described above, will depend on the road position relative to hillslope saturated subsurface throughflow and linkages between the road and stream. In addition, road redirection of subsurface throughflow may act in combination with increased soil moisture and subsurface throughflow associated with forest removal upslope of the road. In this case, road construction and forest harvesting may act to enhance (and in some scenarios diminish) the effects on hydrologic response. The potential for modeling to integrate these various different effects and spatial linkages between them requires adequate modeling of spatially distributed landscape organization. The goal of this work therefore is to both (1) assess the ability of a physically based hydro-ecological model to represent drainage organization and (2) to illustrate how this modeling can be used to generate a hypothesis about road construction and forest harvesting effects.

There are a number of issues that complicate modeling landscape drainage organization. Three key concerns are addressed in this document including the methodology used to model spatially distributed soil moisture and runoff production, calibration and landscape

representation. Because of the sensitivity of hydrologic response to drainage organization, these are issues which must be addressed before modeling can be used as a reliable tool for assessing landscape level sensitivity to forest harvesting, across a range of watersheds within a given region. Once these issues are addressed, the modification of drainage organization caused by roads must be implemented in the model. The model can then be applied to a set of different scenarios.

For this investigation I focus specifically on the Pacific Northwest region where the impact of forest harvesting on hydrologic response remains an important and controversial issue. In terms of hydrologic response, this document will focus specifically on seasonal responses, and consider daily, monthly and annual hydrologic response in both wet and dry periods. As a study site within this region, I use the H.J.Andrews experimental forest in Western Oregon Cascades (Figure I.1). H.J.Andrews is typical of the Western Cascade region, with significant relief, warm dry summers and cool wet winters. Vegetation is dominated by douglas fir (Pseudotsuga menziesii), western hemlock (Tsuga heterophylla) and western red cedar (Thuja plicata) in lower elevations and by noble fir (Abies procera) and Pacific silver fir (Abies amabilis) in the upper elevations. Figure I.2 illustrates forest cover in one of the smaller sub-watersheds used in this study. Forests in this region are exceptionally productive, reaching heights of greater than 70m. Soils range from clay to sandy and gravelly loam. Underlying bedrock is volcanic material from Oligocene-lower Miocene including basalts, tuffs and breccias. H.J.Andrews is also part of the LTER network and serves as site of extensive field study, including several paired catchment harvesting experiments. Thus, it offers a good test catchment for model development and testing.

The Pacific Northwest region supports some of the greatest forest productivity in the world and is an area where forest harvesting plays a key economic role. Forest harvesting, in this region, often competes with other land uses such as natural habitat maintenance, including commercial fish habitat, recreation and a growing human population. The linkage between forest harvesting and hydrology is also an important issue in this region. The augmentation of peak flow response due to forest harvesting has been linked to increases in winter flooding

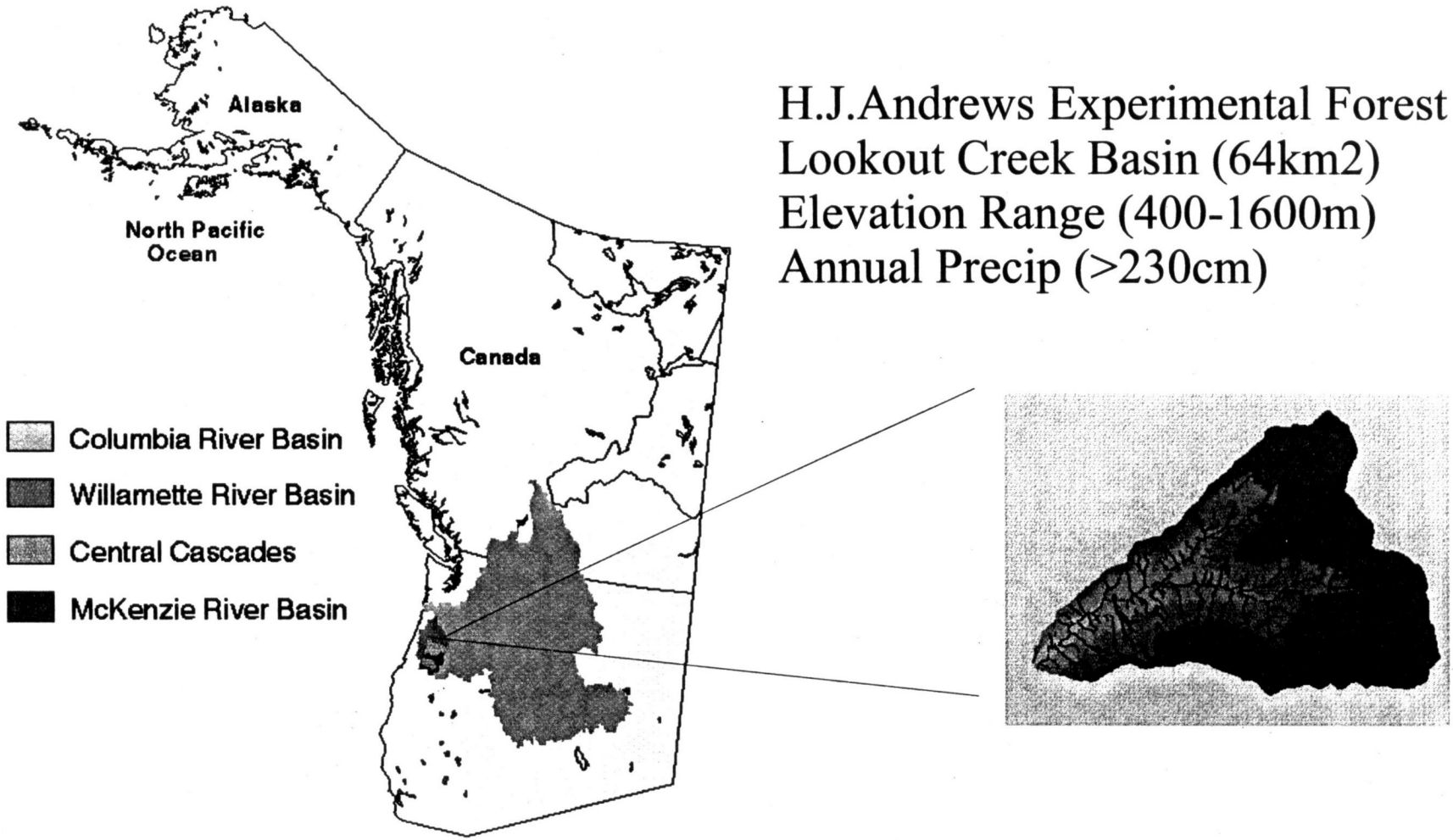

Figure I.1: Location of the H.J.Andrews Forest

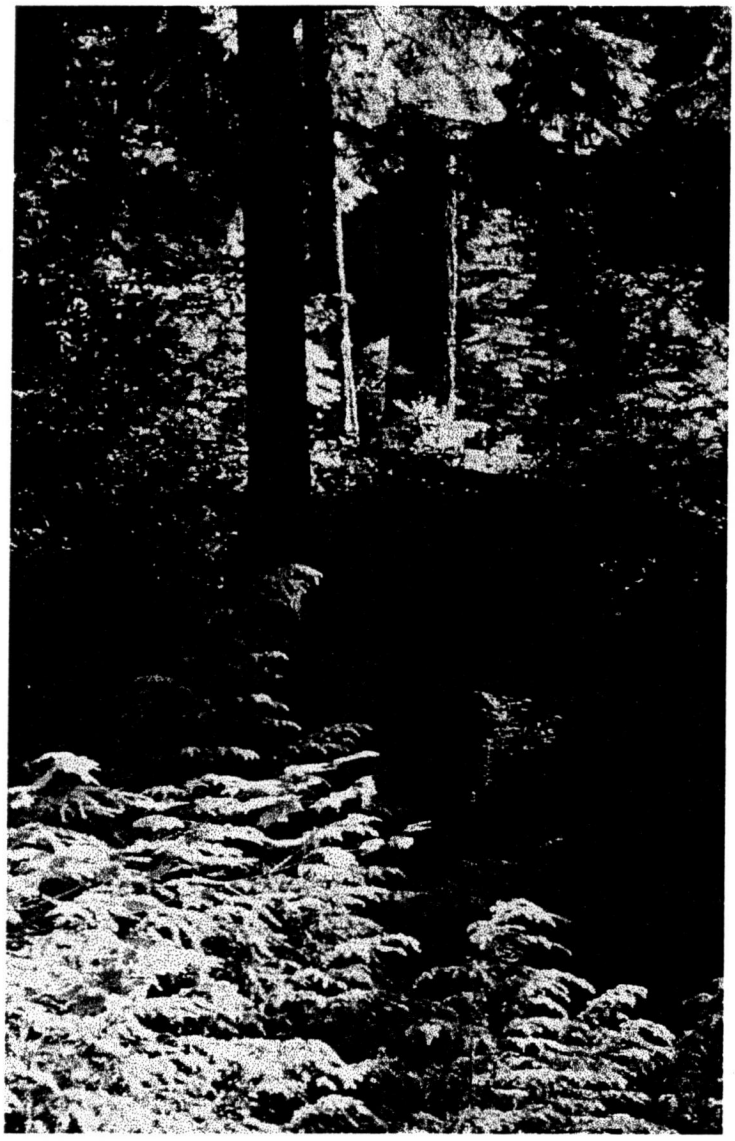

Figure I.2: Streamside forest cover in the H.J.Andrews study catchment.

and stream sedimentation. In terms of hydrologic response, much of the modeling and field study in the Pacific Northwest has been done on assessing peak flows. Issues around low flow and summer soil moisture, however, are also important from the perspective of ecological assessment in this region where summer drought often occurs. Changes in summer low flow response related to harvesting can have effects on stream habitat quality and changes in soil moisture can have effects on re-growth potential subsequent to harvesting, fire sensitivity and ultimately on species composition.

Strategy

I begin by presenting the Regional Hydro-Ecologic Simulation System (RHESSys) modeling framework (Band et al., 1993) and recent modifications to the model, which contribute to its use as tool for assessing hydro-ecological impacts. In the following two chapters, I discuss specific issues related to landscape drainage organization in RHESSys, and other similar models. The second chapter examines the trade-off between using a spatially explicit routing approach versus a less detailed statistical approach to modeling distributed hydrology. I compare different strategies for partitioning the landscape and modeling processes at multiple scales. The intention is to determine an efficient and reasonably accurate approach to modeling hillslope drainage and to establish the sensitivity of this method to error in topographic and soil input data. The third chapter expands upon the importance of landscape representation in modeling hillslope soil moisture and drainage using an explicit routing approach. In particular, I examine the importance of incorporating fine scale topographic variability associated with areas adjacent to and including streams. This paper highlights the significant role played by drainage organization in these areas and its potential importance in assessing hydrologic response.

Having established a methodology for landscape representation and modeling with respect to drainage organization, the final section considers an application of this approach by examining the potential for altering this organization through road construction. The issue of the hydrologic effects of road construction is particularly amenable to spatially distributed

modeling issues because of the link with drainage organization. The potential effect of road construction is largely dependent upon the position of the road relative to other hillslope hydrologic processes including drainage organization and the spatial distribution of vegetation and its water use. Road construction in low wetland areas near to the stream, for example, may produce significantly different effects on hydrologic response when compared with road construction in midslope areas. Conditions upslope from road construction such as forest cover and drainage patterns will also alter watershed hydrologic response. The final section offers a conceptual model of road construction effects on hillslope hydrologic response, presents how this conceptual model can be incorporated into RHESSys, and provides an illustration of how modeling can be used to provide insight into the complex interactions involved.

References

Adams, P. W., Flint, A. L., Fredriksen, R.L. 1991. Long-term patterns in soil moisture and re-vegetation after a clearcut of a Douglas-fir forest in Oregon, *Forestr. Ecol. Man.*, 41, 249-263.

Band, L.E. P.Patterson, R.R. Nemani, and S.W.Running. 1993. Forest ecosystem processes at the watershed scale: incorporating hillslope hydrology. *Agriculture Forest Meteorology* **63**: 93-126.

Berris, S.N. and Harr, R.D. 1987. Comparative snow accumulation and melt during rainfall in forested and clear-cut plots in the western Cascades of Oregon, *Wat. Res. Research* 23:1, 135-142.

Bosch, J.M and Hewlett, J.D., 1982. A review of catchment experiments to determine the effect of vegetation changes on water yield and evapotranspiration. *J. of Hydrol.*, 55, 3-23.

Harr, R. D., Levno, A, Mersereau, R. 1982. Stream flow changes after logging 130-year-old douglas fir in two small watersheds, *Wat. Res. Research* 18:3, 383-393.

Harr, R.D. 1983. Potential for augmenting water yield through forest practices in Western Washington and Western Oregon, , *Wat. Res. Research* 19:3, 637-644.

Harr, R.D., Harper, W.C., Krygier, J.T, Hsieh, F.S. 1975. Changes in storm hydrographs after road building and clear-cutting in the Oregon Coast Range, *Wat. Res. Research* 11:3,436-444.

Hicks, B.J., Beschta, R. L., Harr, R.D., 1991. Long-term changes in streamflow following logging in Western Oregon and associated fisheries implications, *Wat. Res. Bull.*, 27, 217-225.

Hornbeck, J.W., Adams, M.B., Corbett, E.S., Verry, E.S., Lynch, J.A., 1993. Long-term impacts of forest treatments on water yield: a summary for northeastern USA, *J. of Hydrol.*, 150, 323-344.

Johnson, R. 1998. The forest cycle and low river flows: a review of UK and international studies, *Forest Ecology and Management*, 109, 1-7.

Jones, J.A., and Grant, G.E. 1996. Peak flow responses to clear-cutting and roads in small and large basins, western Cascades, Oregon, *Wat. Res. Research*, 32:4, 959-974.

King, J.G., Tennyson, L.C. 1984. Alteration of streamflow characteristics following road construction in north central Idaho, *Wat. Res. Research*, 26:7, 1159-1163.

Luce, C.H., Cundy, T.W. 1994. Parameter identification for a runoff model for forest roads, *Wat. Res. Research*, 30:4, 1057-1069.

Sahin, V., Hall, M.J. 1996. The effects of afforestation and deforestation on water yields, , *J. Hydrol*, 178, 293-309.

Stednick, J. 1996. Monitoring the effects of timber harvest on annual water yield, *J. Hydrol*, 176, 79-95.

Thomas, R. B. and Megahan, W.F. 1998. Peak flow responses to clear-cutting and roads in small and large basins, western Cascades, Oregon: A second opinion, *Wat. Res. Research*, 34:12, 3393-3403.

Wemple, B. C., Jones, J.A., Grant, G.E. 1996. Channel network extension by logging roads in two basins, western Cascades, Oregon, *Wat. Res. Bulletin*, 32:6, 1195-1207.

Wright, K.A., Sendek, K.H., Rice, R.M, Thomas, R.B. 1990. Logging effects on streamflow: Storm runoff at Caspar Creek in Northwestern California. *Wat. Res. Research* 26:7, 1657-1667.

Chapter 1: The RHESSys modeling framework - an overview and summary of recent modifications

Introduction

This section presents an overview of the RHESSys modeling system. RHESSys (Figure 1.1), is a GIS-based, hydro-ecological modeling framework that combines both a set of physically based process models and a methodology for partitioning the landscape and parameterizing the model. The process models simulate carbon, water and nutrient fluxes at a daily time step over multi-year time periods. The RHESSys architecture models the spatial distribution and spatial-temporal interactions between these different processes at the hillslope to regional scale. RHESSys, as described here, presents a significant modification of earlier versions of RHESSys as described in Band et al., (1991, 1993) and developed by Mackay and Band (1997), Creed and Band (1998). In this version of RHESSys, I have, in collaboration with Richard Fernandes redesigned the model structure and implementation, input/output formats, landscape representation and a number of the key ecological-process algorithms. In this section, I discuss these recent changes to the RHESSys model that support the modeling studies done in later sections of this document.

As with previous versions, RHESSys process models have been adapted from several pre-existing models. Specific algorithms within these original models have been modified to reflect various developments in the associated literature or to fit within the RHESSys modeling framework. The original process models used in RHESSys include a climate submodel, an ecophysiological model and a distributed hydrology model. The climate sub-model includes an interpolation scheme based on the MTN-Clim model (Running et al, 1987) which uses topography and user supplied base climate station information to estimate spatially distributed climate variables such as radiation and to extrapolate input climate variables over topographically varying terrain. The ecophysiological model is adapted from BIOME-BGC (Running and Coughlan, 1988; Running and Hunt, 1993) to estimate carbon, water and nitrogen fluxes from different canopy cover types. Many of these algorithms have been modified and are presented later in Appendix A.

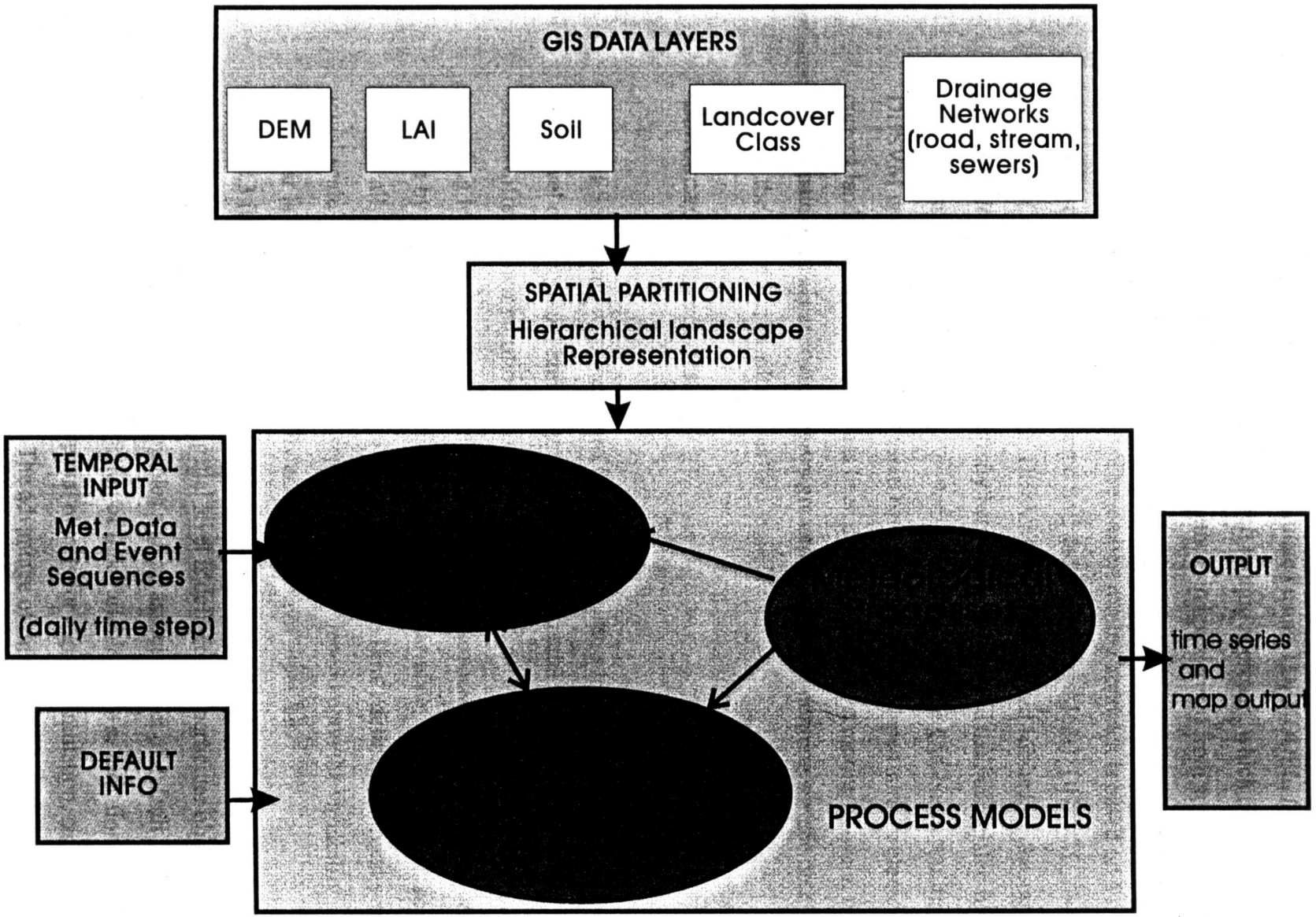

Figure 1.1 Overview of Regional Hydrologic Ecosystem Simulation System, RHESSys

Two distributed hydrologic models are included in RHESSys. In earlier versions of RHESSys, distributed hydrology was simulated using TOPMODEL, (Beven and Kirkby, 1979), a quasi-distributed model or implicit routing approach, which distributes hillslope soil moisture based on the distribution of a wetness index, derived from soil and topographic information. In this version of RHESSys, we have included, in addition to TOPMODEL, a spatially explicit routing approach. The explicit routing approach is based on a modified version of the Distributed Hydrologic Soil and Vegetation Model, DHSVM, routing algorithm (Wigmosta et al, 1994). DHSVM models saturated subsurface throughflow and overland flow via explicit connectivity between grid cells and their associated hydrologic characteristics. In RHESSys, an important modification to the grid-based routing used in DHSVM is to allow water to be routed between arbitrarily shaped surface elements. The current landscape representation has been designed to support routing between irregularly shaped patches. This approach allows greater flexibility in defining surface patches and varying the shape and density of surface tessellation.

Landscape Representation

The RHESSys framework partitions the landscape into a hierarchical structure (Figure 1.2). Each level of this spatial hierarchy fully covers the spatial extent of the world or landscape. Levels differ in their partitioning of the landscape and each level is nested within the preceding level of the spatial hierarchy. Each level is associated with different processes modeled by the simulation system and with a particular scale. At the smallest scale, patches are typically defined on the order of m2; while basins (km^2) define the largest scale. The actual scale used for the different spatial levels will depend upon the variability of the particular landscape and availability and resolution of input data.

Figure 1.3 illustrates how RHESSys associates processes with specific spatial levels and time steps. Within RHESSys, a given spatial level is defined as a particular object type with specific state (storage) and flux variables and an associated set of default parameters. For example, MTN-Clim climate estimation of flux variables such as radiation occurs at the zone level. Thus in deriving the set of spatial objects for a given simulation, zones are chosen to represent areas of similar climate. The advantage of this hierarchical approach is that it allows different processes i.e. climate vs. canopy processes, to be modeled at different spatial

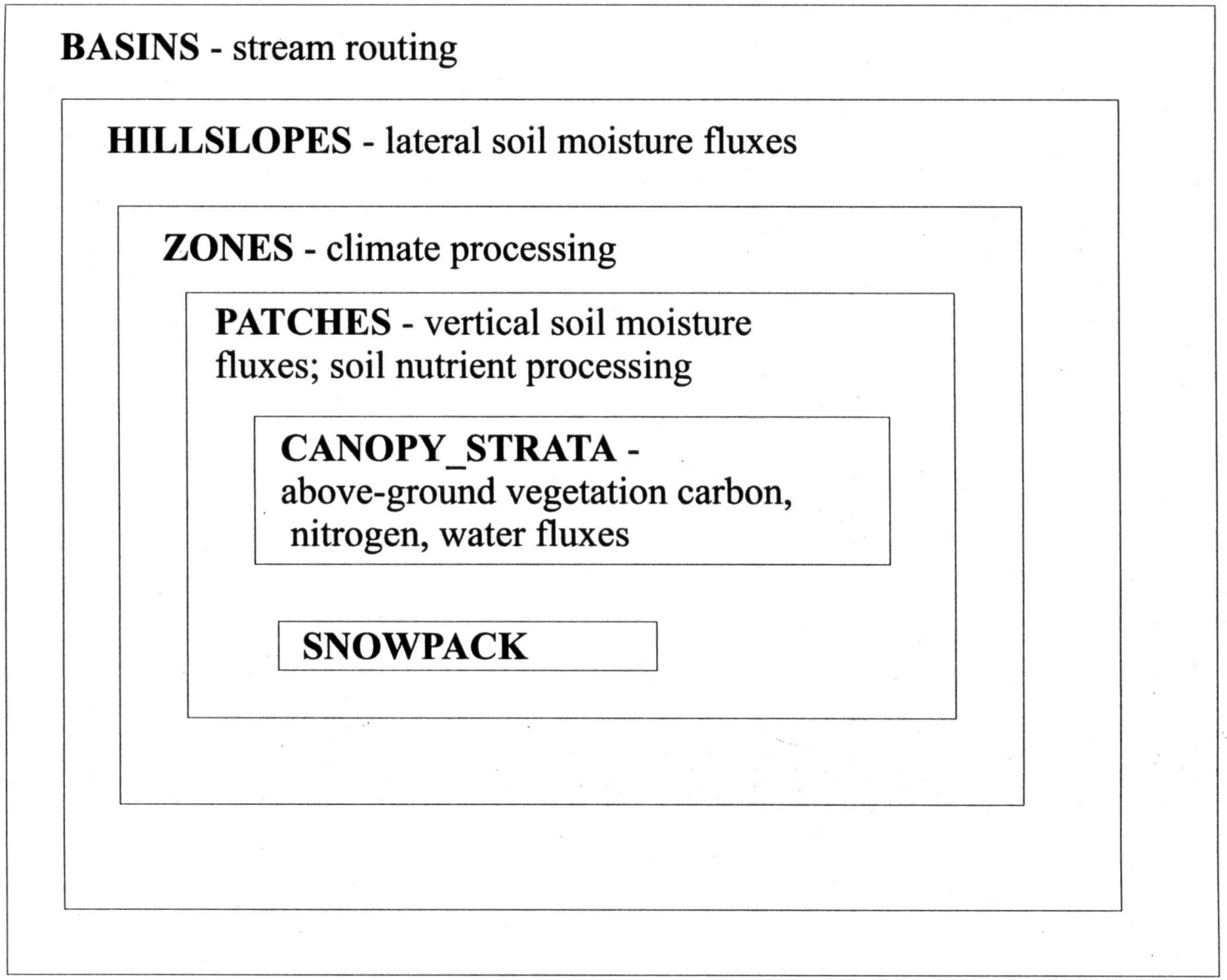

Figure 1.2: RHESSys landscape representation as a set of hierarchical spatial objects

	N/A (ie. no processes implemented at this time)	N/A	Input and interpolation of key climate variables	Calculation of unsaturated zone soil moisture status, including field capacity	Calculation of current canopy moisture status and phenology
	N/A	N/A	Estimation of solar radiation	Infiltration (if hourly rainfall data is available)	
	N/A	Calculation of subsurface and surface routing between patches		Calculation of unsaturated zone soil moisture dynamics, such as infiltration, drainage	Calculation of canopy hydrologic and carbon processes such as ET, interception

Figure 1.3 Temporal and spatial organization of key processes in RHESSys

and temporal scales. It also allows modeling to occur on ecologically meaningful units as opposed to arbitrarily defined grid cells.

The definition of modeling units is done by the user prior to running the simulation. Although the user is given considerable flexibility in choosing a partitioning strategy for the different levels, partitioning should be tailored to take advantage of the patterns of relevant variability within the landscape. This permits efficient parameterization and reduces the error associated with landscape partitioning. Band et al. (1991), Lammers et al. (1997), Band et al. (1995) and Chapter 2 in this document provide further justification for and discussion of partitioning strategies.

The approach to partitioning is specific to each level of the spatial hierarchy and the associated processes modeled at that level. Basins are defined as hydrologically closed drainage areas and encompass a single stream network. Explicit routing is organized at this level to produce streamflow within the basin stream network. Basins can also serve as aggregating units for variables such as photosynthesis.

Hillslopes define areas that drain to a single stream reach. Hillslopes will usually be derived based upon drainage patterns using GIS based terrain partitioning algorithms such as r.watershed in GRASS and as described in Band (1989) and Lammers and Band (1990). Like basins, hillslopes can be used to aggregate sub-level processes. The spatial redistribution of patch soil moisture is organized at the hillslope level and, for TOPMODEL, a hillslope level base flow is defined.

Zones denote areas of similar climate. Zone objects store climate variables such as radiation, and temperature. Each zone is linked to a particular set of climate input files. Thus, a given landscape may utilize data from multiple meteorological stations if this information is available. Data from a particular station such as precipitation and temperature is modified based on zone elevation, slope and aspect relative to the input climate station. Zone processing also estimates additional climate variables that may not be available from base climate station information such as vapour pressure deficit. Numerous strategies exist to

partition areas of similar climate. Elevation bands in a mountainous area, for example, are likely to denote areas of similar climate as discussed in Lammers et al. (1997). Since zones are contained within hillslopes, they will inherit similarity of aspect if hillslopes are generated as facets defined by slope and aspect. The distribution of climate stations can also be used to define zone partitioning, where each zone defines the area associated with a particular climate station.

Patches represent the smallest resolution spatial unit and define areas of similar soil moisture characteristics. Vertical soil moisture processing is modeled at the patch level. Patch state variables include fluxes such as infiltration and storage such as unsaturated zone soil moisture. Figure 1.4 summarizes the hydrologic fluxes associated with the patch level. The spatial resolution of the canopy stratum is also defined by the patch partitioning. Canopy strata are a separate object type but they define vertical above ground layers rather than horizontal spatial layers. Patches must, therefore, also group together areas of similar canopy cover. This is consistent with the definition of patches, which is based on soil moisture, since areas that differ in the type of canopy cover will likely maintain different soil moisture storage and fluxes. Patches therefore are often an overlay of several different maps, such as wetness index, vegetation cover and, when explicit routing is used, stream and road networks. The rationale for including the stream network is discussed later in this document.

As illustrated in Figure 1.5, processes such as photosynthesis and transpiration are modeled at the canopy stratum level. Each stratum corresponds to a different layer such as overstory or understory in the canopy structure. The litter layer is also included as a separate stratum layer. The user defines the number of vertical layers. A height state variable is associated with each layer and defines its processing relative to the other layers. Incoming radiation, precipitation throughfall and wind are extinguished through the multiple layers according to the height and vegetation characteristics of each layer. Litter layers are also considered canopy strata and given a height of zero. RHESSys also permits multiple strata at the same height. This allows mixed vegetation types within the same spatial area to be represented.

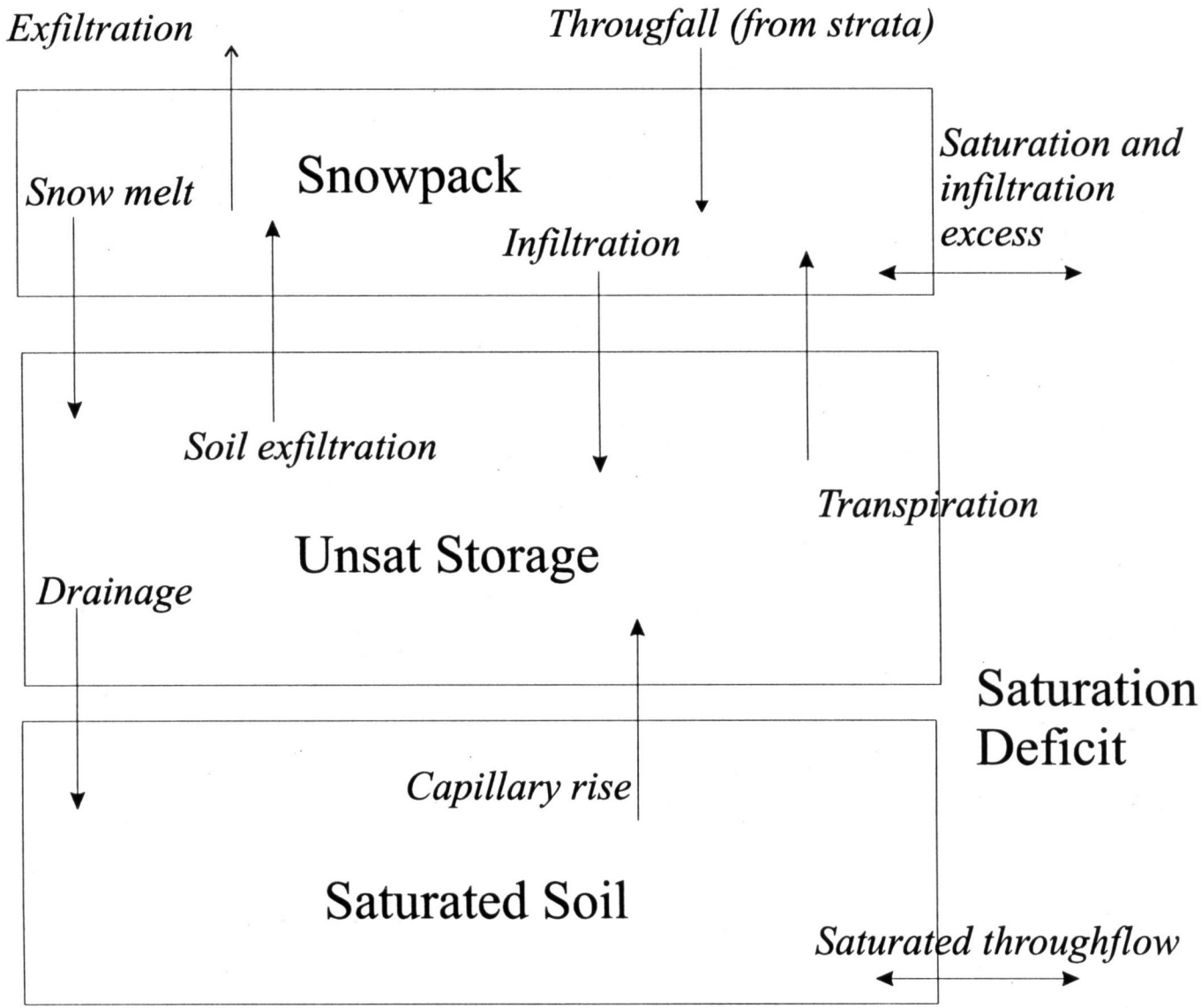

Figure 1.4: Hydrologic processes implemented at the patch level

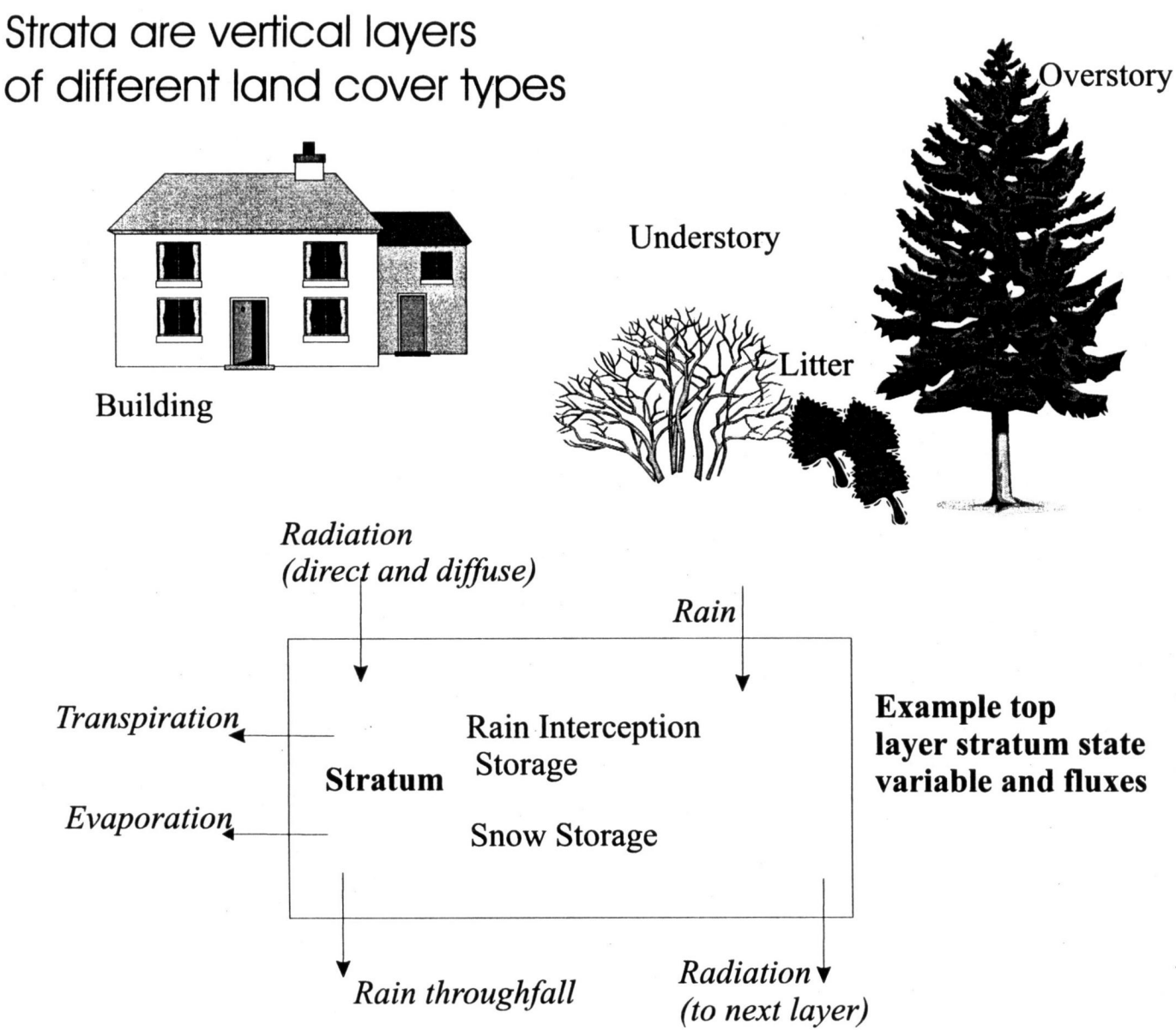

Figure 1.5: Hydrologic processes implemented at the canopy stratum level

Figure 1.6 illustrates an example set of input partition images developed for the H.J.Andrews Forest. A supporting interface program, GRASS2WORLD, was developed, which uses these images to automatically create the required landscape representation input to RHESSys. The basin and hillslope images were both derived using the GRASS GIS r.watershed routine. The zone partition image is derived from documentation on the spatial variation in climate patterns in the area (Rosentrater, 1997). An alternative derivation may have used a map of climate station coverage or considered the impact of elevation. The patch image used here is an overlay of three images, a stream network, a TOPMODEL wetness image and a canopy cover type image, as shown in Figure 1.7.

Process Algorithms

At present, RHESSys performs most of its processes at a daily time step. The exception is climate simulation. Radiation estimation routines execute at an hourly timestep and then are summed to give daily radiation values. All other routines execute at a daily time step. The structure exists, however, for other hourly (or monthly/yearly) routines to be incorporated in the future. Associated with these algorithms are a number of default that are set according to standard soil, vegetation and climatic region characteristics. I will now briefly discuss the various process algorithms applied at the different levels of the spatial hierarchy. Further details on the specific algorithms used are included in Appendix A.

Zone Algorithms

Climate processing is done at the zone level of the hierarchy. A number of climate variables can be optionally included as base station input. If these variables are not available from the base station, they are estimated within RHESSys. These optional climate inputs may be obtained either through measured data or from other external models. Precipitation and minimum and maximum daily temperatures are the only required inputs. Optional climate inputs are listed in Table 1.1.

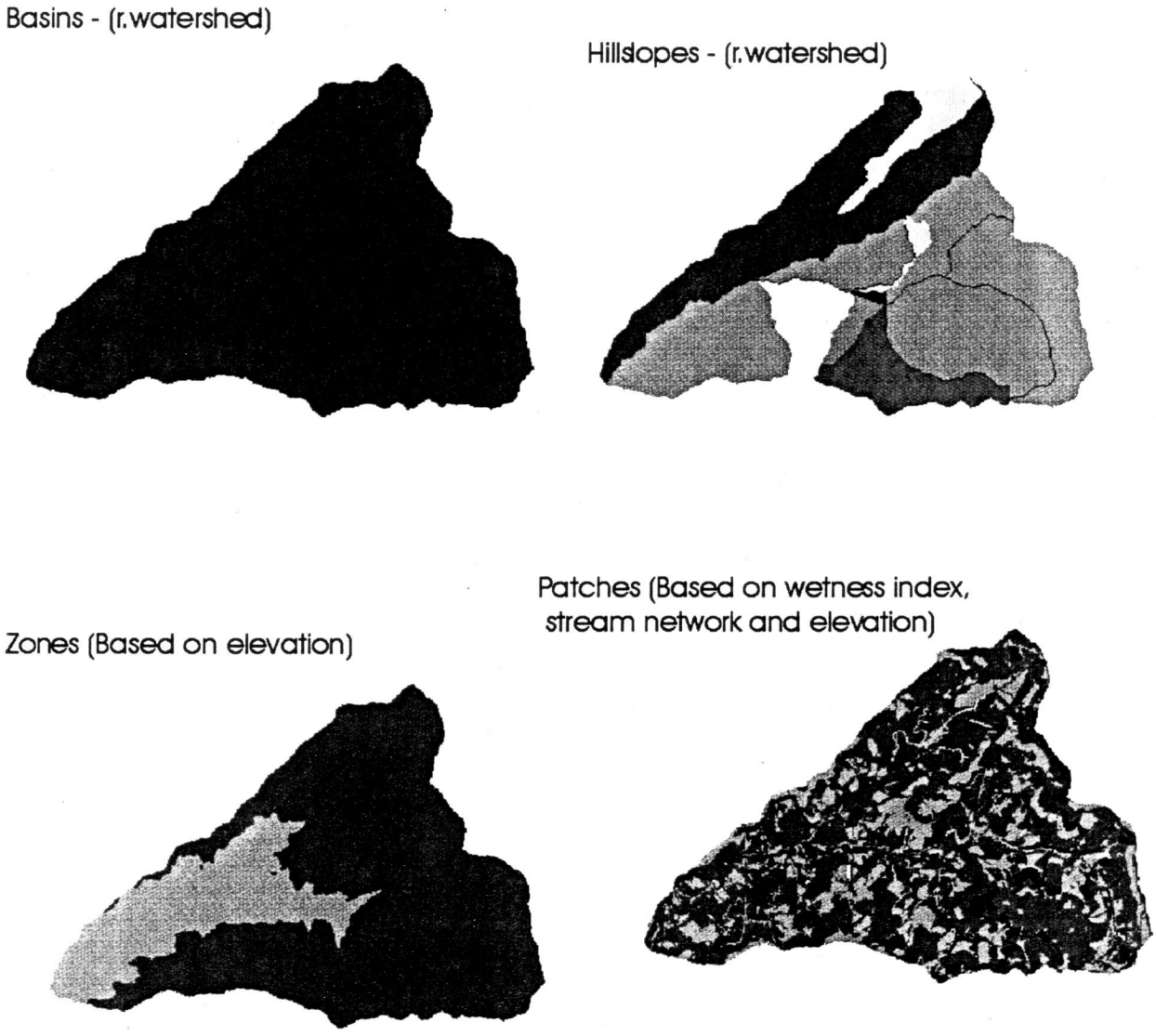

Figure 1.6: H.J.Andrews watershed spatial partitioning – Basins and hillslopes derived using GRASS r.watershed routine; Zones derived from DEM; Patches dervied from a wetness index image, a stream network and DEM.

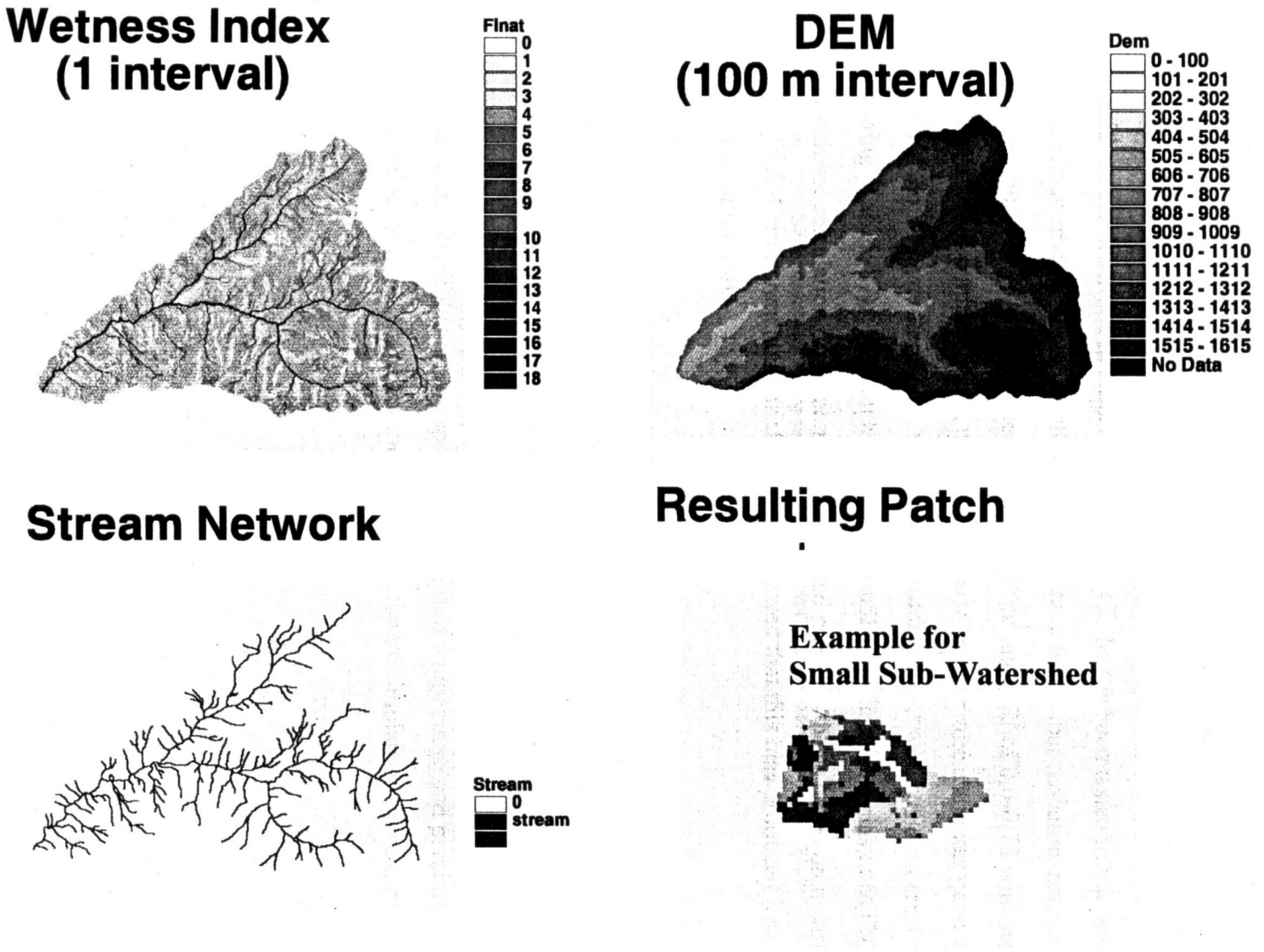

Figure 1.7: Derivation of patch partitioning for H.J.Andrews Watershed – an overlay of a unit interval wetness index, 100m DEM and Stream Network image

Radiation, if it is not input directly, is estimated using MTN_CLIM (Running et al., 1987) which adjusts a monthly incoming solar radiation flux based upon slope, aspect and elevation. Hourly radiation is calculated for both diffuse and direct radiative fluxes taking into account east and west horizon angles. PAR, if it is not input, is calculated as a fixed ratio of short-wave radiation. Hourly values are summed to give daily radiation values. Specific algorithms are described in Appendix A. MTN_CLIM has been tested in numerous mountainous environments. Application in Montana found that radiation estimates gave an average slope of 0.75 with an intercept of $100 W/m^2$ and a R^2 of 0.6-0.78 with standard error $< 100 Wm^2$ when compared with measured values. Temperature estimates gave an average slope of 0.85 with an intercept of <2C and a R^2 of 0.88-0.92 with standard error < 0.5 C (Running et al., 1987). Although the less than unit slope implies a bias in MTN_CLIM estimations, calculation of evapotranspiration and photosynthesis based on measured and MTN_CLIM environmental variables above showed that this bias produced less than a 5% error in resulting fluxes.

Precipitation and temperature are adjusted using topographically defined lapse rates, again following the MTN_CLIM logic. The model assumes an increase in precipitation and decrease in temperature with elevation due to orographic effects. In many situations, however, this model will not apply i.e. temperature inversions, regional convective storms. In these cases, RHESSys allows spatial coverages of temperature and precipitation fields, derived from measured values or more detailed climate simulation, to be directly input.

Climate Input Sequence Name / File Extension	**Description**	**Units**
P	Precipitation (rain + snow) * required	Meters
T_{min}	minimum daily temperature * required	°C
T_{max}	maximum daily temperature * required	°C
Day_{sec}	daylight length	Sec
P_{dur}	duration of daily rainfall	Hours
LAI_scalar	zone and seasonal scaling of LAI. This parameter can be used to simulate within season growth by multiplying current lai by a daily scalar value	Unitless
L	incoming longwave radiation	W / (meters^2)
K_{direct}	incoming direct shortwave radiation	Kj / (meters^2)
$K_{diffuse}$	incoming diffuse shortwave radiation	Kj / (meters^2)
$PAR_{diffuse}$	incoming direct PAR radiation	Kj / (meters^2)
PAR_{direct}	incoming diffuse PAR radiation	Kj / (meters^2)
Rh	relative humidity	Range (0-1)
T_{day}	mean daytime temperature	°C
$T_{nightmax}$	night time temperature at sundown (used for soil heat flux)	°C
T_{soil}	soil temperature	°C
Vpd	vapor pressure deficit	Pa
v	wind speed	Meters/ sec.

Table 1.1: Required and optional climate inputs to RHESSys

Patch Algorithms

Vertical soil moisture processes are modeled at the patch level. The soil column consists of two variable depth layers - an unsaturated zone and a saturated zone. The boundary between the saturated and unsaturated zone is defined by the saturation deficit (s). As shown in Figure 1.4, vertical soil moisture processes include snowmelt, infiltration, capillary rise, exfiltration and drainage from the unsaturated to the saturated soil moisture layer. Within the soil column, both hydraulic conductivity and porosity are assumed to decay exponentially with depth. Beven (1984) gives evidence for an exponential decay in hydraulic conductivity. Evidence for the form of porosity decay is discussed in Kirkby (1997). The shapes of these curves are key parameters in the hydrologic component of the model. Clapp and Hornberger (1978) or vanGenuchten and Nielsen (1985) relationships are used to determine soil moisture characteristics within the profile. Snowmelt processing is done using a modification to a simple degree day model to include melt due to radiation developed by Coughlan and Running (1997). Coughlan and Running (1997) show that this simple model can be used to adequately show linkages between forest cover, topography and snow melt processes although errors for daily predictions of snow water equivalent at some sites could be as high as 20%. In RHESSys, daily melt due to advection from rainfall is also included.

Hillslope Algorithms

Horizontal (spatial) soil moisture and runoff redistribution are organized at the hillslope level, although changes to local soil moisture values occur at the patch level. Soil moisture redistribution through saturated throughflow and associated runoff production can be modeled using either the implicit model, TOPMODEL, or via the explicit routing model which is a modification of the DHSVM approach. Further details on both of these approaches and their relative sensitivity to error and parameterization are given in Appendix A and in Chapter 2. Both approaches are executed at the end of the day, following vertical soil moisture updates.

Stream Processing

Streams and roads are treated as unique objects in the explicit routing routine. At present, any flow produced from a stream patch is assumed to leave the basin during the current time step. The explicit routing routine must also estimate subsurface and overland flow produced by a stream patch. Chapter 3 of this document discusses this issue and shows that the hydrologic response may be quite sensitive to near stream hydrologic representation. To explore this sensitivity, RHESSys considers several different representations of hydrologic characteristics that control flow into the stream.

Flow from a particular patch is a function of the current soil moisture conditions, the gradient and the transmissivity of the patch. In the case of a stream, which is often at a sub-grid scale resolution, the gradient may be difficult to infer. For an incised stream, for example, the local gradient to the stream may be much steeper than the overall patch gradient. For stream patches, it is this local gradient which produces drainage from the patch. In the current version of RHESSys we explore 4 options for computing this gradient:

- A constant value for all stream patches
- The local patch gradient
- A value taken from a random distribution
- The flowpath gradient upslope from the stream

Chapter 3 describes these options in more detail.

In addition to estimation of gradient, flow width to the stream must also be estimated. In the current version, flow width is assumed to be 2 * the stream length within the patch. Pre-processing in RHESSys, however, also permits a scaling or calibration of transmissivity. In this case, calibration of transmissivity can be used to artificially adjust for either the gradient or the flow width associated with stream patches similar to the method described by Francini et al. (1996).

Road patches

Roads have been shown to alter the routing of both overland and subsurface throughflow (Wemple et al., 1996). Road culverts produce channelized flow, which in some cases can connect directly to the stream and effectively extend the stream drainage network. Flow in road culverts is produced from two sources a) runoff from the road surface and b) interception of subsurface routing by the road cut bank. Once flow has entered the road ditches and culverts, it can then be redirected in several different ways. At present we model the re-routing of saturated subsurface throughflow and overland flow by roads following the conceptual model developed by Wemple et al. (1996). Further details on this approach are given in Chapter 4 and in Appendix A. Studies also show that additional infiltration excess runoff is produced by lower infiltration capacities associated with road surfaces (i.e. Luce and Cundy, 1994). This process can be implemented in the current version by changing the hydraulic conductivity associated with patches containing roads.

Canopy Strata Algorithms

Figure 1.5 shows the hydrologic processes modeled at the canopy level. Carbon sequestration and respiration is also calculated for each photosynthetically active canopy layer. Canopy layers are processed sequentially according to height. Radiation, wind and rain or snow throughfall are attenuated as they are absorbed/intercepted by each successive canopy layer. Evaporation of intercepted water and transpiration is also computed, along with intermediate quantities such as canopy conductance. Feedback between soil moisture and plant processes such as transpiration and photosynthesis is incorporated through a single model of stomatal physiology following Thornton (1998). Similarly both evapotranspiration and photosynthesis are controlled by available radiation, temperature, vapour pressure deficit and aerodynamic resistance at each canopy layer. Much of the logic of the canopy algorithms follows that of the BIOME_BGC model. In simulations using BIOME_BGC across a climatic gradient in Oregon, Running (1994) suggests that the canopy model i.e. estimates of evapotranspiration and photosynthesis, will be most sensitive to leaf area index, soil water availability and maximum canopy conductance. Resulting estimates of primary

production for these sites gave an R^2 of 0.82. Again specific algorithms are given in Appendix A.

Interface Design

Associated with the RHESSys simulation are a number of interface programs, which organize input data into the format required by the simulation model. These include a standard GIS-based terrain partitioning programs and RHESSys specific programs that derive landscape representation from GIS images and establish connectivity between spatial units. As part of this research, a prototype GIS interface for RHESSys was developed.

RHESSys is implemented in C, as a command line driven simulation. As illustrated in Figure 1.8, key inputs into RHESSys include:

1. A description (worldfile) of the landscape representation and initial state variables associated with each instance of the spatial hierarchy (i.e. basins, hillslopes, zones etc.). Because of the length and spatial complexity incorporated in this description, a GIS based program was developed to generate this file. A description of this interface can be found in the RHESSys User's Manual (Tague et al, 1998).

2. A flow table describes connectivity between patches within a hillslope when the explicit routing approach is used to modeling distributed hydrology. The flow table is also generated automatically prior to running the main RHESSys simulation and is described in more detail in the RHESSys User's Manual (Tague et al., 1998).

3. The TEC file describes the timing and nature of temporal events, which will occur during the course of the simulation i.e. disturbances such as forest harvesting or road construction. Temporal events refer to events that initiate a change in landscape state variables or parameterization or a new processes in the simulation sequence. Several spin up years are typically run prior to output or disturbance events to remove transient behavior due to initialization.

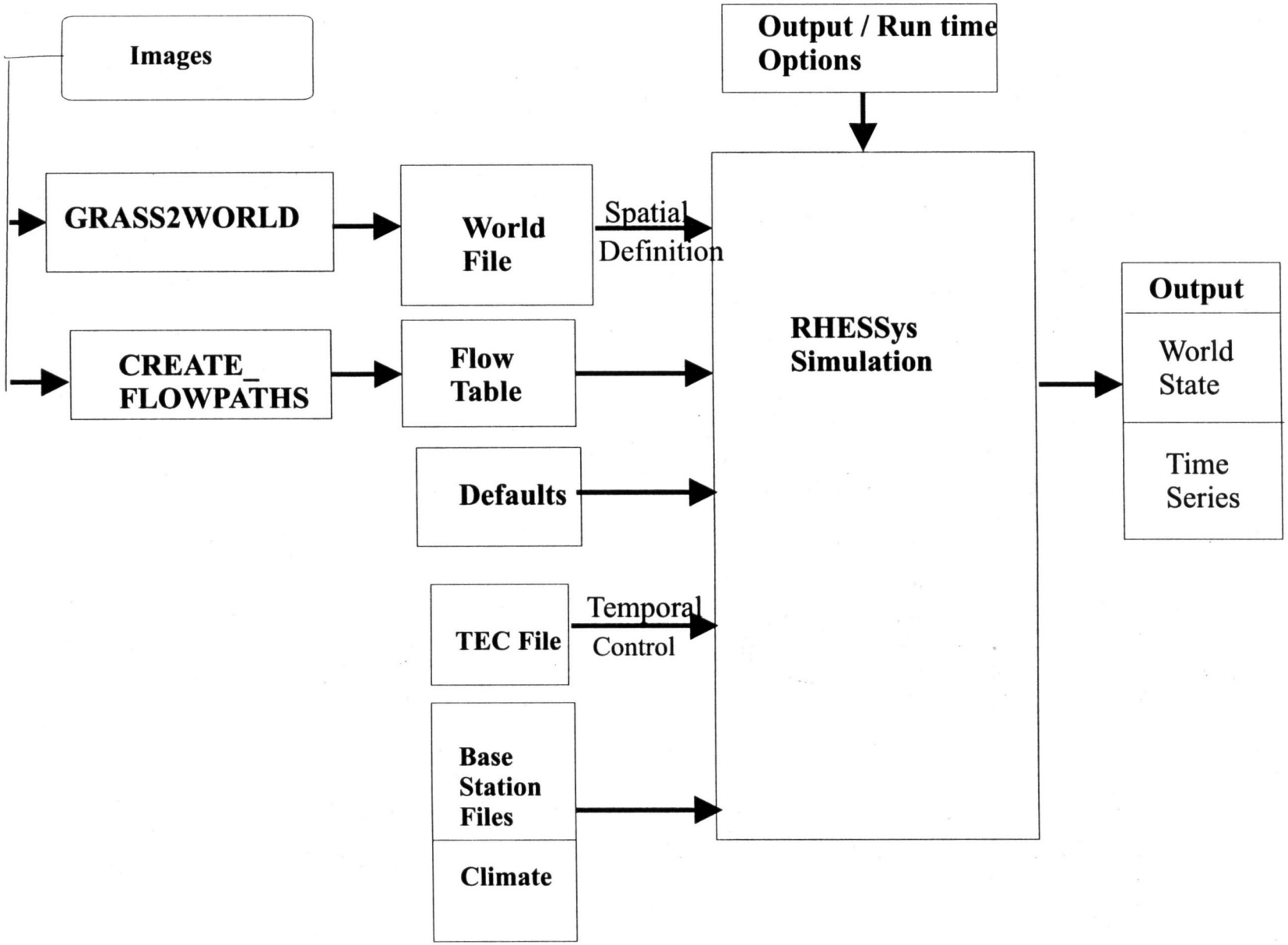

Figure 1.8: RHESSys Framework showing preprocessing, inputs and outputs

4. Climate inputs include both time series inputs of specific climate variables and descriptions of each climate station used in the simulation. Each zone in the spatial hierarchy is associated with a particular base station.

5. Default files are associated with each level of the spatial hierarchy. Canopy stratum default would be associated with specific vegetation types such as a conifer or a grass. Default files associated with patches would be associated with specific soil types such as sandy loam or clay.

Implementation and Future Development

This current version of RHESSys is implemented using an object oriented approach to facilitate the substitution of different process algorithms. All of the processes as well as input/output routines are contained in separate procedures with appropriate names. This allows for relatively easy modification of specific process algorithms. Data structures are similarly defined and named in order to maintain clarity about the level of the spatially hierarchy associated with a specific algorithm. As discussed above, RHESSys execution occurs as a sequence of temporal events which facilitates the implementation of disturbances such as forest harvesting and road construction.

The object oriented approach and hierarchical landscape representation are also designed to facilitate future RHESSys development. Structures exist to allow for the incorporation of canopy growth models and for the development of sub-daily time step models for certain processes such as infiltration. Object oriented landscape representation will also facilitate the implementation of different land covers such as those found in urban areas. Hillslope level organization of drainage and particularly the implementation of roads as mechanisms by which flow can be redirected serve as a foundation for implementation of other man-made controls on flow paths ways such as sewers. Future work with RHESSys will explore these issues. In this document, the behavior and sensitivity of the existing approach is explored, with particular emphasis on the hydrologic modeling components of RHESSys.

References

Band, L.E., 1989. Automating topographic and ecounit extraction from mountainous, forested area, *Artificial Intelligence in Natural Resources*, **3**,1-11.

Band, L.E. 1993. Effect of land surface representation on forest water and carbon budgets. *Journal of Hydrology*, **150**, 749-772.

Band, L.E. P.Patterson, R.R. Nemani, and S.W.Running. 1993. Forest ecosystem processes at the watershed scale: incorporating hillslope hydrology. *Agriculture Forest Meteorology* **63**: 93-126.

Band, L., Peterson, D., Running, S., Coughlan, J., Lammers, R., Dungan, J., Nemani, R. 1991. "Forest ecosystem processes at the watershed scale: basis for distributed simulation", *Ecological Modeling*, **56**, 171-196.

Band, L.E., R. Vertessey and R.B. Lammers, 1995. The effect of different terrain representation schemes and resolution on simulated watershed processes. *Zeitschrift fur Geomorphologie, Suppl-Bd.* **101**, p.187- 199.

Beven, K.J. 1984. Infiltration into a class of vertically nonuniform soils, *Hydro. Sci. J.*, **29**:4, 425-434.

Beven, K and Kirkby, M. 1979. "A physically-based variable contributing area model of basin hydrology, *Hydrologic Science Bulletin*, **24**, 43-69

Clapp,R., Hornberger,G. 1978. 'Empirical equations for some soil hydraulic properties', *Wat. Resour. Res*, **14**, 601-604.

Creed., I.E., Band, L.E. 1998. Exploring similarity in the export behavior of nitrate-H from forested catchments: A mechanistic modeling approach,
Wat. Resour. Res., **34**, 3079-3093.

Coughlan, J.C. and Running, S.W. 1997. 'Regional ecosystem simulation: A general model for simulating snow accumulation and melt in mountainous terrain', *Landscape Ecology* **12**, 119-136.

Francini, M., Wendling, J., Obled, Ch., and Todini, E. 1996. Some note about the TOPMODEL sensitivity to basin topography, *J. of Hydrol.*, 1975, 293-338.

Kirkby, M. 1997. TOPMODEL:a personal view, *Hydrol. Proc.*, 11:9, 1087-1099.

Lammers, R.L, and Band, L.E. 1990, Automating object description of drainage basin", *Computers in Geoscience*, **16**:6,787-810.

Lammers, R.B, Band, L.E. Band C. Tague 1997. Scaling water and carbon budgets to regional extents: Simulation approach. in, *SEB Seminar Series --- Scaling Up*, P. Van Gardingen, ed., Cambridge University Press, Cambridge, 295-317.

Luce, C.H., and Cundy, T.W. 1994. Parameter identification for a runoff model for forest roads. *Wat. Resour. Res*, **4**:1057-1069.

Mackay, D. and Band, L. 1997. "Forest ecosystem processes at the watershed scale: dynamic coupling of distributed hydrology and canopy growth",
Hydrol. Proc., **11**, 197-1217.

Rosentrater, L. 1997 'The thermal climate of the H.J.Andrews Experimental Forest, Oregon", MSc Thesis, Department of Geography, University of Oregon.

Running, S. 1994. Testing FOREST-BGC ecosystem process simulations across a climatic gradient in Oregon. *Ecol. Applic.*, **42**, 238-247.

Running, S., Coughlan, J. 1988. A general model of forest ecosystem processes for regional applications: Hydrologic balance, canopy gas exchange and primary production processes, Ecological Modeling, **42**, 125-154.

Running, S., Hunt, E.R. 1993. Generalization of a forest ecosystem process model for other biomes, BIOME-BGC, and an application for global-scale models, *in Scaling processes between leaf and landscape levels*, ed. J.R. Ehleringer and C. Fields, Academic Press, 141-158.

Running, S., Nemani, R., Hungerfored, R. 1987.Extrapolation of synoptic meteorological data in mountainous terrain and its use for simulating forest evapotranspiration and photosynthesis, *Can.J.For.Res*, **17**:472-483.

Tague, C. L., Fernandes, R. and Band, L.E., 1998. RHESSys 4.6: User Manual.

Thornton, P. 1998. Regional ecosystem simulation: combining surface and satellite based observations to study linkages between terrestrial energy and mass budgets, P.h.D thesis, University of Montana (Missoula), School of Forestry, 280pp.

VanGenuchten, M.T. and Nielsen, D.R., 1985. On describing and predicting the hydraulic properties of unsaturated soils, *Annal Geophys.*, 3: 615-628.

Wemple, B.C., Jones, J.A., Grant, G.E. 1996. Channel network extension by logging roads in two basins, Western Cascades, Oregon, *Wat. Resour. Bull.*, **32**:6, 1195-1207.

White, J. D. and S.W. Running 1994. 'Testing scale dependent assumptions in regional ecosystem simulations', *J. of Veg. Science*, **5**, 687-702.

Wigmosta, M., Vail, L., Lettenmaier, D. 1994. 'Distributed hydrology-vegetation model for complex terrain', *Wat. Resour. Res*, **30:6**, 1665-1679.

Chapter 2: Evaluating Explicit and Implicit Routing for Catchment Scale Models of Forest Hydrology

Preface

In using hydro-ecological models the scale of landscape representation is an important issue particularly in representing drainage organization. Drainage organization occurs at multiple scales from soil processes such as macropore flow that occur at scales of less than a meter to the pattern of river drainage at the landscape (or tens to thousands of kms) scale. The issue of spatial representation or aggregation is closely coupled with the problem of available data and to a lesser extent computational feasibility. A related issue is the problem of generalizing from intensively monitored catchments to populations of watersheds within a region where data sets are typically much sparser. Information to drive models of fine-scale processes is rarely available at larger regional scales. A key issue in modeling is, therefore, given available data resolution, how to represent hydrologic processes and any spatial-temporal variability in the landscape features that control them. In modeling forest hydrology at the hillslope to drainage basin scale, where management takes place, these issues must be addressed. The first two sections of this document will focus specifically on this issue of the adequacy of the algorithms and landscape representation used to model hillslope drainage organization.

Different GIS based hydro-ecological simulation models address the problem of representing distributed hydrology in different ways. At one end of the spectrum, there are point models or bucket models that use mean or effective values of hydrologic variables such as soil moisture capacity and do not consider the effects of lateral redistribution. These models emphasize vertical soil moisture processes and are applicable in flatter areas where redistribution and the spatially variability of hydrologic characteristics at the watershed scale are relatively small. In more spatially variable landscapes, however, representing hydrologic

parameters by mean values can reduce the predictability of the hydrologic response (Band, 1993; White and Running, 1994). At the other end of the spectrum are spatially distributed models, which explicitly model flow in a three dimensional landscape using a Richard's Equation. These models, on the other hand, suffer from considerably greater computational complexity and input data requirements. Different approaches exist to simplifying the full three dimensional routing approach. Explicit two-dimensional routing models, such as the DHSVM (Wigmosta et al., 1994) approach discussed in the following paper, model lateral transport of saturated subsurface throughflow based on topographic gradients and soil transmissivity. An even simpler approach is the TOPMODEL approach, which represents spatial variability in soil moisture and runoff production via a statistical distribution. Both of these approaches can be linked with a vertical model of unsaturated soil moisture dynamics. In this next paper, I consider these two approaches to modeling spatially distributed soil moisture and runoff production and assess their utility, both in terms of input requirements and results for the test H.J.Andrews catchment. In addition, I illustrate and discuss issues related to the scaling and generalizing of these results to larger areas by considering the sensitivity to different landscape representations and to input error.

*paper submitted as Tague, C. and Band, L.E. , Evaluating Explicit and Implicit Routing for Catchment Scale Models of Forest Hydrology, *Hydrologic Processes*.

Abstract

This paper explores the implications of the method used to model the spatial distribution of soil moisture and runoff production. In applications such as modeling the landscape-scale effects of forest harvesting, interactions between soil moisture, runoff and ecological processes are important. Because climate, soil and canopy characteristics are spatially variable, both the pattern of soil moisture and the associated outflow must be represented in modeling these processes. This particular study addresses the implications of using different methodologies - implicit and explicit routing, to model lateral soil moisture re-distribution and spatially variable runoff production. The paper considers the tradeoffs between including computationally costly data requirements for explicit routing approaches, such as DHSVM, and reducing information about connectivity and hydrologic flowpaths in statistical approaches, such as TOPMODEL. Both approaches are incorporated into a physically based hydro-ecological model, RHESSys. Results illustrate that both approaches can be calibrated to achieve a reasonable fit between observed and modeled outflow. Calibrated values for effective watershed hydraulic conductivity are higher for the explicit routing approach, which illustrates differences between the two approaches in the representation of internal hillslope dynamics. The two approaches also differ in the resulting spatially distributed soil moisture. The explicit approach illustrates a seasonal shift in drainage organization from hillslope to more local control as climate goes from a winter wet to a summer dry period. The implicit approach maintains the same pattern of drainage organization throughout the season. The implicit approach is also more sensitive to random error in soil and topographic input information, particularly during the winter wet period. Comparison between the two approaches illustrates the advantage of the explicit routing approach, although the loss of computational efficiency associated with the explicit routing approach is noted. This paper also explores a related issue of using different strategies for partitioning the landscape used in modeling the spatial distribution of soil moisture and runoff production. In particular, the use of a non-grid based method of partitioning, based on indices of hydrologic similarity is introduced and shown to be comparable grid based partitioning. This study presents the results of calibration and application of these different approaches on a small forested

watershed in Western Oregon and discusses implications for representing distributed hydrology within the context of modeling forest ecosystem processes.

Introduction

Representing the distribution and lateral flux of soil water is a critical component of modeling hydrological and ecological processes and the impacts of disturbances such as forest harvesting. Watershed models used to assess and understand these impacts must consider the vertical and horizontal interactions between canopy structure and function and hydrologic processes including interception, evapotranspiration, surface and subsurface runoff production and streamflow. This paper examines the issue of representing lateral soil water flux on the behavior and sensitivity of a watershed hydro-ecological model in terms of runoff production and spatial patterns of soil water and key canopy processes. Two basic approaches have been implemented for this project. One approach is an explicit routing model based upon a modified form of the Distributed Hydrologic Soil and Vegetation Model, DHSVM (Wigmosta et al, 1994). The other is TOPMODEL (Beven and Kirkby, 1979), an implicit approach to modeling spatially variable soil moisture and runoff production. In comparing the explicit and implicit routing approaches, we are interested in the implications of (1) including information about connectivity and (2) maintaining a finer resolution of response and soil moisture variability during model simulations. This paper explores how the behavior of each approach influences the spatial and temporal dynamics of the model when only the subsurface routing scheme is varied and considers the relative sensitivity of each approach to error in input information. We also consider the role played by landscape representation, particularly in the explicit routing approach. We illustrate the potential for gaining flexibility and efficiency by adapting a grid-based routing scheme to allow the size and shape of modeling units to vary and incorporate information about local hydrologic characteristics.

The explicit and implicit routing approaches used in this study represent two basic approaches to modeling lateral soil moisture flux. Explicit routing approaches have been applied in models such as TOPOG (O'Loughlin, 1990), VSAS (Bernier, 1985), CLAWS (Duan, 1996) and DHSVM (Wigmosta *et al*, 1994), which explicitly transfer water between connected patches. These explicit routing models are generally applied over areas where sufficient information on the spatial variability of the topographic and soil parameters that

control water movement is available. In these situations, landscape representation, both in terms of the size and the shape of modeling units, can influence simulation results. The need for generalizing from intensely studied sites to broader landscapes with sparse data sets presents a problem for these explicit routing approaches. Fine resolution information, particularly with respect to soils, may not be readily available for large areas. At the same time, particularly in mountainous regions, high spatial variability within a watershed may preclude the use of averaged values (Band, 1993). This issue is also part of a more general scaling problem where the estimation and, ultimately, the meaning of parameters become problematic (Bloschl and Sivapalan, 1995; Beven, 1995).

Spatial variability in soil moisture can also be addressed implicitly using statistical distribution methods such as TOPMODEL (Beven and Kirkby, 1979) which distribute saturation deficit across a non-spatial distribution of hydrologic parameters within a catchment. Statistical methods can be thought of as providing a compromise between the processing intensive explicit routing methods and mean value or bucket model approaches. Statistical approaches use readily available topographic information to incorporate estimates of variability in hydrologic properties. Processing efficiency is much greater for these approaches in comparison with explicit routing methods but the information about connectivity between specific areas is lost. Estimation of the distribution of hydrologic parameters can be made from widely available topographic information. Previous work, however, has shown that the modeled streamflow response is sensitive to the resolution of the topographic information used to derive this distribution of hydrologic parameters (Bruneau *et al.* 1995; Wolock and Price, 1994; Zhang and Montgomery, 1994).

The implicit and explicit routing approaches, TOPMODEL and the modified DHSVM and associated landscape representation strategies are implemented within the Regional Hydrologic Ecosystem Simulation System, RHESSys, which provides the same canopy process model, vertical soil moisture flux model and climate forcing for each approach. Comparisons are done for a small catchment within the H.J.Andrews watershed, which is a Long-Term Ecological Research (LTER) site. This site represents an area with considerable field data within a larger region where understanding the impacts of forest harvesting is an

important issue. Part of the impetus for this comparison is to assess the potential for using modeling to assess impacts in similar areas within a broader region where less information may be available for model parameterization and calibration.

Representation of Distributed Soil Moisture

TOPMODEL (implicit routing)

TOPMODEL is a statistically based approach that distributes water based on an index of hydrologic similarity. TOPMODEL has been incorporated into biophysical models such as RHESSys (Band *et al*, 1993), TOPLATS (Famiglietti and Wood, 1994) and several soil-vegetation-atmosphere transfer models, SVATS, such as Troch *et al*, (1996).
TOPMODEL distributes a mean soil moisture deficit (s) based on a local wetness index

$$w_i = \ln\{\frac{aT_i}{T_o \tan\beta}\} \qquad [1]$$

where T_i and T_o are local and mean hillslope saturated soil transmissivity, respectively, tan β is local slope and a is upslope contributing area. Soil transmissivity is calculated as:

$$T = \int_{s_i}^{\infty} K_o e^{(-\frac{s}{m})} ds \qquad [2]$$

where K_o is saturated hydraulic conductivity at surface, s is depth expressed as a saturation deficit, s_i is local saturation deficit and m is a soil parameter, which scales hydraulic conductivity with depth .

Local saturation deficit is computed as

$$s_i = \bar{s} + m\{\bar{\lambda} - w_i\} \qquad [3]$$

where λ is mean wetness index value, s_i and s are local and mean hillslope saturation deficit.

TOPMODEL generates saturation excess flow for rain falling on areas with local saturation deficit, s_i, less than or equal to zero. In RHESSys, saturation excess flow is not routed but assumed to reach the stream within a daily time step. TOPMODEL also computes a catchment level base flow, which is subtracted from the mean catchment saturation deficit. Baseflow, q_b,is calculated as:

$$q_b = e^{(-\bar{\lambda})} e^{(\frac{-\bar{s}}{m})} \qquad [4]$$

where, λ is the mean hillslope wetness index calculated as:

$$\bar{\lambda} = \int (\ln(\frac{a_i T_i}{To \tan \beta_i})) \qquad [5]$$

Assumptions and Limitations

As a statistically based approach, TOPMODEL represents a simplified method that has been applied and tested against observed outflow responses for a number of catchments as reviewed by Beven (1997). TOPMODEL relationships are based on the assumption that saturated hydraulic conductivity varies exponentially with depth; that water table gradients can be approximated by local topographic slope, that recharge is spatially invariant and that steady state flux is achieved within the modeling time step. The implications of these assumptions have been explored by comparing TOPMODEL predictions of saturation deficits with observed values in several catchments. In general, TOPMODEL assumptions appear to hold in humid catchments with rolling topography. Several studies, (Barling et al, 1993; Woods et al, 1997; Ostendorf and Mandersheid, 1997) have found that the assumption of steady state flux is violated during drier periods. In drier periods, areas of the catchment may become disconnected and thus, the extent of effective contributing areas becomes more local. In contrast, the TOPMODEL assumptions lead to a constant distribution of contributing area and a constant catchment water table shape through time. Moore and

Thompson (1996) found a reasonable correspondence with the TOPMODEL steady state assumption for a humid mountainous catchment in British Columbia but found a weak correspondence between saturation deficit and TOPMODEL predictions. This catchment has similar topographic and climatic conditions to the H.J.Andrews catchment used in this study. Moore and Thompson (1996) attribute the difference in model and predicted saturation deficit to sensitivity to input errors in both soil parameters and topographic information. Burt and Butcher (1986) also cite the potential for error due to soil properties including situations where the TOPMODEL calculation of soil transmissivity may not be valid (i.e. where hydraulic conductivity does not decay exponentially with depth or where hysteretic behavior occurs). In very shallow soil layers, for example, the assumption of exponential decay with depth may not be valid. TOPMODEL has been modified to consider other relationships (i.e. parabolic and linear) between hydraulic conductivity and depth (Ambroise et al., 1996). However, the model will always be sensitive to the appropriateness of the chosen relationship.

Explicit Routing

The explicit routing approach used in this study is a modified form of an algorithm used in the DHSVM model (Wigmosta *et al*, 1994). The DHSVM routing scheme assumes that throughflow from pixel a to pixel b is given as

$$q(t)_{a,b} = \{ T(t)_{a,b} \tan\beta_{a.b}\omega_{a.b} \} \qquad (6)$$

where ω is flow width, tan β is local slope, and T is soil transmissivity as defined above for the TOPMODEL implementation. Flow widths are assumed to be 0.5 * grid size for cardinal directions and 0.354 * grid size for diagonal directions, after Quinn *et al* (1991). The original DHSVM approach is adapted and generalized here to consider irregularly shaped patches, such that the usual use of grid cells can be considered a special case. The advantage of this broader definition of a patch is that it allows the landscape to be represented as ecologically meaningful units rather than arbitrary grid cells. Previous studies such as Band et al. (1991)

have shown that definition of modeling units based upon ecological properties can reduce within unit variance. This definition of patches also provides a method for increasing efficiency by reducing the number of modeling units, without losing important spatial information.

An assumption of exponential decay of hydraulic conductivity with depth is also used with the explicit routing approach. As with TOPMODEL, however, this profile can be replaced with alternative functions including a prescribed bedrock/soil interface.

The partitioning of the landscape into patches used in this paper is described below. Throughflow is calculated using (6) where flow widths are summed along the shared boundary between adjacent patches. Connectivity between patches is derived using automated GIS-based routines. Neighbors and associated perimeters between irregular areas or patches are extracted from an image of defined patches. Slopes are calculated based on the mean elevation for each patch area.

Routing between patches permits multiple flow paths. Stream patches, defined by an imposed stream network, however, are restricted to single, steepest descent pathways. This is consistent with Quinn *et al* (1991) who observe that multiple flow methods yield more realistic patterns in hillslopes but single flow paths are more appropriate for stream flow routing. There is no catchment level baseflow defined for the explicit routing scheme since baseflow contributions are assumed to be produced directly from saturation subsurface throughflow from patches adjacent to the stream network.

Connectivity between patches is traversed to detect pits or circular flow. O'Callaghan and Mark (1984) note that actual pits are rarely observed in mountainous regions at the scales used in this study. Thus, pits are considered to be spurious products of the DEM or the alternative patch partitioning strategy. Pits are removed by redirecting flow going into the pit to the minimum elevation upslope patch which points to a receiving patch lower than the bottom patch in the pit. All patches in the pit are then assigned to point to this receiving patch. This method is similar to that employed by O'Callaghan and Mark (1984).

Figure 2.1 compares the landscape representation used in the explicit routing approach with TOPMODEL. The explicit routing approach removes the steady state assumption included in TOPMODEL and permits the shape of the water table to vary through time. This explicit routing scheme, however, makes similar assumptions about soil transmissivity and hydraulic gradients. Both models will, therefore, be sensitive to errors in soil hydraulic conductivity and topographic information. The inclusion of information about spatial connectivity between modeling units in the explicit routing approach may change the sensitivity to these errors relative to the TOPMODEL implementation.

Implementation and Partitioning Strategies

Both TOPMODEL and the explicit routing approach are incorporated into RHESSys (Regional Hydrologic Ecosystem Simulation System). RHESSys is an ecological modeling system which combines distributed flow modeling with an ecophysiological canopy model, based on BIOME_BGC (Running and Hunt, 1993) and a climate interpolation scheme based on MTN_CLIM (Running et al, 1987). These sub-models are combined within a GIS framework to allow for organized and efficient modeling of landscape systems. Outputs from RHESSys include both hydrologic and carbon fluxes at a daily time step. By incorporating both explicit and implicit approaches to modeling distributed hydrology into RHESSys, we control for all hydro-ecophysiological feedback and responses, such as evapotranspiration and unsaturated zone dynamics that do not vary between the two approaches. Similarly, climate forcing i.e. radiation, temperature and precipitation, does not vary between the two approaches. The different approaches are compared in terms of resulting runoff production and spatial pattern of soil moisture and evapotranspiration.

The TOPMODEL wetness index distribution can be derived from assumptions made about the shape of the catchment or computed from a DEM. In the former case, TOPMODEL can be run when detailed DEM information is not available. We chose the latter approach following Lammers *et al* (1997). Scaling in the TOPMODEL approach occurs by changing

Fully Distributed Approach Vs. Aspatial Distribution Approach

Explicit Routing
(i.e DHSVM)

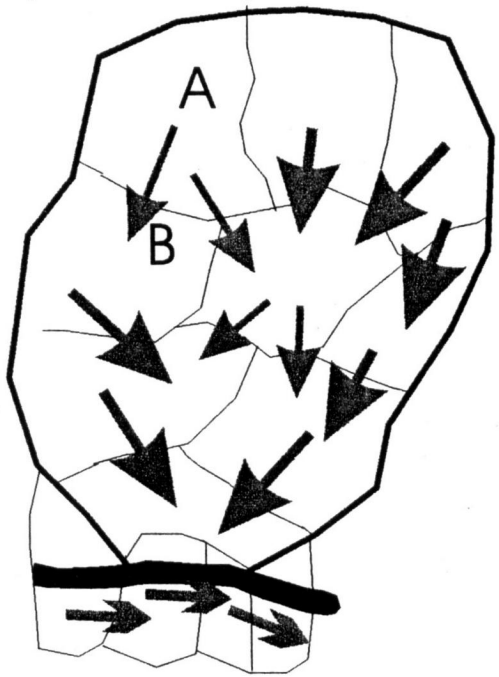

Statistically-Based
Methods
(i.e. TOPMODEL)

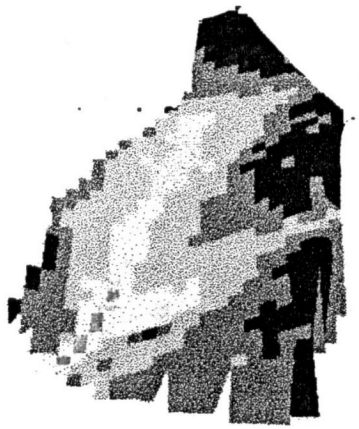

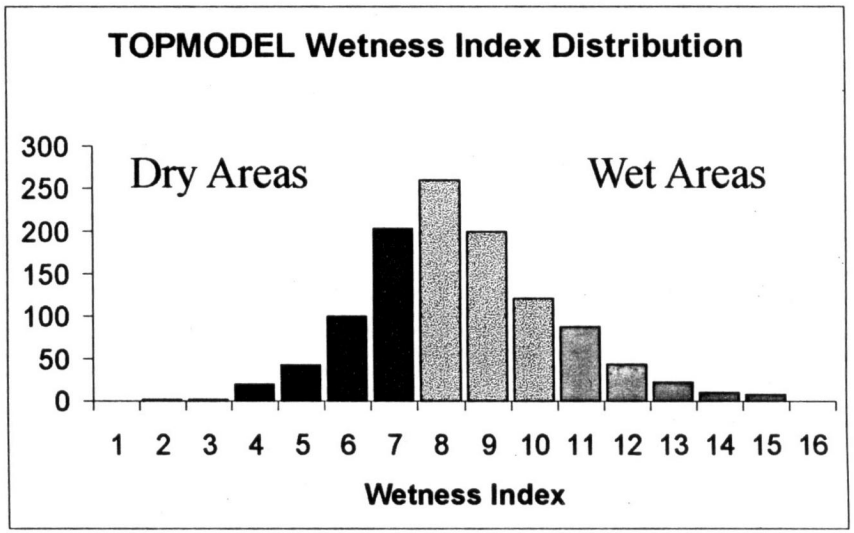

Figure 2.1: Comparison of landscape representation for explicit and implicit routing approaches – Explicit routing approach uses contiguous spatial patches; Implicit routing uses a statistical distribution of aspatial patch types.

the resolution of the underlying information that is used to generate the distribution of the wetness index.

For explicit routing, the resolution of modeling units is directly tied to the resolution of input information. In addition, because modeling units are spatially explicit, shape can be important. In order to investigate the implications of using variable-shaped patches, which include information about hydrologic organization, three different partitioning strategies are explored. The first is based on 30m DEM pixels (PR) and is used as the baseline of finer resolution grid-based information. We also consider two methods of reducing resolution: grid-based aggregation (SQ) and irregular-shaped, hydrologically defined patch aggregation (TR). Partitioning is implemented using an automated GIS-based scheme. The aggregation scheme for developing irregular patches uses landscape information to derive patches of similar soil moisture characteristics. Aggregation by TOPMODEL wetness interval (TR) is accomplished by using a connected component routine applied to a combination of the wetness index image and an image of 50m elevation intervals as shown in Figure 2.2. Explicit routing using patches defined by wetness indices can be thought of as a hybrid of TOPMODEL and explicit routing approaches. The hypothesis is that since the wetness index tends to denote areas of hydrologic similarity, routing between patches defined by the TOPMODEL wetness index will provide an efficient method of aggregation and minimize the loss of information due to aggregation. The 50m elevation intervals are included as an additional limitation on patch size.

Figure 2.3 illustrates the different partitioning strategies used for the explicit routing and for the TOPMODEL implicit routing approach. The number of effective modeling units with TOPMODEL is usually significantly smaller (<20 wetness intervals) and less variable with scale in comparison with the explicit routing approach, which requires 654 modeling units for the pixel based landscape representation for the 60ha study catchment. As shown in Figure 2.3, for the explicit routing approach, spatially explicit modeling units vary significantly in number and shape as a function of the partitioning strategy.

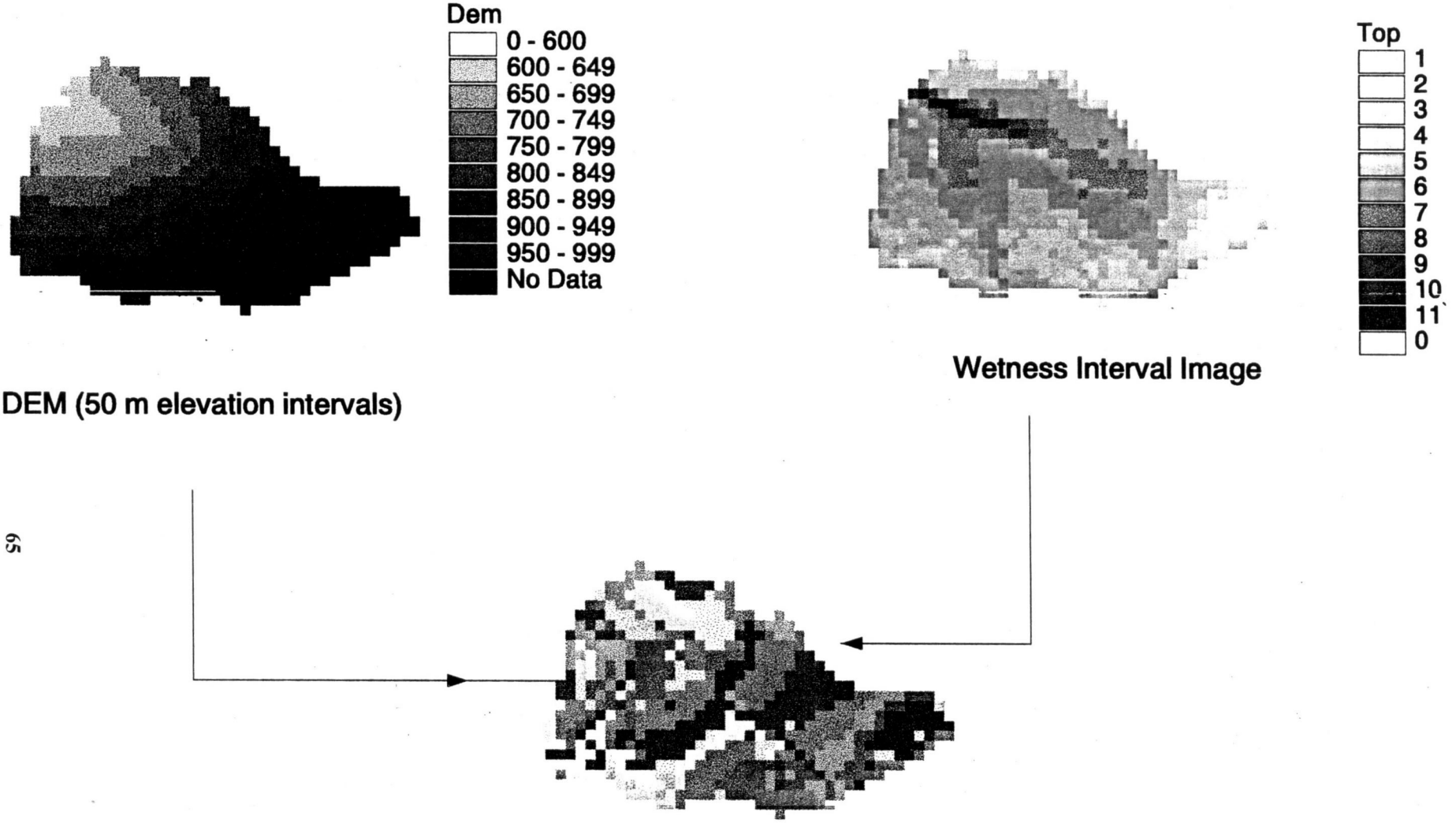

Figure 2.2: Construction of patches based on wetness index and DEM images

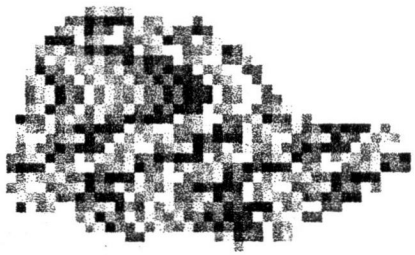

a) PR - Partitioning based on 30m pixels; highest resolution approach

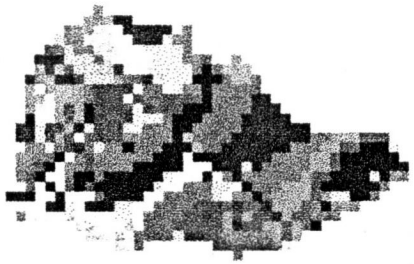

b) TR - Partitioning based on a combination of wetness index and 50m elevation intervals; spatially contiguous patches

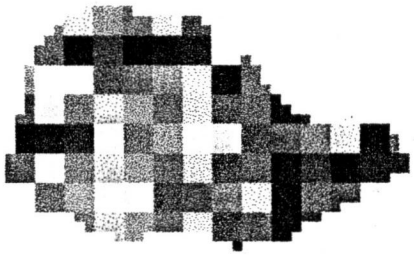

c) SQR - Partitioning based on 90m pixels

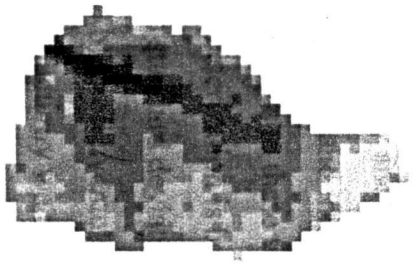

d) TOPMODEL Partitioning based on unit interval wetness intervals; with non-contiguous patches

Figure 2.3: Landscape Partitioning Strategies including a) 30m pixels, b) contiguous patches based on a wetness index image and a DEM, c) 90m pixerls and d) non contiguous patches based on a wetness index

Error Sensitivity

In addition to comparing the resulting model behavior for explicit and implicit routing, we also compare the implicit and explicit routing approaches in terms of their sensitivity to error in input information. Errors in the DEM model of topography and errors in soil information are the two main sources of error that occur for both explicit and implicit routing approaches. In order to test the relative sensitivity of the two approaches to these two sources of error, we perform several additional simulations in which parameterization is based on a) a DEM corrupted with Gaussian noise (with zero mean and a standard deviation,σ, equal to 5m. RMSE estimates for USGS 30m DEM is 7.5m.) and b) a soil hydraulic conductivity image corrupted with Gaussian noise. For soil hydraulic conductivity we test two scenarios. We consider a high noise case with zero mean and a standard deviation equal to 1/6 of the K_{sat} range (0.5 to 200 m/day) for the study watershed. A 50% variation illustrates results for a conservative estimate of conductivity variation at the patch scale. A 50% variation in K_{sat} is low in the context of local point variation in hydraulic conductivity. For larger patches, however, variation in effective and averaged conductivity should be lower. We also consider a low noise scenario with 1/30 of the K_{sat} range. Although calibration alters the mean catchment hydraulic conductivity parameters, it does not change the spatial distribution. Use of the corrupted soil hydraulic conductivity image permits testing of the effect of changing the spatial pattern of soil properties on hydrologic response and assess the robustness of the model for applications in other catchments with potentially less available information.

Parameterization and Calibration

The study site is a small 60h unlogged catchment, Watershed 2, in the H.J.Andrews Experimental Forest in the Western Cascade region of Oregon with an elevation range of 500-1000m. Climate in this region is characterized by warm, dry summers and cool, wet winters. Annual precipitation for years used for calibration and testing ranges from 1500 to

2300 mm. During the winter, climate in this basin is often at the threshold between rain and snow, where heavy rain, rain-on-snow and snowmelt are all common runoff and potential flood producing events. During the summer, precipitation is much lower, and the maintenance of low flows can become an important ecological issue.

Topographically, stream erosion, landsliding and glaciation have produced a steep and highly dissected landscape. Soils range from clay to sandy and gravelly loam. In general, soils are characterized by both high porosity and hydrologic conductivity due to the aggregated character of the soil material and in many areas a high stone content as a result of glacial or mass movement deposition (Ranken, 1974). Some areas, however, contain subsoils of lower porosity and permeability. Underlying bedrock is volcanic material from Oligocene-lower Miocene including basalts, tuffs and breccias. Solid bedrock in many areas is covered by a thick layer of weathered, unconsolidated material (Rothacher et al., 1967) which also facilitates rapid subsurface flow to the stream.

Watershed 2 is covered primarily by mature-old growth Douglas fir. Outflows for this basin, during the study period, range from 850-1300mm per year. Precipitation and temperature inputs are taken from a single base station within the catchment. Variation in incoming radiation with elevation and aspect is accounted for using MTN_CLIM logic (Running et al, 1987). Precipitation lapse rates with elevation are derived from PRISM (Daly et al, 1994). Use of PRISM and the density of climate stations (i.e. there are more than 6 climate stations within the H.J.Andrews Basin, including one within Watershed 2). allows the complex patterns of local precipitation to be accounted for. Temperature lapse rates were estimated by Rosentrater (1997) using the multiple climate stations available in the H.J.Andrews Basin to account for temperature inversions associated with this area, which improved the temperature interpolation associated with the MTN_CLIM approach. Since both routing approaches are implemented within the larger RHESSys simulation framework, both receive the same climate forcing, canopy coverage and soil distribution information.

Parameters for the two models of distributed hydrology are derived from a 30m DEM, and 30m soil texture maps derived from a 1:15000 soil survey map. Canopy information such as

estimated LAI, and ecophysiological parameters for Douglas Fir forests are assigned from literature values (Running, 1994; Jarvis and Leverenz, 1983). Calibration is done separately for the explicit routing and TOPMODEL approaches and for each of the different partitioning strategies. Calibration of the model applies a scale factor to the initial estimates for two soil parameters, m and K_{sat}, which together define soil transmissivity. The same scale factor is applied to the entire watershed so that calibration does not alter the initial spatial distribution of the soil parameters. The initial values for the specific soil parameters, m and hydraulic conductivity, K_{sat}, are derived from soil map information as described below. The initial values of m and K_{sat} fix the spatial distribution of relative transmissivity within the catchment. Other soil parameters, porosity, air entry pressure, and pore size index are not calibrated and are set based upon literature estimates, shown in Table 2.1, for different soil textures following Clapp and Hornberger (1978).

The different approaches are calibrated for 1988, a relatively wet year (annual pcp = 2319mm). Each approach is subsequently tested for 1987, which received less annual precipitation (1607mm) and 1986 that received a slightly larger amount (2427mm). Calibration maximizes the Nash Sutcliffe efficiency (Nash and Sutcliffe, 1970) for 1988.

To set initial parameters, the m parameter is estimated from point measurements by Rothacher et al (1967) of soil percolation rates taken for different soil depths (z) for a selection of soils with measured porosity, $\varphi = 0.5$, in the H.J.Andrews watershed as follows:

$$m = \varphi \cdot \frac{z}{\ln(\frac{K(z)}{K_o})}. \qquad (7)$$

The range of *m* is 0.05 to 0.2. In this implementation of TOPMODEL and the explicit routing scheme, soil depth is indirectly defined by m, since m controls the depth of active hydraulic conductivity.

Dryness (1969) found that hydraulic conductivity and soil-water-holding capacity of soils in the H.J.Andrews watershed can be directly related to the stone content in the soil. Stone content was able to account for 80-90 percent of the variation in soil moisture storage between different soils. He also found that soil series classifications did not yield a significant relationship with storage capacity. Maps of distributed soil series and soil texture are available for the H.J.Andrews catchment. Saturated hydraulic conductivity, K_{sat}, in this region are very high with some measured soil sample values above 150 m / day. They are also highly variable, thus it is not realistic to derive K_{sat} from a limited number of point samples. As an approximation, hydraulic conductivity for the most common texture (gravelly loam) is estimated from average values for different soil samples described in Dryness (1969). Values for other texture classes are extrapolated from that of gravelly loam using typical relationships between texture and conductivity following Clapp and Hornberger (1978). We also assume greater stone content and assigned a higher conductivity for most matric soils. Thus, the variation between conductivity in rocky vs soils such as loams which typically have a much lower conductivity, is reduced. Table 2.1 shows the values used.

Calibration of hydraulic transmissivity through m and K_{sat} is necessary in both the explicit and implicit routing approaches because measurement of soil matrix hydraulic conductivity does not completely determine resistance to water flux given by the soil. The inclusion of macro-pores for example can increase the rate at which water is able to move through the soil. Calibration estimates an effective conductivity that includes these and pathways involved in controlling the movement of water through a patch.

Soil Texture Class	K_{sat} (m / day)	Porosity	Air Entry Pressure (m)	Pore Size Index	Areal % of W2
Rocky	200	0.45	0.001	0.28	3.77
Cobbly	160	0.5	0.007	0.26	1.98
Cobbly Loam	140	0.5	0.005	0.25	0.81
Gravel_Sandy Loam	100	0.6	0.008	0.22	35.99
Gravelly Loam	80	0.6	0.01	0.2	45.18
Gravel_Clay Loam	60	0.6	0.012	0.18	5.84
Light Clay Loam	0.1	0.5	0.1	0.12	1.18
Poorly Drained	0.01	0.5	0.12	0.1	5.27

Table 2.1: Hydrologic parameter values for specific soil classifications in Watershed 2, derived from field measurements (Dryness, 1969) and typical literature values (Clapp and Hornberger, 1978)

Results

Explicit vs. Implicit Routing – Watershed Outflow and Evapotranspiration

Final calibrated values of m and K_{sat} for the TOPMODEL and the explicit routing scheme are shown in Table 2.2. Calibration differences between the different partitioning strategies used for explicit routing are small. Calibrated effective transmissivity for the explicit routing implementations are substantially larger than those used for TOPMODEL (i.e. both m and K_{sat} calibrated values are larger for routing). The larger transmissivities required for explicit routing may reflect the sensitivity of explicit routing to local conditions. The explicit flowpaths associated with routing, for example, may create areas of convergence with

relatively low initial hydrologic connectivity, which force required transmissivities to increase. In addition, the explicit routing model allows for re-infiltration of surface runoff generated by upslope patches, which may slow the transport of hillslope water to the stream. In comparison, the TOPMODEL approach assumes that all surface runoff generated reaches the stream within the daily time step. TOPMODEL also implicitly assumes full connectivity, as pointed out by Barling et al. (1993). Transmissivity values for the TOPMODEL method are, therefore, more representative of hillslope level organization rather than local patch flowpaths and thus are less susceptible to local irregularities in the pattern of flow.

TOPMODEL also differs in its approach to modeling baseflow. In TOPMODEL, baseflow is calculated on a catchment wide basis. Local flow connectivity is assumed in TOPMODEL and does not need to be maintained for baseflow to occur. Thus, baseflow can partially reflect deeper groundwater sources, organized at the hillslope level. For explicit routing, baseflow is implemented as a local process in patches adjacent to the stream and is therefore sensitive to seasonal changes in local connectivity patterns and to the representation of local areas near to the stream. Baseflow, in this case, is a function of local gradient and transmissivity of the streamside patch. The assumption that the local hydrologic gradient is parallel to topographic slope, as is assumed in this explicit routing implementation, may not be appropriate for baseflow production from streamside areas. In these areas, low topographic gradients may increase the importance of matric-potential in controlling flow. The larger calibrated transmissivity associated with the explicit routing approach may therefore compensate for an under-estimation of local streamside hydraulic gradient.

Method	M	Mean K_s (m/day)	Efficiency	# of patches	Patch shape	Average patch size
$PR_{Routing}$	0.17	120	0.68	507	Grid (30m)	900 m^2
$TR_{Routing}$	0.17	150	0.60	113	Irregular	4000 m^2
$SQ_{Routing}$	0.17	150	0.58	92	Grid (90m)	5000 m^2
TOPMODEL	0.09	6	0.47	9 (wetness intervals)	Non-spatial	Non-contiguous areas

Table 2.2: Comparison between different routing strategies and landscape representation approaches showing calibration results and the number of spatial patches

High calibrated transmissivity values for the explicit routing approach also suggest that, even for this more physically based method, m and K are essentially tuning parameters and do not necessarily reflect observable soil properties although they may reflect dominant physical processes. The high calibrated transmissivities may reflect the importance of macropore flow over soil matrix properties in controlling the hydrologic response. Calibrated transmissivity is therefore an effective value rather than a reflection of soil based measurements. Initial soil texture classifications, however, do indicate hillslope scale (i.e. between 30m patches) relative variability in hydrologic properties.

Table 2.3 shows predicted ET and annual outflow values for the different approaches. In all cases the total annual outflow is under-estimated by both explicit and implicit approaches, although under-prediction is greater for the TOPMODEL approach. This could suggest an over-estimation of ET. Error in the estimation of leaf area index inputs based on stand age and literature rather than measured values may result in lower ET values.

	1986		1987		1988	
Method	ET (mm)	Outflow (mm)	ET (mm)	Outflow (mm)	ET (mm)	Outflow (mm)
$PR_{Routing}$	914	1455	728	861	816	1442
$TR_{Routing}$	908	1463	718	873	810	1446
$SQ_{Routing}$	913	1452	728	869	815	1437
TOP.	1061	1312	855	844	1083	1133
Observed		1641		979		1539

Table 2.3: Evapotranspiration and Outflow for 1986 to 1988; Comparison between implicit and explicit routing schemes and landscape partitioning strategies.

Figure 2.4 compares 3-day averaged winter (January-March) and summer (June-September) observed outflow with TOPMODEL implicit routing and the explicit routing implementation, using the full pixel landscape partitioning. Both models capture the pattern of response fairly well. The explicit routing implementation produces flashier hydrograph responses than the corresponding TOPMODEL response. In general explicit routing implementations tend to overestimate the rate of peak flow decay. TOPMODEL tends to underestimate it. Both models overestimate summer baseflow as shown in Table 2.4 below. TOPMODEL also shows a consistent delay in stormflow response.

TOPMODEL and the explicit routing implementation are applied in RHESSys with the same canopy evapotranspiration, snowmelt, and vertical unsaturated flow sub-models. Thus, differences between them reflect differences in rates of transport through hillslope to the stream network. The rapid of peak flow decay associated with the explicit routing approach reflects its corresponding large values for calibrated transmissivity. High transmissivities are required for the explicit routing implementation in order to match peak flows. The Nash Sutcliffe calibration metric used in this study is more sensitive to high flows and thus, matching peak flows may occur at the expense of adequately modeling recession periods. In the case of explicit routing, high rates of peak flow decay may also reflect the lack of explicit treatment of baseflow. In TOPMODEL, however, the assumption that the water table follows

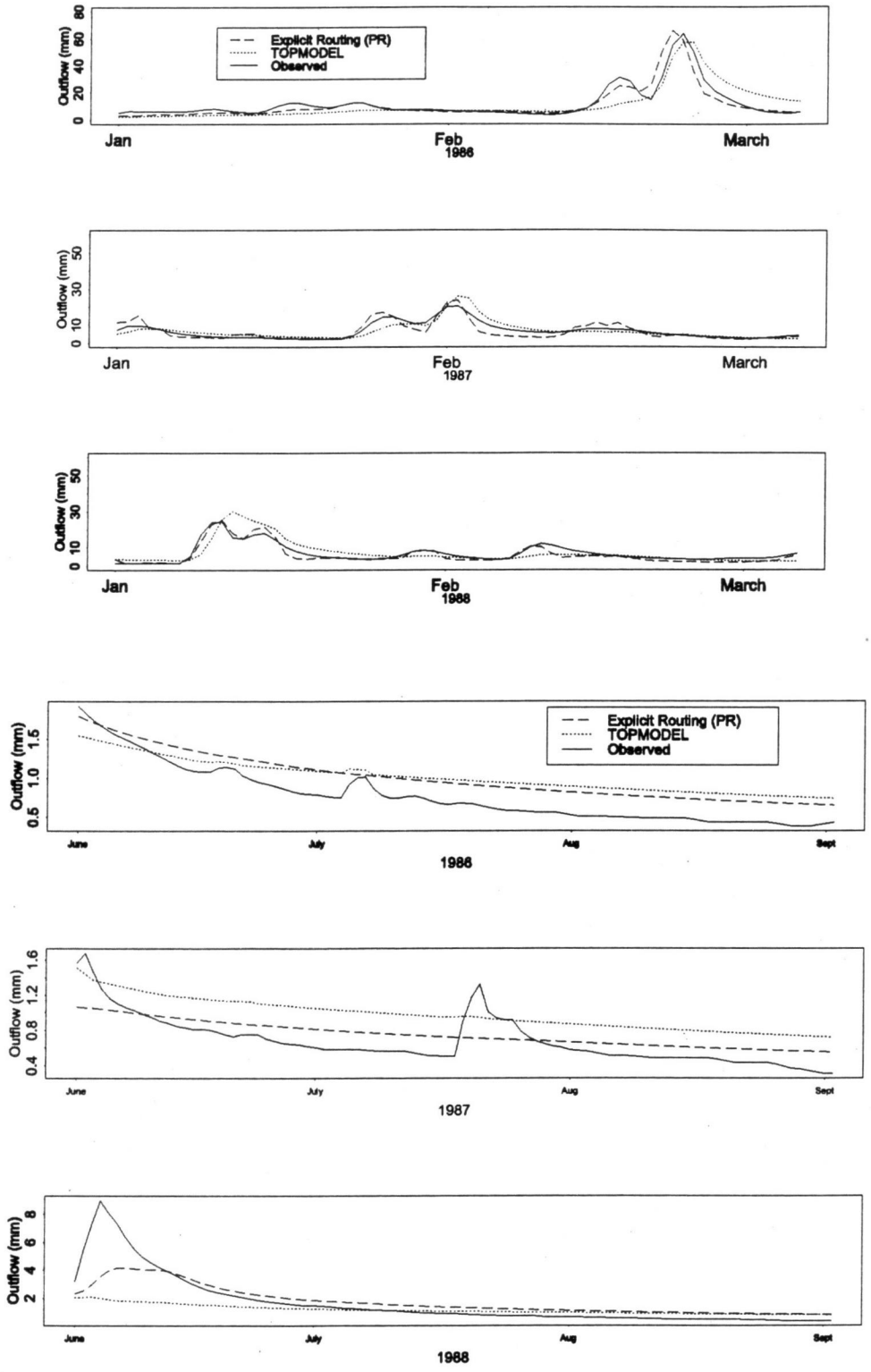

Figure 2.4: Watershed 2 Outflow, Comparison between simulations using TOPMODEL (implicit routing) , explicit routing and observed outflow for 1986-1988.

the shape of the topography may create a limitation in calibrating to fit both peak and recession flow conditions.

The difficulty in matching the pattern of peak flow, recession and low flow periods in both approaches may be related to the calibration of effective conductivity. As noted above, hydrologic conductivity is typically higher than hydrologic conductivity recorded for particular soils. This effective value takes into account other processes involved in the transport of water in addition to matric flow through soil pores. In particular, pipe flow and preferential flow paths through root channels, bedrock fractures etc, are included in this effective conductivity. McDonnell (1990) notes that access to these preferential flow paths, however, may change with soil water content. In this case, calibrated effective conductivity will vary over time. To account for this effect, an extension of the model and calibration procedure to include both matric and preferential flow paths as separate processes would be necessary. In this case the density of macropores across the hillslope and as a function of saturation deficit would need to be estimated. Again assumptions could be made based on relationships between macropore density and catenary sequence or soil type. In the current model, the assumption of a temporally constant effective conductivity independent of conditions controlling macropore flow may prevent matching both peak and recession flow periods. Similarly, the assumption that conductivity decays exponentially with depth may not always be valid and may limit the ability of the model to capture all flow dynamics. Modeling of spatially variable profile functions, however, would considerably increase the complexity of the model and the degree of required parameterization.

	June-Sept. Outflow (mm)			June-Sept. Evapotranspiration (mm)		
Method	**1986**	**1987**	**1988**	**1986**	**1987**	**1988**
$PR_{Routing}$	95	70	164	189	163	238
$TR_{Routing}$	96	71	175	184	156	233
$SQ_{Routing}$	95	69	164	187	163	238
TOPMODEL	95	90	110	124	155	374
Observed	72	63	155			

Table 2.4: Summer outflow comparison between observed and modeled outflow using TOPMODEL and explicit routing with various landscape partitioning strategies

Both approaches are also sensitive to other sources of error in the model including error in climate input, vegetation characteristics, snowmelt modeling and errors in measured outflow. As notes above, error in the estimation of vegetation parameters, particularly LAI, may account for the overall (annual) under-estimation of outflow response. During low flow periods, small values may be within the precision of weir measurements. In addition there are now available estimates of deeper groundwater flow that lost from the catchment but not measured by the weir. We assume these to be negligible.

Given the high density of climate station input in this region, error in climate input should also be small. One exception to this is the estimation of snow versus rainfall events based upon temperature. (The meteorology station records do not distinguish between precipitation falling as rain or snow – we assume the snow/rain proportion varies linearly from –3C (all snow) to 3C (all rain)). Watershed 2 can often contain the boundary between precipitation falling as rain and as snow and, therefore, presents a complex pattern of rain vs. snow across the landscape and over time. Similarly snowmelt processes in this region are complex, including rain on snow melt events. Considerable error, particularly in the timing of snowmelt processes can be expected given the daily time step snowmelt model used in

RHESSys. Although watershed 2 does not maintain a seasonal snowpack in the winter; daily to weekly snow accumulation events and subsequent melt can alter the timing and characteristics of runoff events over a period of several days. Snowfall events during the simulation period were few. However, modeling of these few events may account for some of the differences between observed and modeled hydrographs. In addition, the daily time step used in the model means that differences in rainfall intensities are ignored. Seasonal differences in rainfall intensities i.e. high intensity convective storms during the summer vs low intensity rainfall during winter months, may account for some differences in summer vs winter hydrograph responses. Given the high infiltration capacities associated with humid forest soils, however, these effects are likely to be small.

Explicit vs. Implicit Routing – Spatially distributed soil moisture patterns

Differences between implicit and explicit routing approaches are more dramatically reflected by the pattern of soil moisture distribution. The pattern of soil moisture deficit across Watershed 2 is shown in Figures 2.5 and 2.6 for two sample days - January 10 1988 and August 20 1988, a wet and dry day respectively. TOPMODEL and the explicit routing patterns match fairly well for the wet day. For the dry day, however, TOPMODEL predicts a significantly different pattern of saturated area for the same amount of generated outflow (0.4 mm). Comparing upland and streamside soil moistures during wet and dry periods depicts a clear and potentially field testable difference between the two approaches. TOPMODEL assumes a constant difference between upland and bottomland areas while routing predicts an increased divergence during drier summer periods.

TOPMODEL is restricted by the assumption that the water table follows the shape of the topography. Routing, on the other hand, permits water table shape to vary over the hillslope and throughout the year. Figure 2.7 illustrates saturation deficit along a single flowpath, from the ridge to the stream, for both January and August. The pattern of saturation deficit illustrates the invariance in water table shape associated with TOPMODEL and the ability of the explicit routing model to capture the production of local, subcatchment patterns of soil moisture.

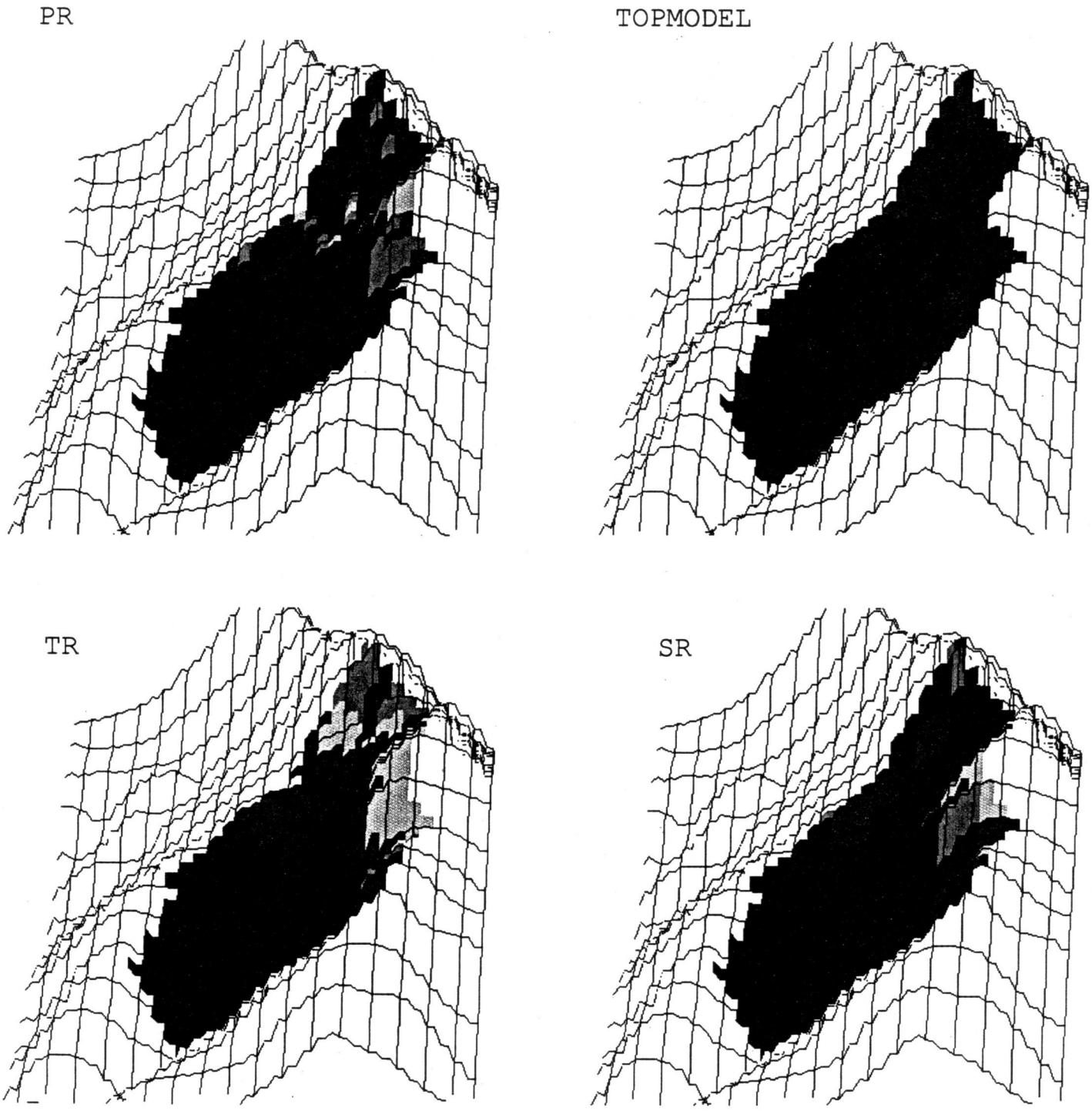

Figure 2.5: Soil Moisture Distribution for January 10, 1998 - Comparison between different routing approaches.

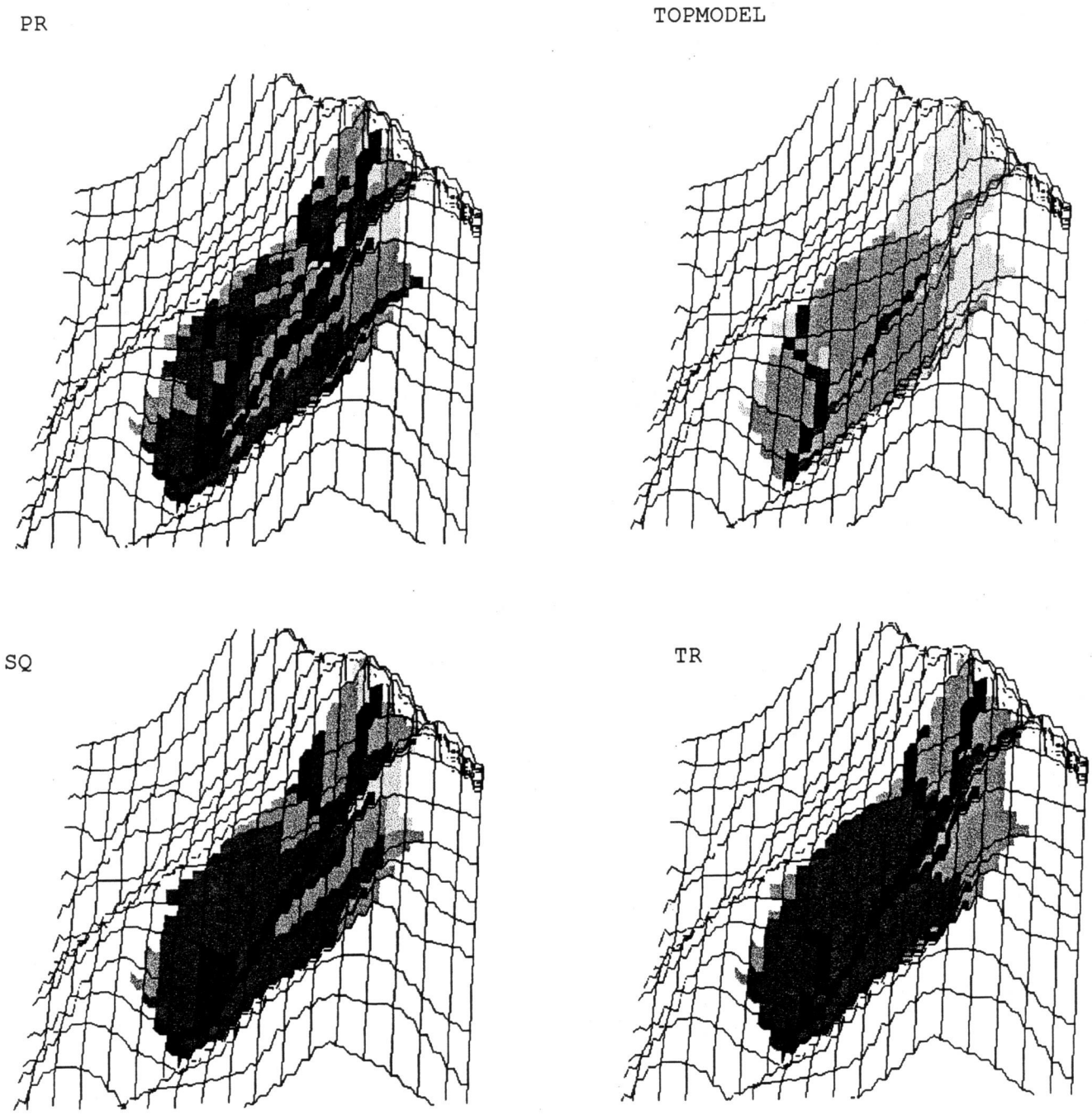

Figure 2.6: Soil Moisture Distribution for August 20, 1998 - Comparison between different routing approaches

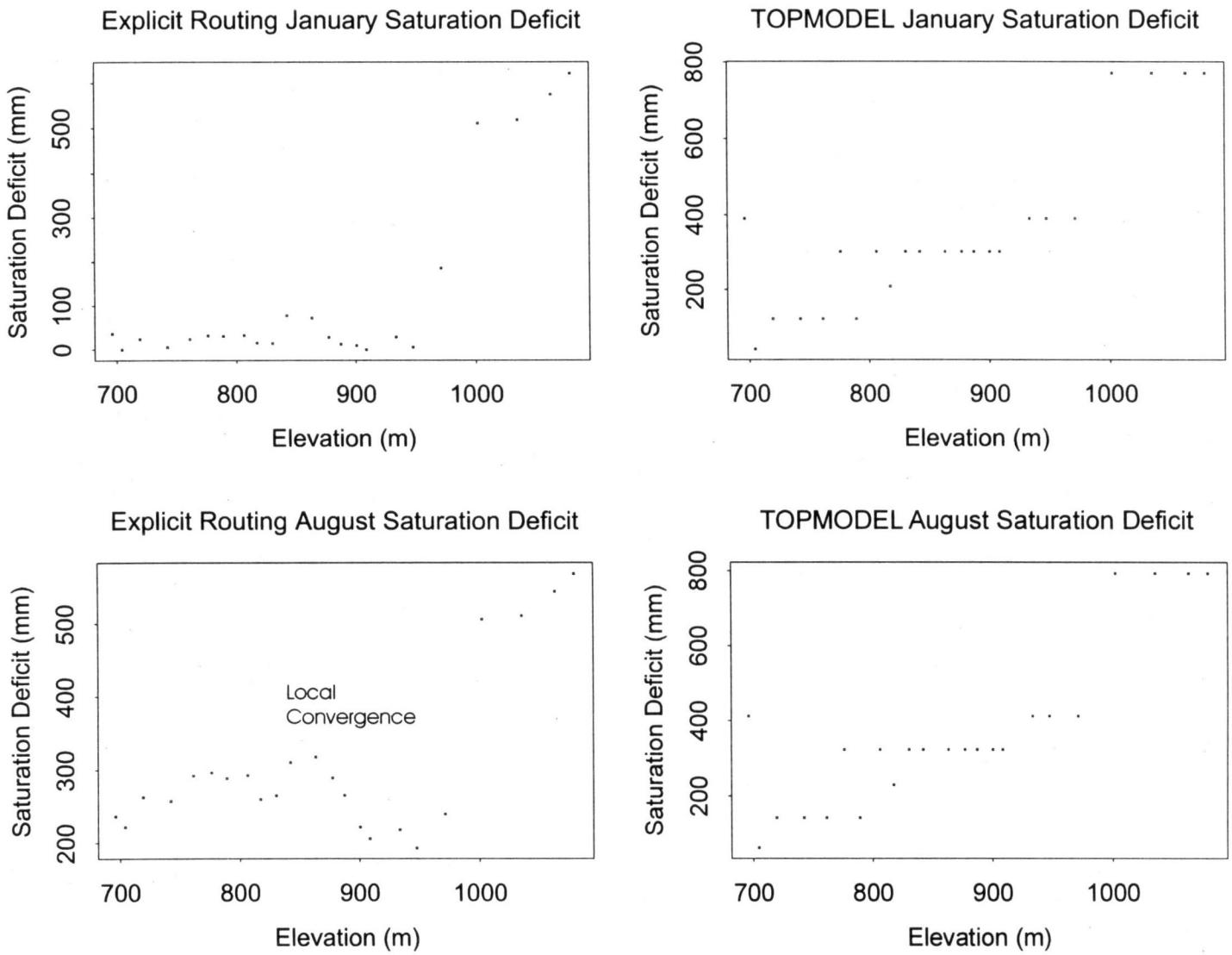

Figure 2.7 Saturation deficit along a single flow path - from stream to ridge. Comparison between TOPMODEL and explicit routing for January (wet period) and August (dry period).

Monthly soil moisture patterns, shown in Figure 2.8, further illustrate the dynamic versus static spatial variation in soil moisture associated with explicit routing and TOPMODEL respectively, for a single hillslope within Watershed 2. With explicit routing there is a decreased spatial variability in saturation deficit as the hillslope goes from the dry period in August to nearly full saturation in January. TOPMODEL, however, does not capture this pattern to the same extent.

Over the year, these differences in soil moisture patterns between the two approaches result in a higher annual evapotranspiration (Table 2.2) for TOPMODEL. In local areas, however, evapotranspiration from the explicit routing can be higher, due to the greater variability in soil moisture associated with the explicit routing approach. This suggests that the explicit routing approach offers a significant improvement over the TOPMODEL approach in terms of the ability to capture the seasonal dynamics that control the pattern of soil moisture. These differences influence secondary prediction of ecologically important variables such as evapotranspiration and by extension, productivity.

Sensitivity Analysis

The inclusion of connectivity information in the explicit routing approach permits the pattern of local contributing area to vary seasonally. Including this information, however, may make the explicit routing approach more sensitive to errors in both soil and topographic input information. To explore this issue, we examine the sensitivity of both approaches to input information degraded by Gaussian noise. Table 2.5 shows the sensitivity to error in input topographic and soil information for the two approaches. Sensitivity is expressed as both a mean daily relative and a mean daily absolute difference in simulated outflow obtained using initial and corrupted input information. Figure 2.9 illustrates the daily relative difference between simulations with degraded and original input information for both routing approaches.

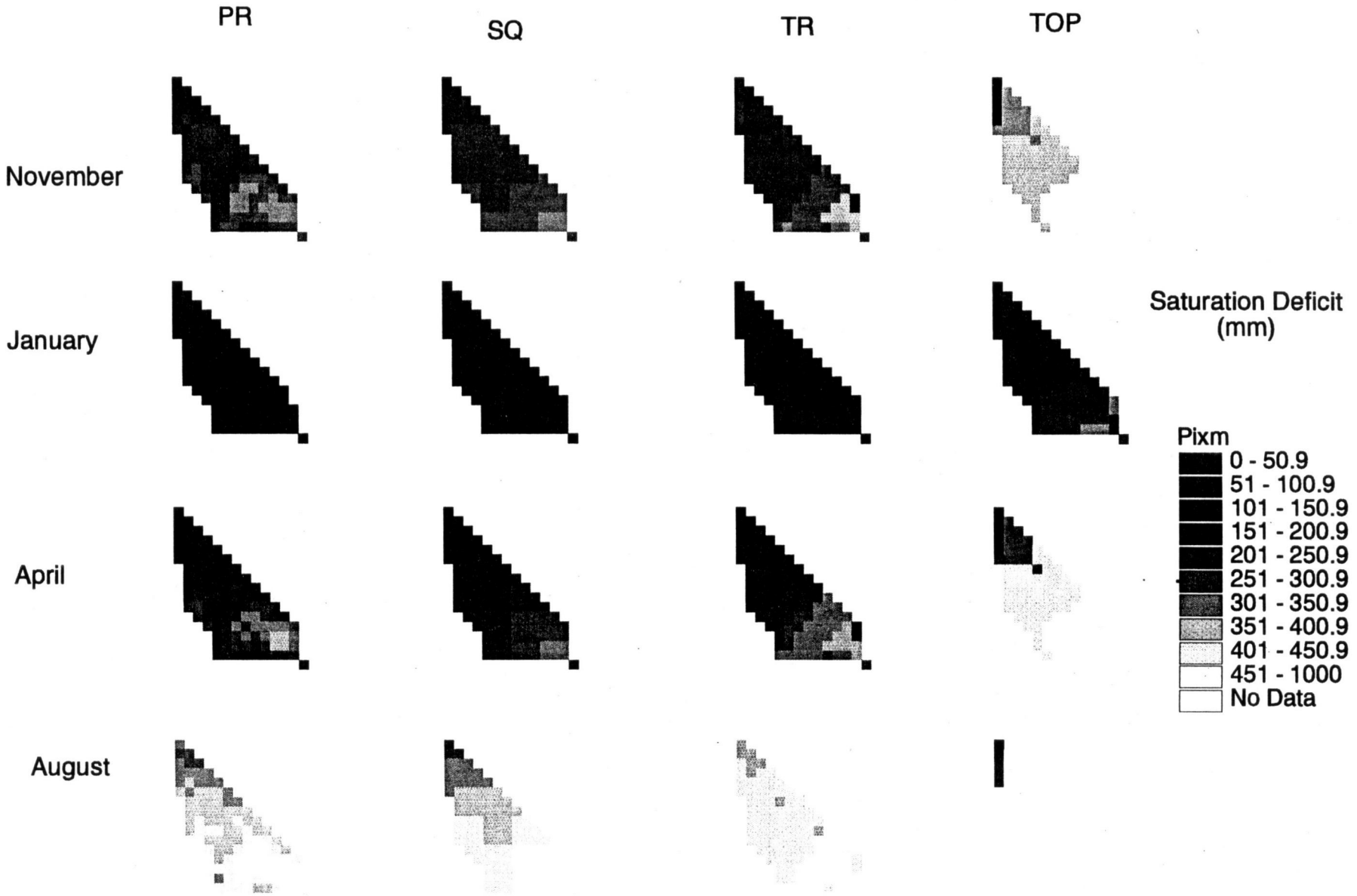

Figure 2.8: Spatially Distributed Mean Monthly Saturation Deficits for a small sub-hillslope in Watershed 2: Comparison between different routing methods

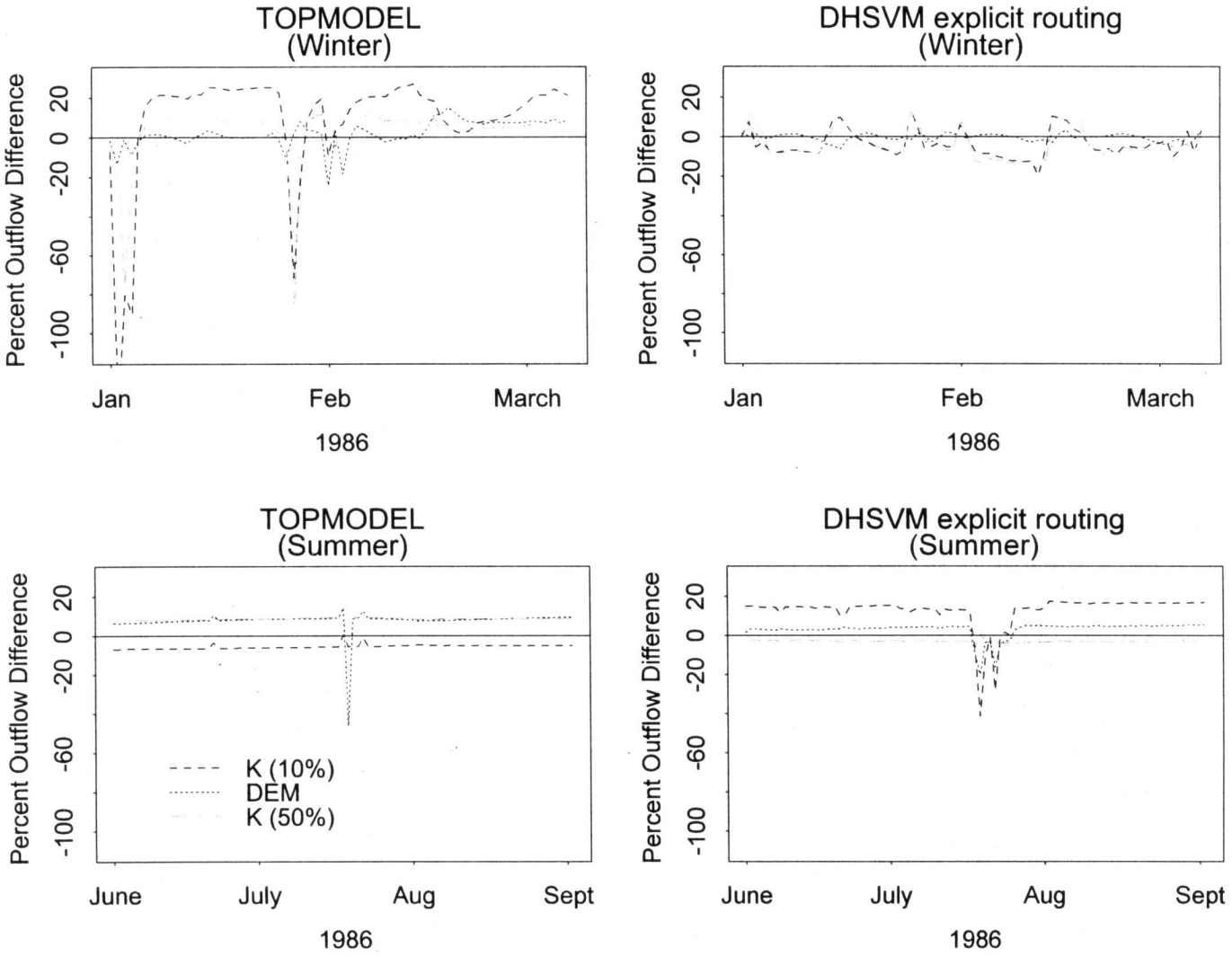

Figure 2.9: Sensitivity to simulated outflow to error (Gaussian noise) in input DEM and in the spatial pattern of soil hydraulic conductivity, K_{sat}; Comparison between TOPMODEL and the explicit routing approach (PR). Random Gaussian noise (μ=0; σ= 5m) is applied to the DEM; Two scenarios of Gaussian noise are applied to the Ksat image: low (μ=0; σ= 8m/day) and high (μ=0; σ= 40m/day) noise scenarios

Daily relative difference is defined as:

$$\sum_{all\ i} \frac{(q_i - q_{obs_i})}{q_{obs_i}} \quad (8)$$

where q_i is modeled outflow, q_{obs} is observed outflow.

Both TOPMODEL and the explicit routing approach result in a reasonably small (< 5%) mean difference in outflow for both the DEM noise and for noise in soil K_{sat} inputs. In terms of absolute error, TOPMODEL is significantly more sensitive to noise in both the input DEM and input K_{sat} information. In terms of relative error, TOPMODEL and the explicit routing approach show a more similar response, although TOPMODEL is still more sensitive.

However, on a daily basis, explicit routing shows relative differences in outflow for corrupted simulations of up to 20% during the summer, shown in Figure 2.9. TOPMODEL simulations show differences of up to 150% during the winter. Figure 2.9 also illustrates that TOPMODEL sensitivity to noise is more pronounced during peak flow events. Explicit routing shows a somewhat greater sensitivity to noise during summer low flow events and a consistent reduction in summer outflow response with the addition of noise for both K_{sat} and DEM inputs. In the case of TOPMODEL, the impacts of Gaussian noise are reflected in changes in the distribution of the wetness index as shown in Figure 2.10. Runoff production in TOPMODEL is particularly sensitive to the upper tail of this distribution, which expands with the addition of noise for the DEM and high noise K_{sat} scenarios. For TOPMODEL, changes in the distribution of the wetness index translate local noise into catchment scale changes, since baseflow is computed at the hillslope rather than individual patch scale. In the explicit routing approach, the effects of noise remain more local. In the winter, flow is dominated by the catchment scale topographically driven flow patterns and the effects of noise on the explicit routing approach remain small and unbiased. In summer, however, subcatchment flow networks play a relatively stronger role in runoff production and the addition of noise disrupts the dominant local runoff production mechanisms.

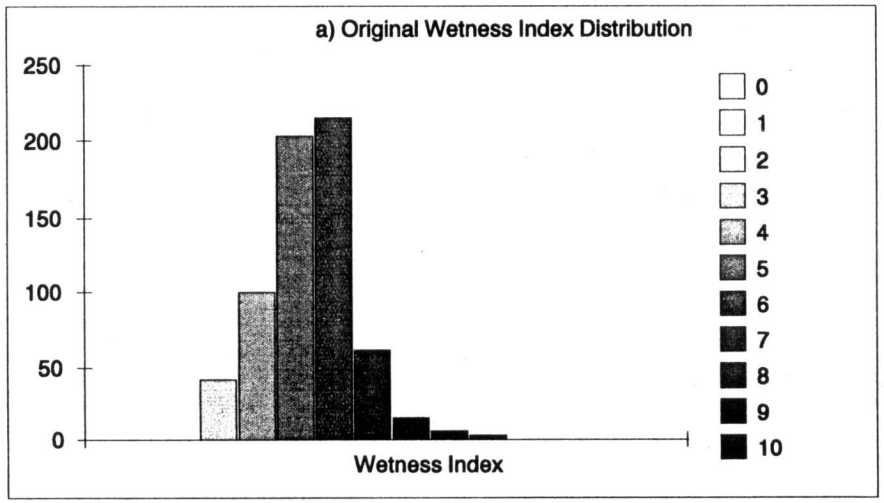

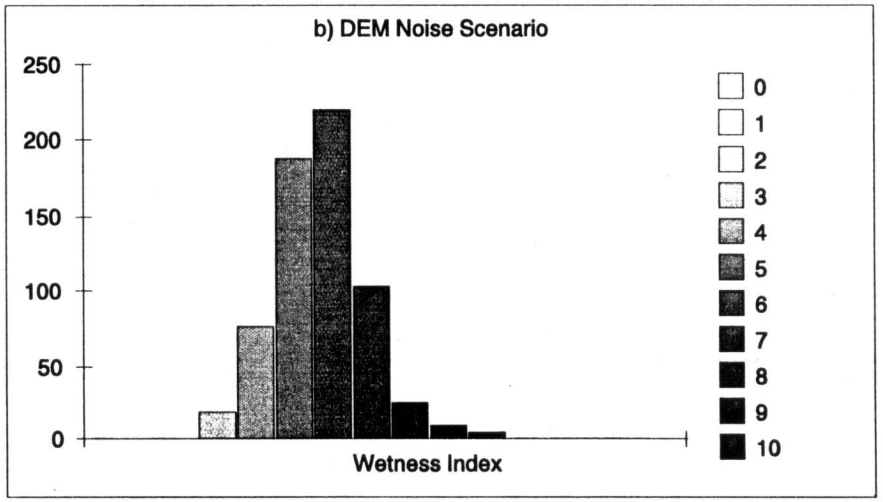

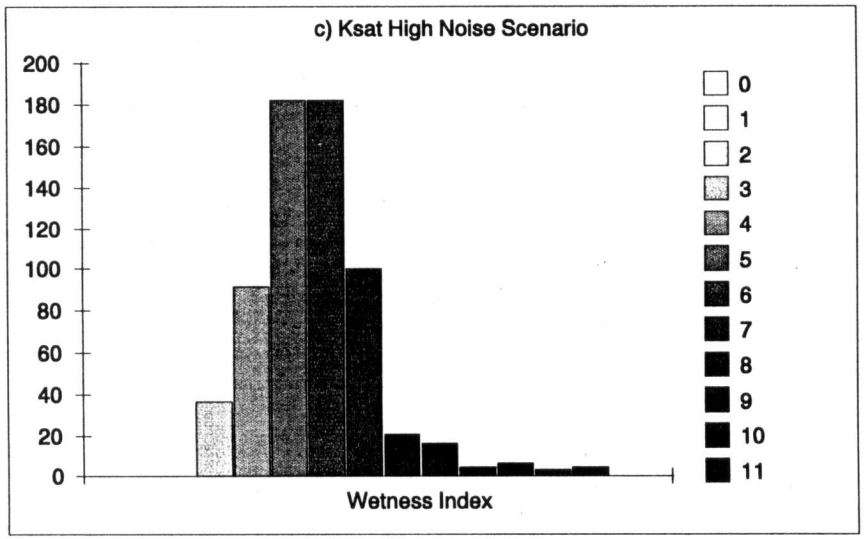

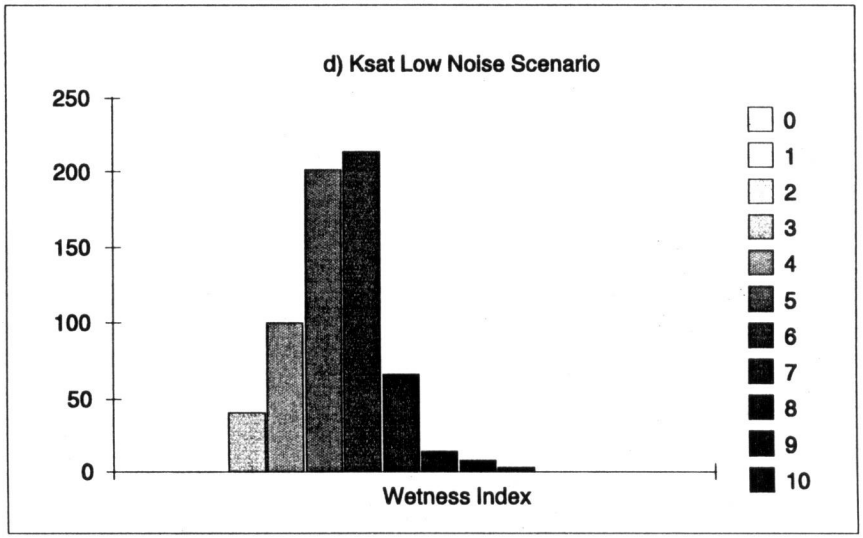

Figure 2.10: The effect of Gaussian noise in DEM and Ksat input information on the
a) original distribution of TOPMODEL wetness index.
b) Random Gaussian noise (mean = 0; std=5m) is applied to the DEM;
Two scenarios of Gaussian noise are applied to the Ksat image
a) high (mean=0, std=40m/day) and
d) low (mean=0, std=8m/day) and

	Sensitivity to Degradation of DEM by Gaussian noise $\mu=0$; $\sigma=$ 5m		Sensitivity to Degradation of Soil Hydraulic Conductivity, K_{sat}, by Gaussian noise $\mu=0$; $\sigma=$ 8m/day		Sensitivity to Degradation of Soil Hydraulic Conductivity, K_{sat}, by Gaussian noise $\mu=0$; $\sigma=$ 40m/day	
Modeling Approach	Mean Daily Relative Difference (percent)	Mean Daily Absolute Difference (mm)	Mean Daily Relative Difference (percent)	Mean Daily Absolute Difference (mm)	Mean Daily Relative Difference (percent)	Mean Daily Absolute Difference (mm)
TOP-MODEL	1.4	0.92	1.0	0.63	3.0	1.60
explicit routing	0.5	0.15	0.1	0.008	2.0	0.11

Table 2.5: Sensitivity of Outflow to Error in Soil and Topographic Input Information for Explicit and Implicit Routing Approaches

Landscape Representation

Using various methods of aggregation can reduce the input information that is required for the pixel based explicit routing approach. These methods also serve to simplify the landscape representation. As discussed above, we consider a grid-based and a variable-shape partitioning strategy. Neither of the two approaches to aggregation produce significant differences in outflow in comparison with the pixel based approach for calibrated and test years. Aggregation does slightly alter the pattern of soil moisture deficit, although to a lesser degree, than the quasi-spatial TOPMODEL approach. Aggregation smoothes the landscape

topography and consequently can change the pattern of flow. Figure 2.5 and 2.6 compare results from the fine resolution pixel-based routing (PR) and the two approaches for reducing resolution (i.e. aggregating by wetness index (TR) versus aggregation by squares (SQ). The pattern of soil moisture shown in Figures 2.5 and 2.6 are inconclusive in terms of the superiority of a particular partitioning strategy. In these simulations, the grid-based approach and the variable shaped partitioning strategies both show some degradation of soil moisture patterns. Both methods of aggregation show a loss of finer resolution variability in soil moisture. Similarly in Figure 2.8 the pattern of wetting and drying illustrated by monthly hillslope soil moisture deficit is fairly consistent across the different approaches with some loss in fine resolution detail for the aggregate approaches. Comparison of ET, shown in Figure 2.11, show that the resulting differences in ET are also small, although the aggregate approaches tend to under estimate late summer transpiration reductions. During the summer dry period, larger evapotranspiration rates are associated only with a fairly small area of significantly higher soil moisture. Aggregation results in an effective expansion of these areas which results in a small net increase in catchment mean evapotranspiration. This effect can be explained by non-linearity in evapotranspiration-soil moisture relationships. In RHESSys, soil moisture control on evapotranspiration occurs through a non-linear modification of stomatal conductance. When areas of high soil moisture are concentrated in relatively small areas, aggregation can produce relatively greater or smaller net ET, depending on the magnitude and pattern of soil moisture.

Conclusions

This study explored the behavior and sensitivity of watershed hydrologic and ecological processes to different lateral subsurface water flux models and the implications of different landscape representations within these models. The comparison between an explicit routing approach and an implicit routing approach, TOPMODEL, illustrates the implications of the simplification of landscape representation associated with the latter approach. In summary, we suggest that the following tradeoffs exist between the two approaches. TOPMODEL is simpler and computationally more efficient. Specifically by removing information about connectivity and by decreasing the effective modeling resolution, the implicit routing

Figure 2.11: Simulated Late-Summer Evapotranspiration; Comparison between pixel based 30m grid (PR), and aggregation by grids (SQ) and irregular aggregation (PR) landscape partitioning approaches.

approach results in a computationally more efficient approach where the number of modeling units is reduced by more than a factor of 10 and processing time decreases by a similar amount. Even with considerable computational power often available for modeling work, the need for multiple, multi-year simulations for large scale landscapes, particular for calibration and scenario development, means that processing efficiency remains an issue. TOPMODEL also does not require information about connectivity and thus can potentially be parameterized with less information. In this study the topographic information used to derive the wetness index distribution came from the same resolution DEM that was used by the explicit routing approach. Franchini *et al* (1996), however, showed that the effect of scale (of DEM) used to derive the topographic index distribution can be modeled and potentially incorporated into the use of coarser resolution information for TOPMODEL parameterization.

This simplicity which permits analytic solutions to the scaling issues with TOPMODEL, however, also limits the ability of the TOPMODEL approach in capturing the local soil moisture pattern. This limitation presents the main drawback of the TOPMODEL or implicit routing approach. Modeling results show significant differences in the spatial and temporal pattern of catchment soil moisture obtained using TOPMODEL and using the explicit routing approach. The explicit routing approach showed an increased spatial variability in catchment soil moisture, during summer dry periods. These results correspond with results from field studies such as Grayson et al (1998), Western et al (1999), Woods et al (1997) which indicate that the control of saturated subsurface throughflow becomes more local during dry periods. The explicit routing model is designed to capture these effects while TOPMODEL, as shown by the more consistent pattern of soil moisture through time, is not able to adequately model the shift towards more local control of distributed soil moisture. Soil moisture distribution may be important in assessing forest harvesting effects on ecosystem response for assessing effects on forest processes such as evapotranspiration and regrowth potential, particularly in water limited areas. The assessment of hillslope contributions to stream chemistry is also sensitive to the spatial pattern of soil moisture and saturated areas. For these applications where spatially distributed soil moisture is important, explicit routing is clearly the better approach, in spite of the computational costs. The incorporation of a dynamic contributing

area into TOPMODEL as suggested by Barling et al. (1993) and Woods et al. (1997) may overcome some of these TOPMODEL limitations and provide another alternative. However, these approaches also require additional parameterization.

It should be noted that as evidence by TOPMODEL and explicit routing comparison that correspondence between observed and modeled outflow may be derived from multiple soil moisture patterns. In this case, we assume that explicit routing better approximates soil moisture distribution because it makes fewer assumptions and because the seasonal shift in soil moisture patterns follows results found by other researchers, as noted above. Further field testing, however, would be necessary to confirm this finding. Since it is not feasible to obtain distributed soil moisture measurements for the entire hillslope, a field approach based on simulated soil moisture patterns can be used. Sites should be chosen in both upslope areas that show, for explicit routing simulations, a large seasonal difference in soil moisture and in the areas near to the stream that remain wet into the summer dry season. Measurements from these sites can then be used to assess how well each model is able to capture seasonal patterns in soil moisture distribution by comparing relative seasonal changes in soil moisture.

It should also be noted that the explicit routing approach has the potential to incorporate much greater parameter uncertainty than the TOPMODEL approach since each patch can be parameterized separately. In TOPMODEL, on the other hand, the distribution of sub-hillslope variability in hydrologic parameters (hydraulic conductivity) is characterized by only two parameters. In this paper, however, the explicit routing approach used an initial distribution of soil parameters and calibrated based on hillslope level scale factors. This effectively reduces the uncertainty of the explicit routing approach to that of the TOPMODEL approach. As with TOPMODEL, initial parameters may be constrained by assumptions about hillslope structure i.e. initial soil properties may be assumed to follow a catenary sequence as is often found in steep mountainous environments. The comparison between the two approaches made in this paper, therefore, illustrates the advantage of incorporating these assumptions into the explicit routing approach.

Results from this paper also highlight the problem of error in input topographic and soil information used for both modeling approaches. We initially hypothesized that the inclusion of information about connectivity in the explicit routing model also provides opportunity for additional error in comparison with simpler implicit routing approaches such as TOPMODEL. Modeling results, however, suggest instead that TOPMODEL is significantly more sensitive to random noise in both topographic and soil information, particularly during peak flow periods. This again suggests that the explicit routing approaches may be preferable, even in areas where limited data is available. Sensitivity to noise for explicit routing increases during low flow periods. This, however, is related to the more local control of soil moisture dynamics during this period, which is ignored by the TOPMODEL approach We did not test model responses to organized or spatially correlated noise.

Although the mean effect of soil and topographic input error was small, daily peak and low flow values were altered by as much as 20% even for the explicit routing approach. The sensitivity of both distributed hydrologic models to input noise also illustrates the inadequacies of using typically available input information without calibration. This is particularly true in the case of soil parameters, which must often be derived from secondary sources such as soil texture maps. These sensitivities may become important in the application of landscape models to areas without fine resolution information or in uncalibrated applications - a task for which these models are often designed. Sensitivity to soils information may also be important when using these models to examine impacts of disturbance such as forest harvesting since local soil conditions may alter the hydrologic response in the disturbed area. The low flow sensitivity to local areas observed here also suggests that models will be sensitive to soil parameterization in these areas. Calibration can be used to capture hillslope level characteristics of outflow response but cannot be used, with either the TOPMODEL or the explicit routing approach, to capture local variability in soil characteristics which may control the local summer soil moisture patterns. In this case, more sophisticated modeling or calibration approaches would be required.

This study also found that both approaches showed some error in capturing the dynamics of recession and low flow periods. We attribute this to emphasis in the calibration on matching

peak flows and to limitations in both modeling approaches. In TOPMODEL, a temporally constant catchment water table shape limits calibration of both peak and low flow or recession periods. With explicit routing, we suggest that low flow and recession periods may require an explicit treatment of hillslope level baseflow contributions, which was not included in the explicit routing model. In addition in both approaches, the dynamics of effective conductivity, which includes the effects of macropore flow and preferential flowpaths, may account for differences in peak, recession and low flow response. Incorporation of temporally varying model of effective conductivity, as a function of soil moisture, could account for these effects.

Finally, this study found that altering the partitioning strategy used in the explicit routing approach produced much smaller changes to resulting distributed soil moisture in comparison with the TOPMODEL approach. In comparison with TOPMODEL, aggregation approaches offer a viable method for increasing the computational efficiency of the explicit routing approach, at least at the watershed (1-100km^2) scale. Partitioning based on wetness intervals (TR) and simple grid-based partitioning produced patterns of soil moisture that are a reasonable approximation of those given by the finer resolution pixel partitioning (PR). Differences between partitioning strategies in this study are not significant enough to denote superiority of one partitioning strategy method over the other. The irregular patches used in the wetness interval partitioning (TR), which incorporate hydrologic information, did not show a significant improvement nor degradation over the similar resolution grid based approach (SR). There may, however, be other arguments to support the use of the wetness interval strategy for partitioning the landscape since soil and vegetation characteristics may also be organized in this manner. Moore *et al.* (1993) and Band et al. (1993) discuss the advantages of incorporating these spatially organized processes into landscape representation. Further work will explore these issues in more detail.

References

Ambroise, B., Beven, K.J., and Freer, J. 1996. Towards a generalization of the TOPMODEL concepts: topographic indices of hydrologic similarity, *Wat. Resour. Res*, **32**, 2135-2145.

Band, L.E. 1993. Effect of land surface representation on forest water and carbon budgets. *Journal of Hydrology*, **150**, 749-772.

Band, L., Patterson, P., Nemani, R., and Running, S. 1993. 'Forest ecosystem processes at the watershed scale: incorporating hillslope hydrology', *Agric. For. Meteorol*, **63**, 93-126.

Band, L., Peterson, D., Running, S., Coughlan, J., Lammers, R., Dungan, J. and Nemani, R. 1991. 'Forest ecosystem processes at the watershed scale: basis for distributed simulation', *Ecol. Model.*, **56**, 171-196.

Barling, R., Moore, I., Grayson, R. 1993. 'A quasi-dynamic wetness index for characterizing the spatial distribution of zones of surface saturation and soil water content', *Wat. Resour. Res*, **30**, 1029-1055.

Beven, K.1997. 'TOPMODEL: A critique', *Hydrological Processes*, **11**, 1069-1085.

Beven, K. 1995. "Linking parameters across scales: Subgrid parameterizations and scale dependent hydrological models", *Hydrologic Processes*, **9**, 507-525.

Beven, K and Kirkby, M. 1979. "A physically-based variable contributing area model of basin hydrology, *Hydrologic Science Bulletin*, **24**, 43-69l.

Bernier, P. 1985. 'Variable source areas and storm-flow generation: An update of the concept and a simulation effort', *Journal of Hydrology*, **79**, 195-213.

Bloschl, G., Sivapalan, M. 1995. Scale issues in hydrological modeling: a review, in Kalma, J.D., Sivapalan, M. (Eds), *Scale Issues in Hydrological Modeling*, Wiley, Great Britain, pp9-48.

Bruneau, P., Gascuel-Odoux, C., Robin, P., Merot, Ph., and Beven, K. 1995. Sensitivity to space and time resolution of a hydrological model using digital elevation data, *Hydrologic Processes*, 10th Anniversary Issue, 55-69.

Burt, T.P., Butcher, D.P. 1986. Development of topographic indices for use in semi-distributed hillslope runoff models', in Baltenau, D. and Slaymaker, O. (Eds), *Geomorphology and Land Management*, Zeits. Geomorph. Suppl. Band 58, 1-19.

Clapp,R., Hornberger,G. 1978. Empirical equations for some soil hydraulic properties, *Wat. Resour. Res*, **14**, 601-604.

Daly, C., Neilson, R.P., Phillips, D.L. 1994. A statistical-topographic model for mapping climatological precipitation over mountainous terrain, *Journal of Applied Meteorology*, **33**:2, 140-157.

Dryness,C. 1969. Hydrologic properties of soil on three small watersheds in the western Cascades of Oregon, USDA Forest Service, Research Note PNW-111, Pacific Northwest Forest and Range Experiment Station, 17pp.

Duan, J. 1996. A coupled hydrologic model for evaluating effects of vegetation change on watersheds, P.h.D Thesis, Oregon State Universty, 131pp.

Famiglietti, J.S., Wood, E.F. 1994. Multi-scale modeling of spatially-variable water and energy balance processes, *Wat. Resour. Res*, **30**, 3061-3078.

Franchini, M., Wendling, J., Obled, Ch., and Todini, E. 1996. Physical interpretation and sensitivity analysis of the TOPMODEL, *J.Hydrol.*, 175, 293-338.

Grayson, R., Moore, I., McMahon, T. 1992. Physically based hydrologic modeling: Is the concept realistic, *Wat. Resour. Res*, **23**, 2659-2666.

Jarvis, P., Leverenz, J. 1986. Productivity of temperate, deciduous and evergreen forests, in Lange, O.L., Nobel, P.S., Osmond, C.B., Ziegler, H., *Physiological plant ecology. Encyclopedia of plant physiology, New Series*, Vol 12D, Springer-Verlag, 233-280.

Lammers, R., Band, L., Tague.C. 1997. Scaling behavior of watershed processes, in van Gardingen,P. Foody, G. and Curran, P. *Scaling-up*, Cambridge University Press.

Lammers, R.B., Band, L.E. and Csillag, F. 1996. A comparison of partitioning strategies for complex terrain Paper presented at American Geophysical Union, Spring Meeting, Baltimore, May 21, 1996 at an IGBP - BAHC Special Session on Scaling Issues in Hydrometeorology and Ecohydrology.

McDonnell, J.J. 1990.`A rational for old water discharge through macropores in a steep humid catchment, *Wat. Resour. Res*, **26**,2821-2832.

Moore, R.D. , Thompson, J.C. 1996. Are water table variations in a shallow forest soil consistent with the TOPMODEL concept, *Wat. Resour. Res*, **32**, 663-669.

Moore, I., Turner, A.K., Wilson, J.P., Jenson, S., Band, L., 1993. 'GIS and land surface-subsurface process modeling', in Goodchild, M., Parks, B., Steyaert, L. (Eds), *Environmental Modeling with GIS*, Oxford University Press, pp196-230

Nash, J., and Sutcliffe, J. 1970. 'River flow forecasting through conceptual models: Part 1 - a discussion of principles', *Journal of Hydrology*, **10**, 282-290.

O'Callaghan, J., Mark, D. 1984. 'The extraction of drainage networks form digital elevation data', *Computer Vision Graphics and Image Processing*, **23**, 323-344.

Ostendorf, B., Manderscheid, B. 1997. Seasonal modeling of catchment water balance: A two-level cascading modification of TOPMODEL to increase the realism of spatio-temporal processes. *Hydrol. Processes* , 11, 1231-1242.

O'Loughlin, E.M.1990 'Modeling soil water status in complex terrain', *Agric. For. Meteorol.* ,**50**, 23-38.

Quinn, P., Beven, K., Chevallier, P., and Planchon, O. 1991. 'The prediction of hillslope flow paths for distributed hydrological modeling using digital terrain models', *Hydrological Processes*, **5**, 59-79.

Ranken, D.W., 1974. *Hydrologic properties of soil and subsoil on a steep, forested slope*, M.S. thesis, Oregon. State Univ., Corvallis, 177p.

Rosentrater, L. 1997 'The thermal climate of the H.J.Andrews Experimental Forest, Oregon", MSc Thesis, Department of Geography, University of Oregon.

Rothacher, J., Dyrness,C, and Frediiksen, R. 1967.'Hydrologic and related characteristics of three small watersheds in the Oregon Cascades', U.S. Department of Agriculture Forest Service, Pacific Northwest Forest and Range Experiment Station, Portland, Oregon, 54pp.

Running, S.W. 1994. 'Testing FOREST-BGC ecosystem process simulations across a climatic gradient in Oregon'. *Ecological Application*, **4**: 238-247.

Running, S. W. and R. E. Hunt. 1993. 'Generalization of a forest ecosystem process model for other biomes, BIOME-BGC, and an application for global-scale models'., Ehleringer, J. D., Field, C.D. (Eds) in *Scaling Physiologic Processes: Leaf to Globe*. Academic Press, San Diego, CA. pp. 141-158.

Running, S. W., R. R. Nemani and R. D. Hungerford. 1987. Extrapolation of synoptic meteorological data in mountainous terrain and its use for simulating forest evapotranspiration and photosynthesis. *Can. J. For. Res.* **17**:472-483.

Troch P.A., Su Z., Debruyckere L., Debels P., Verhoest N., Cosyn B., Nachtergale L., De Troch F.P. 1996. Spatial and temporal soil moisture mapping from distributed SVATS modeling and remote sensing.'; *Annales Geophysicae*, *Supplement II* , **14**, C361.

Western , A., W., Grayson, R.B., Bloschl, G., Willgoose, G.R., McMahon, T.A. 1999. 'Observed spatial organization of soil moisture and its relation to terrain indices', *Wat. Resour. Res*, **35**, 797-810.

Wigmosta, M., Vail, L., Lettenmaier, D. 1994. 'Distributed hydrology-vegetation model for complex terrain', *Wat. Resour. Res*, **30:6**, 1665-1679.

Wolock, D., Price, C. 1994. 'Effects of digital elevation model map scale and data resolution on a topography based watershed model', *Wat. Resour. Res*, **30**, 3041-3052.

Woods, R. A., Sivapalan, M., Robinson, J.S. 1997. 'Modeling the spatial variability of subsurface runoff using a topographic index', *Wat. Resour. Res*, **33**, 1061-1074.

Zhang, W., Montgomery, D. 1994. 'Digital elevation model grid size, landscape representation and hydrologic simulations', *Wat. Resour. Res*, **30**, 1019-1028.

Chapter 3: Modeling seasonal hydrologic response: sensitivity to landscape representation and stream channel parameterization.

Preface

The previous chapter presents arguments that suggest that in order to capture seasonal changes in drainage organization, an explicit routing model is required. The previous chapter also discusses some of sources of error associated with this approach and the potential problems of finding adequate input data. Given the goal of applying the explicit routing approach within the RHESSys modeling framework and exploring the relationship between drainage organization and disturbances such as forest harvesting, some further analysis of this approach is warranted. This next section continues the investigations of the previous section by focusing on the sensitivity to landscape representation for the explicit routing model. This chapter highlights the importance of representation of near stream areas and illustrates the key role that these areas play in controlling summer low flow production.

Abstract

This study addresses the sensitivity of modeling hydrologic response, particularly during summer low flow periods, to landscape representation of local streamside areas. In this paper, we use a physically based hydro-ecosystem model, RHESSys, to illustrate sensitivity of seasonal streamflow response to the representation of stream and near stream areas for a representative headwater catchment in the H.J Andrews Experimental Forest in the Western Oregon Cascades. We consider 5 different approaches to partitioning the landscape including both grid based and irregular shaped partitioning strategies that incorporate information about hillslope drainage organization. We also consider 4 different approaches to representing landscape modeling units or patches that contain streams, since these are particularly sensitive areas within the landscape. Stream patch representations differ in terms of the local gradients used in routing subsurface and overland flow to the stream. To address seasonal variation in sensitivity, we calibrate the model for both annual and summer flow. Results from these simulations show a seasonal sensitivity to landscape and stream patch representation. In comparison with annual or winter flows, summer low flow production show a much greater sensitivity to calibrated soil transmissivity. Results also show that in order to capture summer low flow dynamics, landscape representation must include fine resolution patches in near stream areas and that variance in hydrologic characteristics, in this case implemented as gradient to the stream, must be included in patches containing streams. We use this modeling study to discuss implications of this sensitivity in terms of scaling and generalizing studies of seasonal hydrologic response to other watersheds where data availability may be limited.

Introduction

Seasonal streamflow response is an important component of understanding ecosystem behavior and the environmental impacts of land use change and climate variability. In regions such as the Pacific Northwest, warm dry summers and wet cooler winters produce relatively small summer flows and much higher winter water yields. Summer low flows and winter peak flows both play important roles in maintaining riparian ecosystems, aquatic habitat and the human uses of streams. Large winter flows contribute to flooding, erosion, stream sedimentation and the modification of other channel characteristics. Although low flow values comprise only a small portion of annual water yields, low flow dynamics can have important ecological implications as they contribute to water supply and aquatic health (Hicks et al, 1991). Streamflow quality is also related to low flow dynamics and the associated pattern of soil moisture.

Alteration of landscape vegetation cover and drainage patterns has been shown to have significant but variable impacts on seasonal streamflow patterns (Stednick, 1996; Johnson, 1998; Harr et al, 1982). To better understand these processes and their variability, hydro-ecological modeling presents one method of generalizing information derived from intensive field studies to a population of hillslopes within a regional landscape. Applying these models across a heterogeneous landscape requires spatially distributed input information on soil, topographic, vegetation, streamflow and climate characteristics. Given the potential for limited availability of this information at a fine resolution for many catchments, it is important to assess model sensitivity to input information resolution and to explore techniques which may reduce necessary data collection.

Seasonal streamflow response is controlled by spatial and temporal interactions between climatic, topographic, soil and vegetation patterns. These interactions determine the patterns of antecedent moisture status and the mechanisms that translate that pattern of antecedent moisture into streamflow. In regions where streamflow response is dominated by variable source area runoff production, specific spatial areas within a hillslope or landscape can be particularly important in controlling hydrologic response. In addition, the spatial extent and

degree of this sensitivity may vary with seasonal and inter-annual variations in climate. Field evidence of a seasonal shift in dominance of near stream areas to broader hillslope contributions in the production of runoff has been shown by Tani (1997) and McDonnell (1990). Woods et al (1997) also show that drier periods produce a greater spatial variability in soil moisture patterns. Grayson et al. (1997) and Western et al (1999) show that more local soil and vegetation patterns rather than hillslope topography tend to dominate during drier periods as controls on soil moisture pattern. Modeled streamflow will therefore be sensitive to the seasonal variation in the spatial extent and organization of runoff producing areas and how topographic, soil and vegetation patterns in these local areas, typically in valley bottoms or hollows near to the stream, are represented in a given model.

Considerable analysis of the effect of representation has been done for the TOPMODEL approach to modeling distributed soil moisture and runoff production. TOPMODEL (Beven and Kirkby, 1979) is a quasi-spatially distributed approach which models soil moisture redistribution based on a statistical distribution of topographically defined wetness indices. In TOPMODEL, the distribution of wetness indices and calibrated saturated conductivity have been shown to shift towards larger values as grid cell resolution decreases (Zhang and Montgomery, 1994; Band *et al.*, 1995). Saulnier *et al* (1997b) note that this effect is related to an increasing area being treated as channels in the calculation of the wetness index distribution. They also propose a method for compensating for this scale effect in TOPMODEL by restricting the accumulated area of channel crossing pixels to hillslope rather than channel contributions. It is important to note that this approach requires the additional input information detailing the location of channels.

These results illustrate that, for TOPMODEL, the representation of streamside areas becomes important in model applications across different scales. There is also evidence of seasonal variability in this sensitivity related to seasonal shifts in connectivity between streamside and the surrounding contributing hillslope area. TOPMODEL assumes that the connectivity between stream side and hillslope area remains unchanged across a range of antecedent soil moisture conditions. In contrast, field and modeling studies have shown that the relationship between upslope and near stream area can change between relatively wet and dry periods and

that these changes in connectivity between different hillslope areas result in an effective change in the TOPMODEL wetness distributions or associated calibrated transmissivity (Ostendorf and Manderscheid, 1997; Barling et al., 1993).

The above discussion illustrates the sensitivity of the TOPMODEL approach to the spatial representation of near stream areas. TOPMODEL, in its simplicity, offers analytical approaches to scaling but has several limitations. It may not be appropriate for modeling the effects of land use change since it assumes net recharge to be spatially invariant and ignores explicit connectivity between patches. Thus, TOPMODEL cannot directly address downslope impacts of vegetation removal on upper areas of a hillslope. The assumption of spatially invariant recharge also becomes important in the drier periods where variability in evapotranspiration becomes a dominant control on soil moisture. In addition, as we have noted, calibration based on transmissivity in TOPMODEL may obscure variability in the function of and relationship between streamside and upper hillslope areas. Explicit routing methods are able to more closely model combined effects of land use and can be used to investigate the importance of explicit and variable connectivity between land areas. Explicit routing approaches, however, are more data intensive and potentially more complex in terms of scaling.

In this paper, we examine an explicit routing approach and the sensitivity of streamflow patterns to landscape representation. Following the results from scaling studies using TOPMODEL, we examine changes in calibrated effective transmissivity due to representation of the landscape and streamside areas and explore how this sensitivity varies seasonally. Several spatially distributed hydro-ecological models are available including TOPOG (O'Loughlin, 1990), DHSVM (Wigmosta *et al.*, 1994) and CLAWs (Duan, 1995). For this study we use, RHESSys, which incorporates a modified version of the DHSVM explicit routing approach described below. Using RHESSys, we consider alternative approaches to landscape partitioning. We consider both grid based approaches and irregular shaped partitioning strategies. The irregular shaped partitioning strategies are used to explore the feasibility of varying surface tessellation to maximize resolution in sensitive streamside areas and relax input requirements in areas of the watershed that are less critical

to modeling runoff response. We use the TOPMODEL wetness index to define local areas of high sensitivity. To address the issue of local control of runoff production during drier periods, we also explore model sensitivity to the information included in local streamside areas. In particular, we consider the importance of variability in the local gradient to the stream as a control on catchment level streamflow response.

Model Description

RHESSys is a GIS based hydro-ecological modeling system which combines distributed hydrologic modeling with an ecophysiological canopy model, based on BIOME_BGC (Running and Hunt, 1993) and a climate interpolation scheme based on MTN_CLIM (Running et al., 1987). The various components of RHESSys and the overall approach have been tested in numerous applications (Band, 1993; Running, 1994; White and Running, 1994). Landscape representation and numerous process algorithms have been modified in the current version of RHESSys. The current version incorporates a hierarchical landscape representation that models specific processes at different spatial resolutions. Figure 3.1 illustrates this hierarchy. Stream flow processes are modeled at the basin level, lateral soil moisture fluxes at the hillslope level; climate processes at the zone level; vertical soil moisture flux at the patch level and canopy hydro-ecological processes at the stratum level. Note that strata are vertical objects that use the same spatial resolution as the underlying patch layer.

The hierarchical objected-oriented approach facilitates the exploration of scaling issues for different processes. In this paper, we will focus specifically on the scaling of lateral soil moisture flux. Lateral hydrologic modeling occurs between patches within a hillslope. The basic landscape hydrologic modeling unit in RHESSys is the patch, which represents areas of similar soil moisture and canopy cover. The use of irregularly shaped patches rather than grid cells permits more efficient parameterization of the watershed and allows patches to represent ecologically meaningful units at different scales. Lammers et al (1996) and Band et al (1995) discuss the advantages of non-grid based representation.

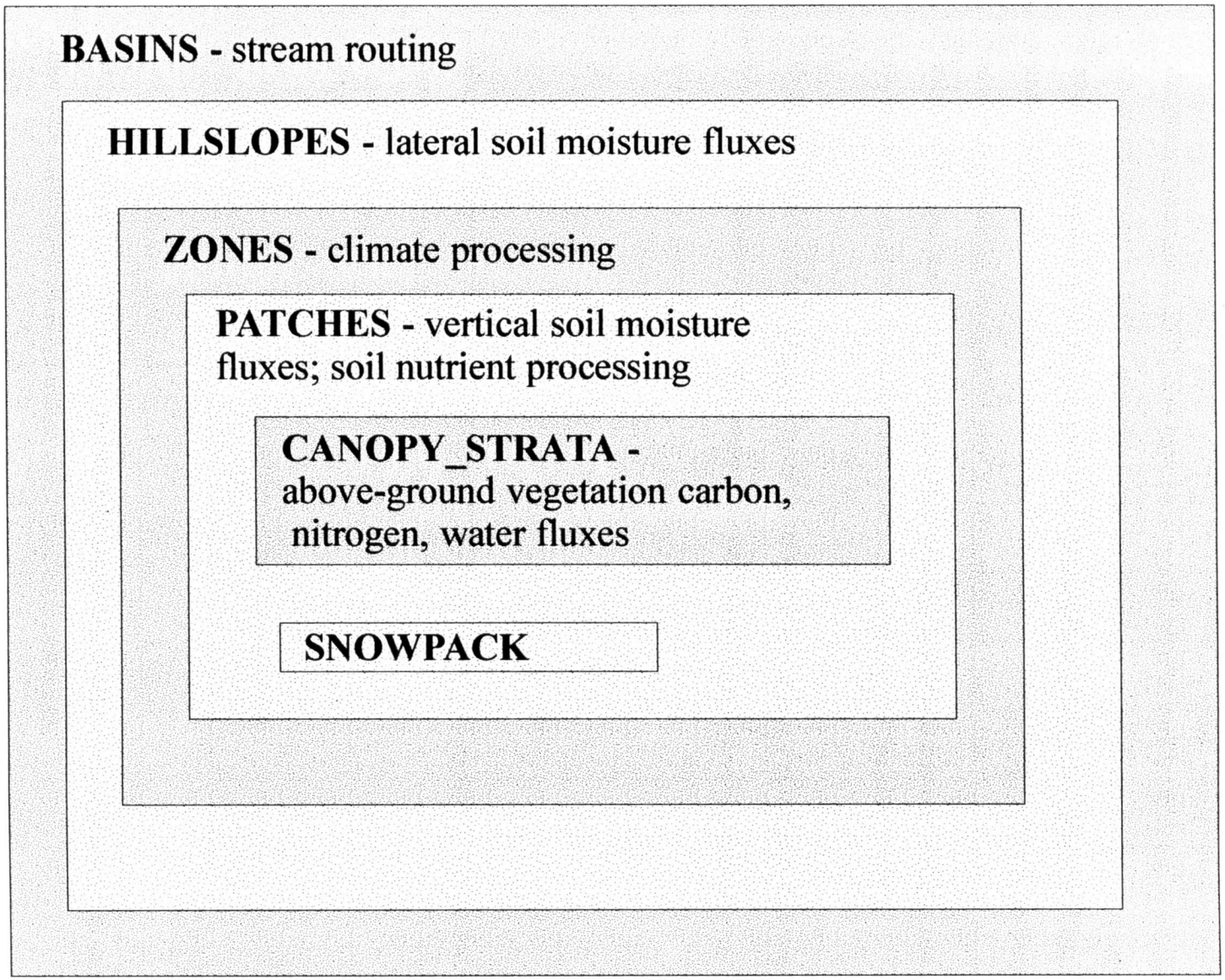

Figure 3.1: Hierarchical landscape objects in RHESSys and associated key hydro-ecological processes

Modeling of distributed hydrology in RHESSys has been expanded to include an explicit routing of saturated zone soil moisture based on DHSVM (Wigmosta et al. 1994), which has been adapted for variable shaped patches as described in Tague and Band (submitted). Soil moisture dynamics in RHESSys have been modified from earlier versions. A single layer unsaturated zone is used to model infiltration, drainage to unsaturated zone and capillary rise over a soil depth with vertically variable hydraulic conductivity and porosity. Details of the unsaturated zone model are described in Fernandes (1999). Canopy process routines have also been modified from BIOME_BGC (Running and Hunt, 1993) to consider clumped, multi-layer, and multiple cover type canopies and a separation between diffuse and direct radiation. These process modifications are also described in Fernandes (1999).

In the DHSVM model of explicit routing, saturated subsurface throughflow is computed as:

$$q(t)_{a,h} = \{T(t)_{a,h} \tan \beta_{a,h} \omega_{a,h}\} \qquad [1]$$

where ω is flow width, tan β is local slope, approximated by topographic slope, and T is transmissivity as defined as:

$$T = \int_0^D K_0 e^{(\frac{s\Delta\Theta}{m})} dz \qquad [2]$$

where K_o is saturated hydraulic conductivity at surface; *m* is a soil parameter; $\Delta\Theta$ is soil moisture capacity and s is saturation deficit and D is soil depth.

For land surface patches, flow widths are the shared perimeter between adjacent patches and the gradient is defined by relative patch elevation.

Estimation of Streamside Gradient

RHESSys considers patches containing streams as distinct patch types within the flow routing network. Flow routing between stream patches assumes that all water entering the stream reaches the outlet within a single time step. Thus, there is no routing between stream patches. This is appropriate for the daily time step used in RHESSys and for study catchments less than 100km^2 in area. The amount of flow entering the stream from a patch containing a stream is a function of subsurface flow from that patch as defined by (1). In the case of a patch containing a stream, subsurface throughflow flow width is defined by the stream length rather than the boundary with the neighboring patch. Flow width for stream patches is assumed to be twice the number of grid cells in the patch times the grid resolution.

Since stream widths at the small watershed scale are typically smaller than the 30m-grid resolution, local gradients to the stream may not be reflected by the mean land surface gradient of the patch or pixel. TOPMODEL deals with a similar issue in the calculation of accumulated area for streamside pixels (Saulnier,1997a). In this study, we consider four alternatives for the estimation of the gradient to the stream within a patch:

a) constant gradient for all stream patches within a given sub-basin
b) random gradient
c) contributing flowpath gradient
d) local patch gradient

A constant gradient is used to explore the issue of scaling, where the gradient for stream network within a given area is represented by a mean value. This illustrates model sensitivity to scenarios where detailed information about near stream areas is not available. The random gradient assumes a uniform distribution of local slopes ranging from gentle to highly incised and is used to explore the contribution of local small scale streamside topographic variance in the production of streamflow. The random gradient approach allows gradient to vary along the stream reach but does not require additional input information about local patch gradient. The next two approaches include topographic information about stream containing patches. Gradient is derived either from local patch gradient or from upslope flow gradient to the

stream patch. The distinction between using a local patch gradient and the contributing flowpath gradient is outlined in Figure 3.2.

Flow from a patch into a stream is also a function of the soil transmissivity of that patch. Since fine resolution soil information is not always available, there may be considerable sources of error in estimating transmissivity. Hillslope transmissivity is calibrated in this model. Outflow, however, may also be sensitive to local stream side transmissivity. Since transmissivity follows the effect of local gradient in the calculation of flow (1), sensitivity to gradient may also reflect sensitivity to soil transmissivity.

Landscape "Patch" Representation

At the finest resolution, patches can be defined based upon the DEM resolution. In order to facilitate more efficient parameterization and computation or to consider ecologically meaningful units, patches can also be defined based upon indices of hydro-ecological similarity. Patches then represent areas of similar soil moisture characteristics. In this study, we develop several different strategies for patch partitioning using several GIS data layers including the TOPMODEL wetness index, a 100m elevation interval and stream network layer. Patches are defined by a connected component algorithm applied to the intersection of the various supporting data layers. In areas with variability in land cover, a land cover classification scheme would also be incorporated into the patch definition. Figure 3.3 illustrates patch derivation schemes used in this study.

The five alternative landscape partitioning strategies used in this study are compared and summarized in Table 3.1.

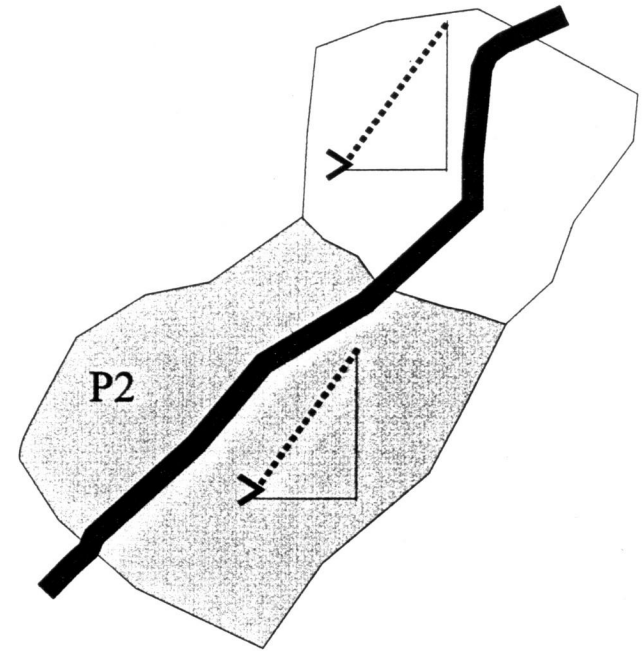

Local Patch Gradient

Gradient of P1, containing the stream, is used for gradient defining patch output to the stream

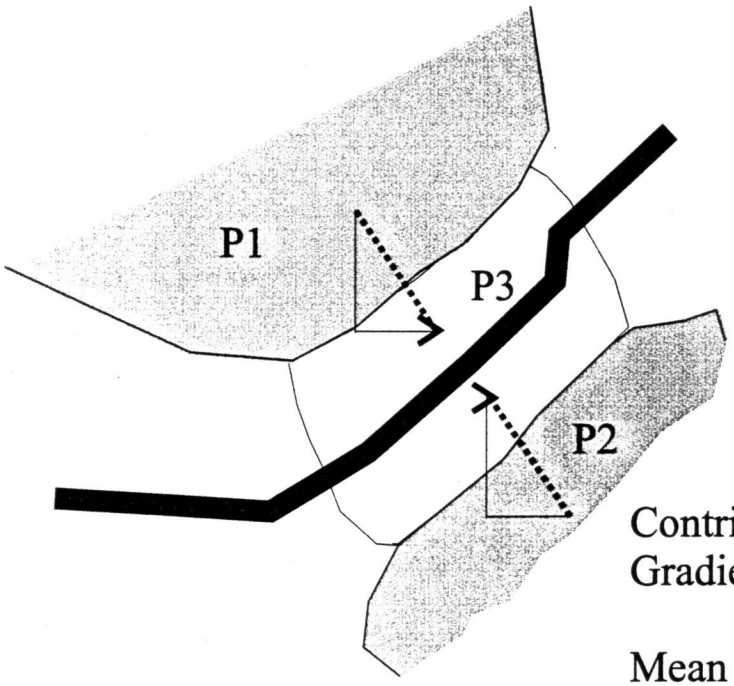

Contributing Flowpath Gradient

Mean gradient between upslope patches (P1 and P2) and the patch containing the stream, P3, is used for gradient defining patch output to the stream

Figure 3.2: Estimation of Streamside Gradient: Local patch gradient vs contributing flowpath gradient

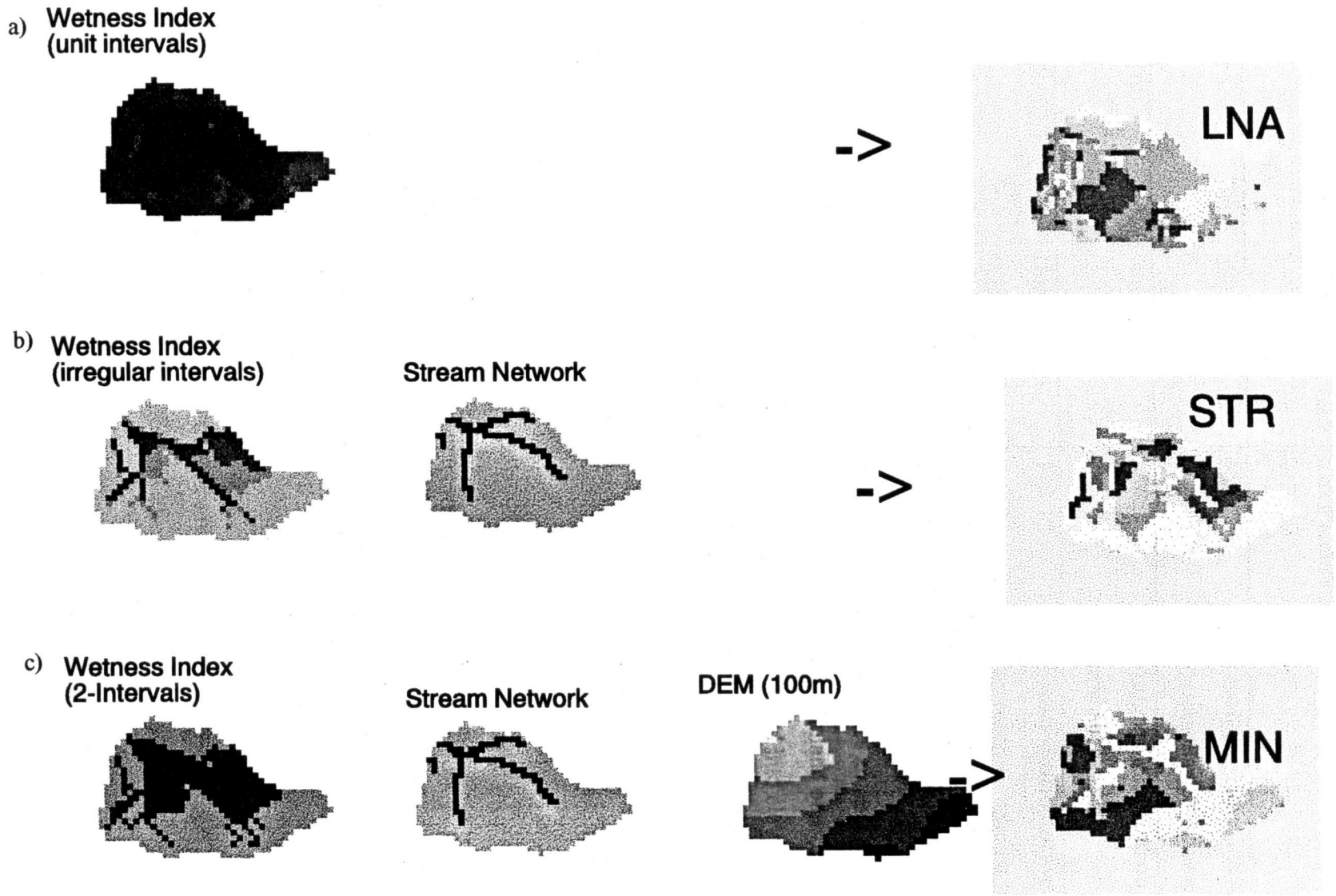

Figure 3.3: Patch partitioning strategies based on different GIS data layers
a) LNA, using a unit interval wetness index;
b) STR using an irregular wetness index with high resolution in typically wet areas and
c) MIN, using a simplified wetness index with high resolution near to the stream and a DEM

Partitioning Strategy	Supporting GIS layers	# of Patches	Description
PIX	30m pixel	654	Finest resolution approach; uses rectangular grid based partitioning
SQR	90m pixel	86	Aggregation based on rectangular grid approach
LNA	Unit-interval Wetness index	120	Evenly distributed wetness index approach – grouping together cells of similar soil moisture
MIN	Two wetness intervals; stream network; 100m elevation bands	55	Minimum number of patches; assumes an upland, a stream and a bottomland object, each further sub-divided into elevation intervals
STR	Irregularly-spaced wetness index intervals*; stream network	148	Compensates for greater sensitivity of hydrologic response to near stream areas by including finer resolution partitioning in high wetness index areas (i.e. areas near to stream and local hollows)

* For the STR patch representation; areas with wetness indices in the range from 1-5 are aggregated to a single interval. Higher wetness indices are grouped using a high resolution (0.5) wetness interval.

Table 3.1: Description of partitioning strategies

In the set of partitioning strategies, there are two grid -based approaches that permit comparison between fine and coarse resolution grid based landscape representation. We also compare the grid-based scaling or aggregation approach to several different irregularly shaped patch partitioning strategies. These strategies use patches based on the TOPMODEL wetness index (Beven and Kirkby, 1979) to define contiguous areas of similar soil moisture.

The simplest representation (LNA) is based on a unit interval wetness index distribution. The more complex approach (STR) compensates for sensitivity of hydrologic response to near stream areas or local hollows by generating a higher density of patches in these areas. Figure 3.4 illustrates the increase in streamside resolution associated with this approach. Finally, we consider a coarse hillslope object approach, (MIN), which defines upland and bottomland areas, subdivided into 100m elevation zones but maintains fine resolution in stream patches. The MIN approach produces the minimum number of patches.

Site Description

The test site catchment for this study is Watershed 2, a 60.3 ha unlogged sub-watershed in the Lookout Creek basin in the H.J.Andrews forest. Some additional comparison is done using a neighbouring sub-watershed, Watershed 1. This watershed is also unlogged for the time period used in this study. Annual precipitation of greater than 2000mm occurs mostly during winter months. Watershed 2 elevation ranges from 400 to 1070m. Slopes are steep and highly dissected as a result of fluvial erosion and landsliding. Climate input, as temperature and precipitation, for the simulation is taken from a meteorological station within Watershed 2. A spatially variable climate surface is then derived using MTN_CLIM as embedded in RHESSys, with modified temperature and precipitation lapse rates based upon climate investigations by Rosentrater (1997) and modeling by the PRISM model (Daly et al., 1994) for the H.J.Andrews basin. The partitioning of precipitation into rain and snow is based upon air temperature. (The proportion of precipitation falling as rain or snow varies linearly from –3C to +3C, with all precipitation falling as snow at –3C and all precipitation falling as rain at +3C). Uncertainty in precipitation values, and particularly the partitioning between rain and snow events, can have significant effects on the estimation of winter peak flow events in this region (Harr, 1981). For this study we use a daily time step which is somewhat less sensitive to peak flow generation dynamics than storm event driven simulations. We still expect, however, some error due to uncertainty in climate forcing and snow melt estimation.

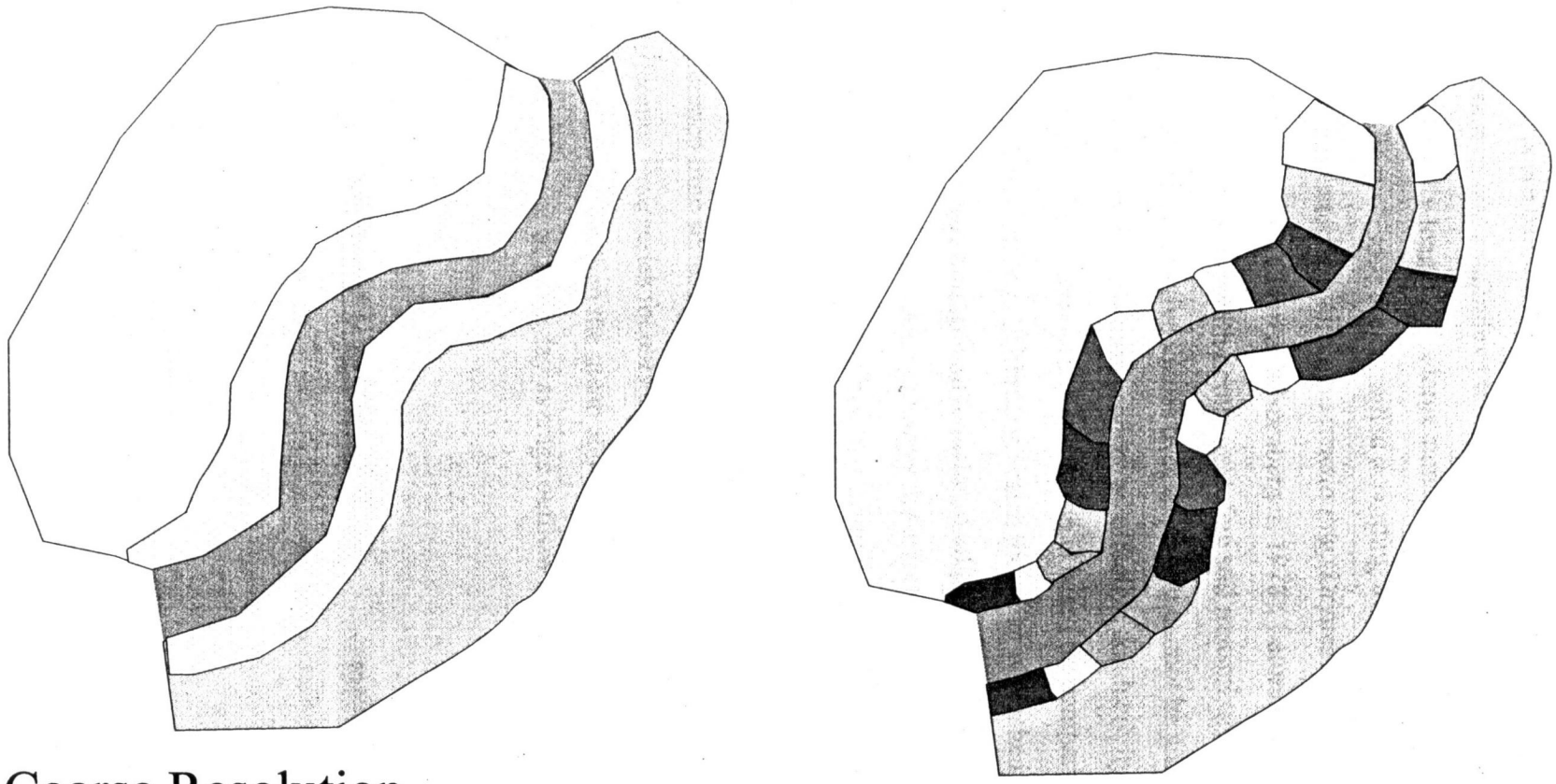

Figure 3.4 Patch spatial partitioning: Including fine resolution information in areas adjacent to streams for the MIN and STR partitioning strategies.

Vegetation is dominated by Douglas fir (Pseudotsuga menziesii). Model vegetation parameters are based upon literature values for Douglas Fir or coniferous forest with the exception of leaf area index that varies according to available maps of stand age. Soils are clay to gravelly loam with a large stone content and high hydraulic conductivity (Dryness, 1969). Although soils are classified according to texture, it is the high stone content that tends to characterize hydrologic functioning (Dryness, 1969). Parameters used are typical for well-drained soils (Clapp and Hornberger, 1978). Saturated hydraulic conductivity, K, and decay of conductivity with depth, m, define soil transmissivity. These values are calibrated, since they act as effective values over space and cannot be adequately estimated through point measurements. Results produce an effective conductivity and transmissivity, which include the effect macropores. Calibration is based on comparison between observed and modeled daily outflow. Calibration scales the mean watershed K and m parameters by applying the same multiplicative factor to all patches, similar to the method used by (Saulnier et al, 1997c). This procedure changes the effective basin transmissivity but does not change the within-basin spatial distribution. Calibration is applied using the Nash-Sutcliffe efficiency criteria (Nash and Sutcliffe, 1970) with a Simplex minimization algorithm (Nelder and Mead, 1965). Additional calibration and comparison is done using the 1st order difference time series for observed and modeled daily outflow. Comparison of 1st order difference time series focuses on the ability of the model to capture the temporal dynamics of streamflow rather than the mean and peak streamflow values. Nash-Sutcliffe efficiency of 1st order difference of three day average outflow is computed as:

$$obs_d(t) = \sum_{i=(t-1)}^{(t+1)} \frac{obs(i+1) - obs(i-1)}{2} \qquad [3]$$

$$Y_d(t) = \sum_{i=(t-1)}^{(t+1)} \frac{Y(i+1) - Y(i-1)}{2} \qquad [4]$$

$$eff_d = \frac{\sum_t (obs_d(t) - \overline{obs_d})^2 - \sum_t (obs_d(t) - Y_d(t))^2}{\sum_t (obs_d(t) - \overline{obs_d})^2} \qquad [5]$$

where obs is observed outflow, Y is simulated outflow.

To explore the potential for variation in drainage organization in summer and winter flow periods, we calibrate for both summer and winter periods for 1963, a moderately wet year. Any significant difference in calibrated transmissivity indicates that there is a seasonal shift in drainage dynamics that is not directly captured by the model or that the different population of events, during the summer, results in a different combination of optimal parameters. It should be noted, however, that the optimal parameter set is not necessarily unique. We also calibrate separately for each of the five landscape partitioning strategies and the different methods of stream patch gradient estimation. Hydrologic responses using the different strategies are then compared to explore the sensitivity to resolution and local topographic information.

Results

Calibration using a constant slope

Table 3.2 shows calibration scaling for m and K and the associated Nash-Sutcliffe efficiency for each of the different landscape partitioning approaches assuming a constant streamside gradient. The resulting transmissivity for larger soil depths can be estimated as m*K and is also recorded. Calibrations for both annual and summer low flow time series for the calibration year, 1963, are shown. Differences between landscape representation approaches are small, although larger for annual calibrations and for K versus m. Bruneau et al (1995) found a similarly higher calibration sensitivity for K as compared to m, using TOPMODEL.

Mean calibrated transmissivity is slightly higher for the annual calibrations. Figure 3.5 and 3.6 illustrate the resulting hydrographs for winter and summer, respectively, using a constant streamside gradient. Winter flows are shown only for the PIX and MIN landscape representations. Other landscape representations follow a similar pattern. Results using both annual and summer calibrated values are shown for winter and summer periods. Winter hydrographs show that the model tends to over-estimate responsiveness of streamflow in all cases. Annual calibration offers a slight improvement over summer calibration by reducing the tendency to over-estimate peak events for the MIN representation but not for the PIX representation. Figure 3.6 shows that for summer periods, the difference between summer and annual calibrated results show a shift in the mean outflow. None of the landscape representations are able to capture low flow dynamics, although the pixel approach, PIX, does show some additional sensitivity.

	Summer				Annual			
Part. Strategy	*m*	*K*	T	*Efficiency*	*m*	*K*	T	*Efficiency*
PIX	0.92	9.2	8.46	0.77	0.86	8.6	7.40	0.61
SQR	0.92	9.2	8.46	0.71	0.99	10.1	10.00	0.67
LNA	0.86	8.6	7.40	0.73	1	14.7	14.70	0.66
STR	0.87	9.1	7.92	0.71	0.86	8.7	7.48	0.67
MIN	0.87	8.6	7.48	0.69	0.96	10.0	9.60	0.66
Mean	0.89	8.94	7.94	0.72	0.93	10.53	9.84	0.65
STD	0.03	0.31	0.51	0.03	0.07	2.87	2.97	0.03

Table 3.2: Watershed 2 calibration, using constant streamside slope in the representation of streamside areas

Calibration using a variable (random) slope

Table 3.3 shows the revised calibrated values for m and K when stream patch slope is estimated from a random distribution i.e. variance in streamside hydrologic characteristics is

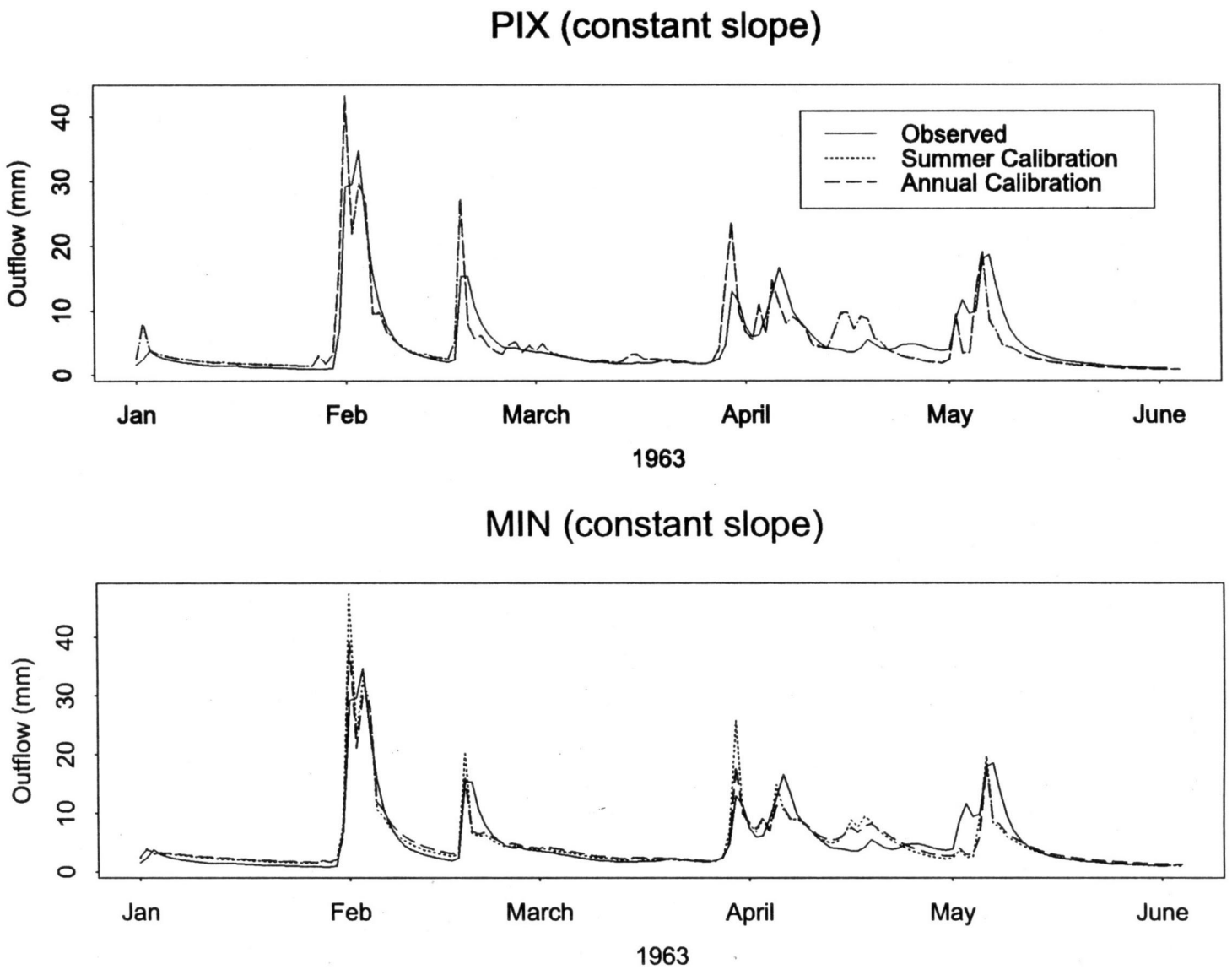

Figure 3.5: Winter Outflow for MIN and PIX partitioning strategies using constant streamside slope: Observed vs Annual and Summer Calibrations

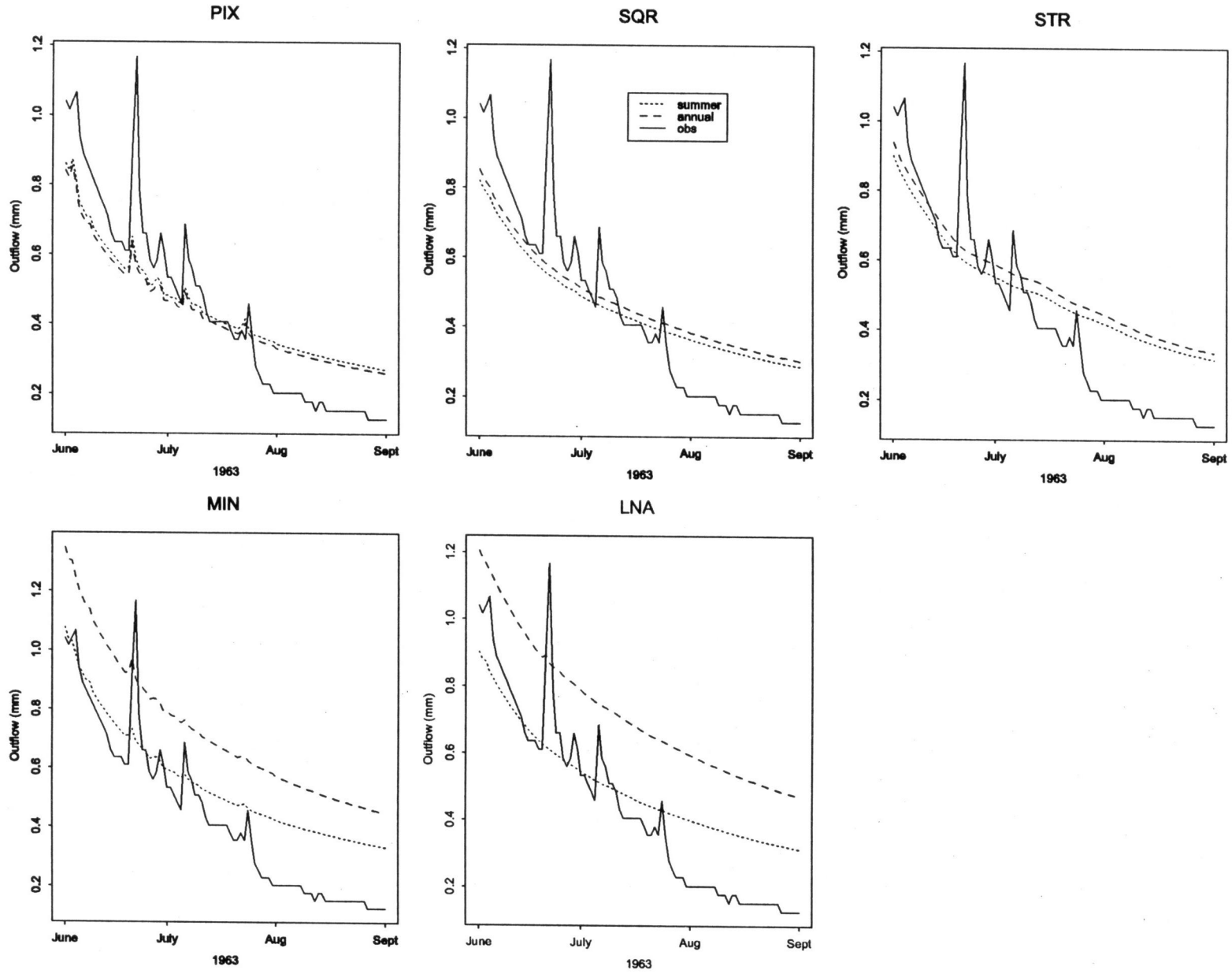

Figure 3.6: Summer Outflow by partitioning strategy using constant streamside slope: Observed vs Annual and Summer Calibrations

included. We initially focus on the implications of simply including variability in the stream patch gradient. Subsequent discussion will explore the importance of including patch specific information about these gradients. Summer calibrated values are similar to those computed for the constant slope approaches, with a similarly small variance between different partitioning strategies. Resulting Nash-Sutcliffe efficiencies, for the variable slope case, are slightly lower for summer calibrations, although visual comparison of outflow response shows a significant improvement in the ability of the model to capture low flow dynamics. This is a key finding since it suggests that the inclusion of variance in streamside slope is necessary in capturing low flow dynamics. This effect is discussed in more detail below.

Winter calibrated values, particularly for effective conductivity are significantly higher than obtained in the constant slope case (i.e. more than double) and produce slightly higher Nash-Sutcliffe efficiencies. Winter calibrated values also show an increased variance across the different partitioning strategies. Figures 3.7 and 3.8 illustrates the resulting summer low flow and winter high flow time series for the different partitioning approaches. Figure 3.7 shows that for winter time series, the variable slope and associated increase in annual calibrated transmissivity results in a slightly improved match between observed and modeled peak. The Nash-Sutcliffe efficiency measure is particularly sensitive to peak flow response. Visual examination of winter time series, however, suggests that difference between winter and summer calibrations is not significant for this period, given the uncertainty in model prediction of peak flow events. Only PIX and MIN representations are presented in Figure 3.7. Other representations produce a similar pattern of winter outflow.

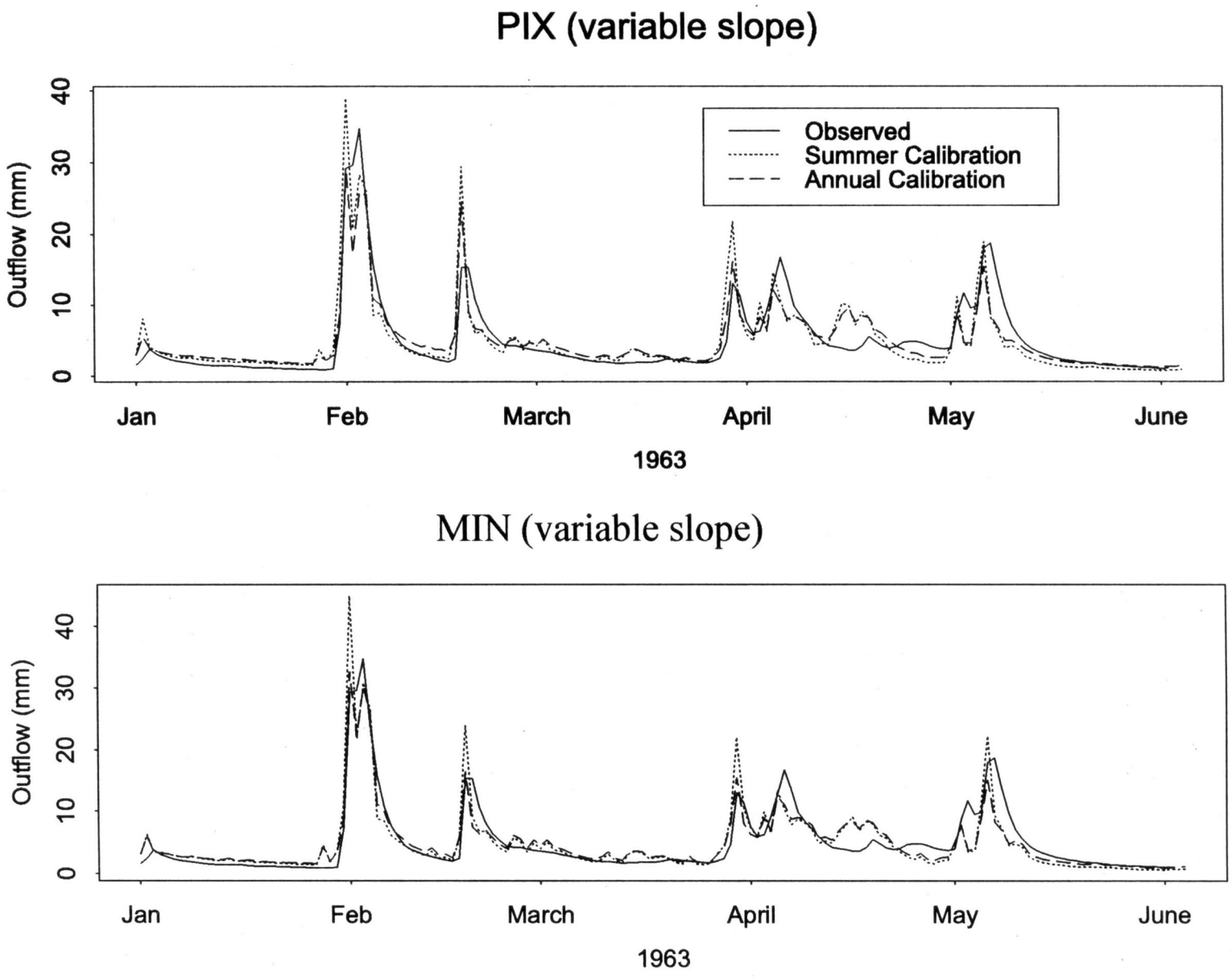

Figure 3.7: Winter Outflow for MIN and PIX partitioning strategies using variable streamside slope: Observed vs Annual and Summer Calibrations

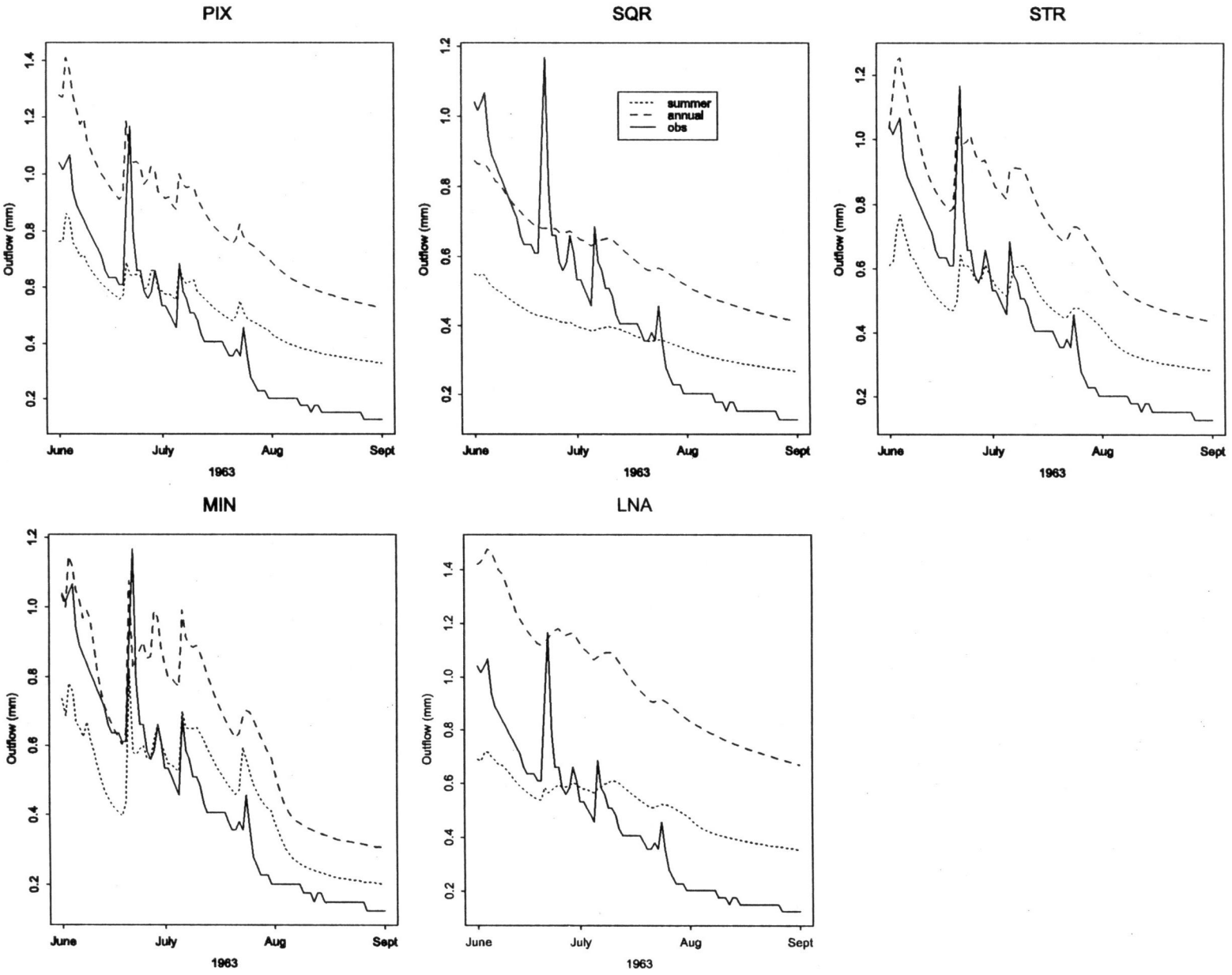

Figure 3.8: Summer Outflow by partitioning strategy using variable streamside slope: Observed vs Annual and Summer Calibrations

	Summer				Annual			
Part. Strategy	*m*	*K*	*T*	*Efficiency*	*m*	*K*	*T*	*Efficiency*
PIX	1.07	10.8	11.56	0.64	1.05	20.56	21.59	0.74
SQR	1.08	10.8	11.66	0.51	1.01	21.7	21.92	0.74
LNA	1.2	11.4	13.68	0.49	1.2	30.3	36.36	0.72
STR	1.02	10.25	10.46	0.59	1.02	17.7	18.05	0.75
MIN	1.02	10.24	10.44	0.65	1.03	15.13	15.58	0.77
Mean	1.08	10.70	11.56	0.58	1.06	21.08	22.70	0.74
STD	0.07	0.48	1.32	0.07	0.08	5.76	8.07	0.02

Table 3.3: Watershed 2 calibration, using a variable (random) streamside slope in the representation of streamside areas

To explore the implications of a high winter effective conductivity value further, we examine the Nash-Sutcliffe efficiency for a range of K and find that the higher effective conductivity associated with annual calibrations for the variable slope case is also associated with a change in parameter space. Figure 3.9 illustrates parameter topology using the MIN landscape representation for both summer and winter calibrations. Figure 3.9 shows a significantly higher sensitivity to K for the summer calibration where only a small range of K result in reasonable values for the Nash-Sutcliffe efficiency metric (i.e. efficiency > 0.5). Winter calibration for the variable slope case produces a significantly more gently sloping parameter surface in comparison with the summer calibration. A more gently sloping surface suggests a wider range of reasonably optimal parameters. The higher transmissivity, therefore, may in part be an artifact of this relaxation in parameter surface slope.

Significant differences between the parameter surfaces for winter and summer calibrations also suggest a seasonal difference in drainage organization. This seasonal change in drainage organization is also illustrated in Figure 3.10 which shows soil moisture deficit against elevation using the PIX landscape representation for a winter (Feb1) and a summer dry day

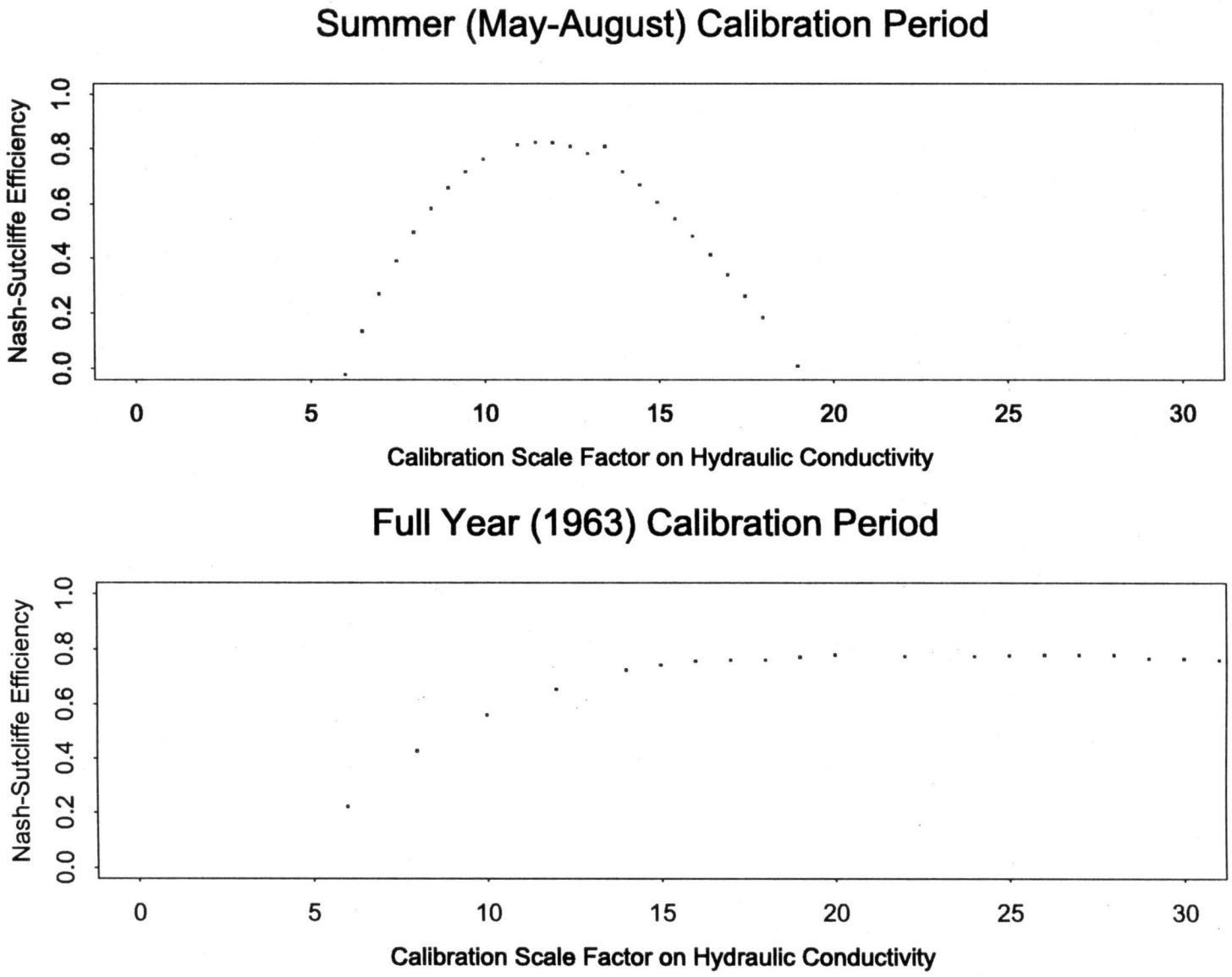

Figure 3.9: Nash-Sutcliffe Efficiency Sensitivity to variation in hydraulic conductivity, K - summer calibration versus winter calibration

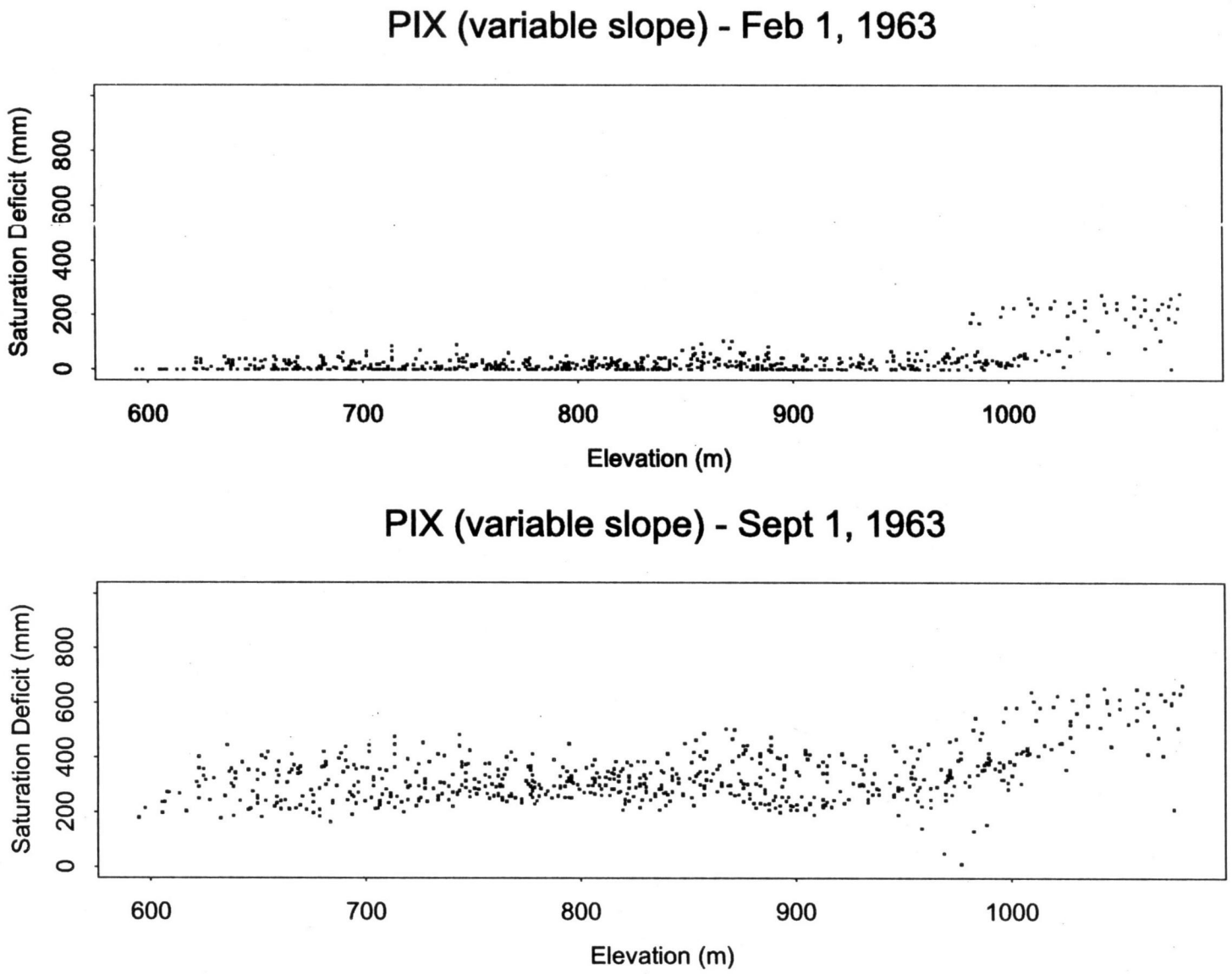

Figure 3.10: Saturation Deficit by Elevation (Estimated water table shape) for a) Winter (Feb 1) and b) Summer dry period (Sept 1)

(Sept 1), both using the summer calibration. The curves give a rough estimate of the shape of the water table. The graph illustrates a significant change in the water table shape from winter to summer period and an increase in soil moisture variance near to the stream, i.e. increased variance at low elevations during the summer. These results are consistent with field studies, discussed earlier, which indicate increasing soil moisture variability and more local organization during summer periods. Higher calibrated winter transmissivity values may also indicate a seasonal shift in effective transmissivity due to increases in the availability of macropore flowpaths and surface flow during wetter periods.

Variation in calibration results indicates a seasonal shift in relative importance of local streamside in drier periods to broader hillslope areas during wetter periods. Outflow results, shown in Figure 3.7 and 3.8, suggest that this effect is best captured by using summer calibrations. In addition, summer hydrographs show a significant over-estimation of baseflow if winter calibrations are used. Outflow comparisons are discussed in more detail below. Examination of the parameter surface in Figure 3.9 for summer and annual flows also shows a sharper gradient for the summer calibrations. Calibration for summer outflow response is, therefore, more sensitive. This reflects the much smaller flow volumes and more local behavior of summer outflow production. Summer storms are also likely to produce higher rainfall intensities. Given high infiltration capacity of soil on the sites, however, these effects should be fairly small.

To test the generalizability of the above results, calibrated values developed for 1963 were then applied to a range of years. Figure 3.11 shows the mean efficiency results for years 1961-1968 using the both annual and summer calibration and both variable and constant stream patch gradients. Results for the MIN landscape representation are shown where (S) denotes variable streamside slope. MIN is used as sample representation; since, from 1963 results, it provides the most efficient partitioning strategy, while still maintaining sufficient near stream resolution to capture summer low flow dynamics. From Figure 3.11, it is evident that (1) summer outflow values are more sensitive to calibration period and stream gradient implementation than winter outflow values (2) winter calibrated transmissivity values are consistently larger than summer calibrated transmissivity values and (3) that the variable

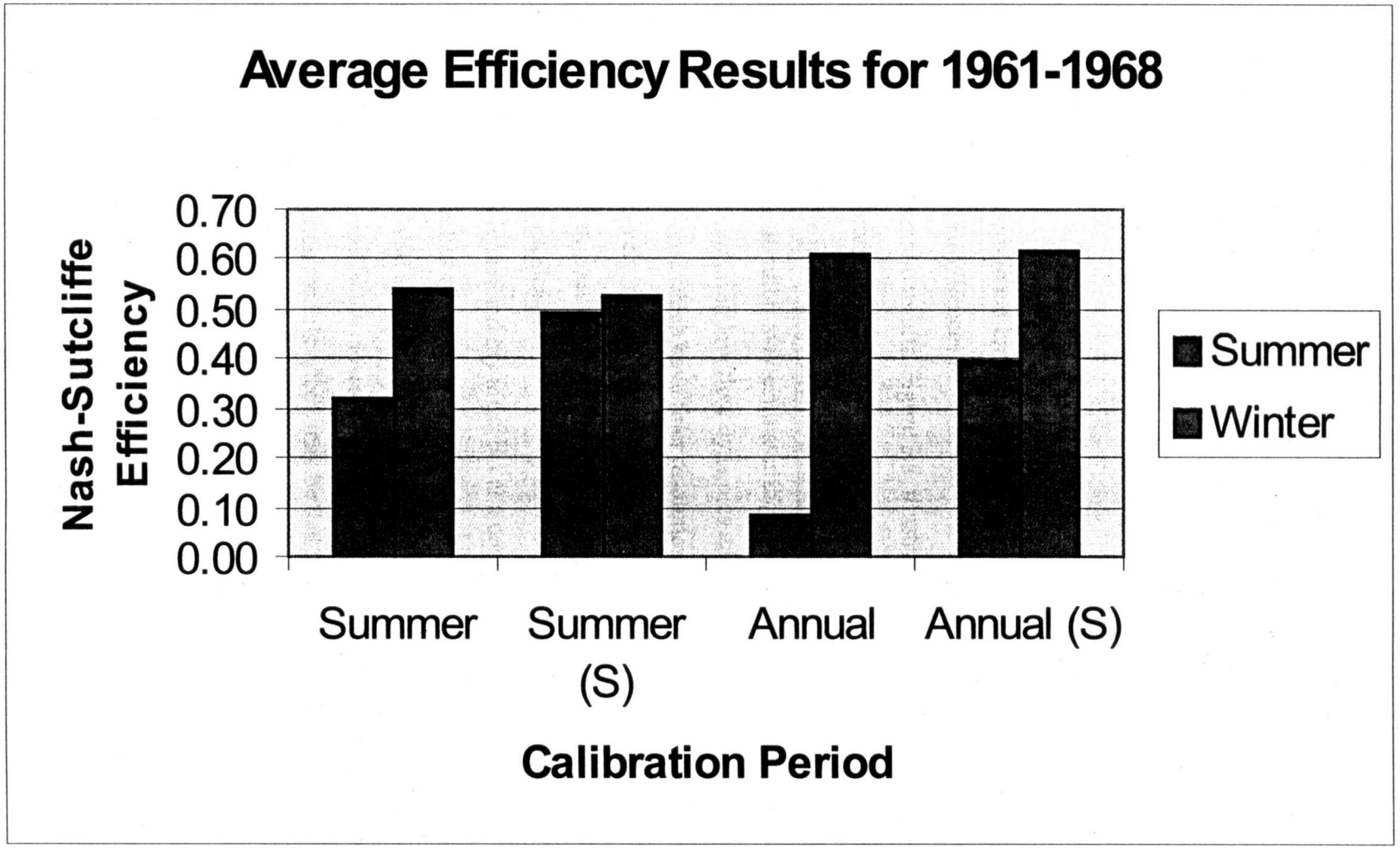

Figure 3.11: Mean Nash-Sutcliffe Efficiency for 1961-1968 for Summer and Annual Calibrations for constant and variable (S) streamside slope using MIN landscape representation

slope implementation is more robust than the constant slope approach. This is consistent with results discussed in detail above for 1963.

Outflow Comparisons

In addition to differences in calibration, both landscape representation and stream patch representation produce differences in simulated outflow. Outflow for the summer time period shows much more dramatic results. Figure 3.8 illustrates that for certain landscape representations the incorporation of variable slope greatly improves the ability of the model to capture summer low flow dynamics. This occurs for both summer and winter calibrations, although the winter calibration over-estimates the mean flow value by a significant amount. This improvement in capturing low flow dynamics occurs only with PIX, STR and MIN landscape representations, which have finer resolution patch structure in stream and near stream areas. Alternatively, the SQR approach, which allows the resolution of stream patch area to decrease to 90m, does not capture these summer low flow dynamics. Similarly in the LNA case, outflow dynamics are not well represented. The LNA landscape representation does partition relatively wet and dry areas but at a coarser resolution in comparison with PIX, STR and MIN approaches where the stream network is explicitly represented as 30m patches. Figure 3.8 also shows that among the landscape approaches with fine near stream resolution, the MIN approach produces the closest correspondence between observed and summer outflow. One explanation for this effect, may be that maintaining coarser resolution in upper portions of the watershed in the MIN approach may more accurately model water table gradients. In this model, water table gradients are assumed to follow topographic gradients. More aggregate landscape partitioning in the upper reaches of the watershed tends to smooth topographic slope, which may be more representative of a more gradually varying water table shape in the upper portions of the watershed. In areas, near to the stream, the water table may more closely follow finer resolution topography.

Figure 3.8 also illustrates the improvement in capturing low flow dynamics obtained by using variable slope in stream side patches. It is interesting to note that this improvement is not reflected in the Nash-Sutcliffe efficiency measures shown in Table 3.2. Simulations using the variable slope have slightly lower Nash-Sutcliffe efficiencies, shown in Table 3.3, than those using the constant slope do. These differences, however, are small in comparison with overall parameter space variation illustrated in Figure 3.8. In addition Nash-Sutcliffe efficiency tends to reflect the correspondence between observed and modeled high flow values rather than the dynamics of hydrologic response.

Comparison of 1st order different time series illustrates more clearly the improvement associated with the use of variable stream patch gradients. Figure 3.12a shows the Nash-Sutcliffe efficiency of the 1st order difference applied to the summer outflow time series for the different landscape partitioning strategies, and variable vs. constant stream patch slope. (Variable stream patch slope is denoted by a subscripted s to landscape partitioning strategy name). Figure 3.12b shows the Nash-Sutcliffe efficiency of the regular summer outflow hydrographs for the different strategies. The 1st order difference efficiencies more clearly illustrates the inability of constant slope and non-stream based partitioning strategies (i.e. LNA and SQR) to capture summer low flow dynamics. Regular time-series efficiencies tend to ignore these outflow dynamic distinctions. One exception is the low efficiency value obtained by MIN for the variable slope case. Figure 3.13 illustrates the time series of 1st order differences for variable slope MIN representation against observed values. This time series illustrates that the low efficiency value for the MIN is related to a temporal shift in the modeled time series results. For the 1st order difference, efficiencies for all strategies are quite low (< 0.25). This may in part be due to the daily time step used in the model, which may result in small shifts in the timing of baseflow augmentation and decay, as illustrated in Figure 3.13 for the MIN approach.

Simulations using the MIN landscape representation are also created for a neighboring watershed, Watershed 1, for 1962 to test the generalizability of these results. 1963 calibration values from Watershed 2 for 1963 are used to scale transmissivity via m and K. Reasonable Nash-Sutcliffe efficiencies, 0.55 and 0.46, are obtained for both summer and winter flows,

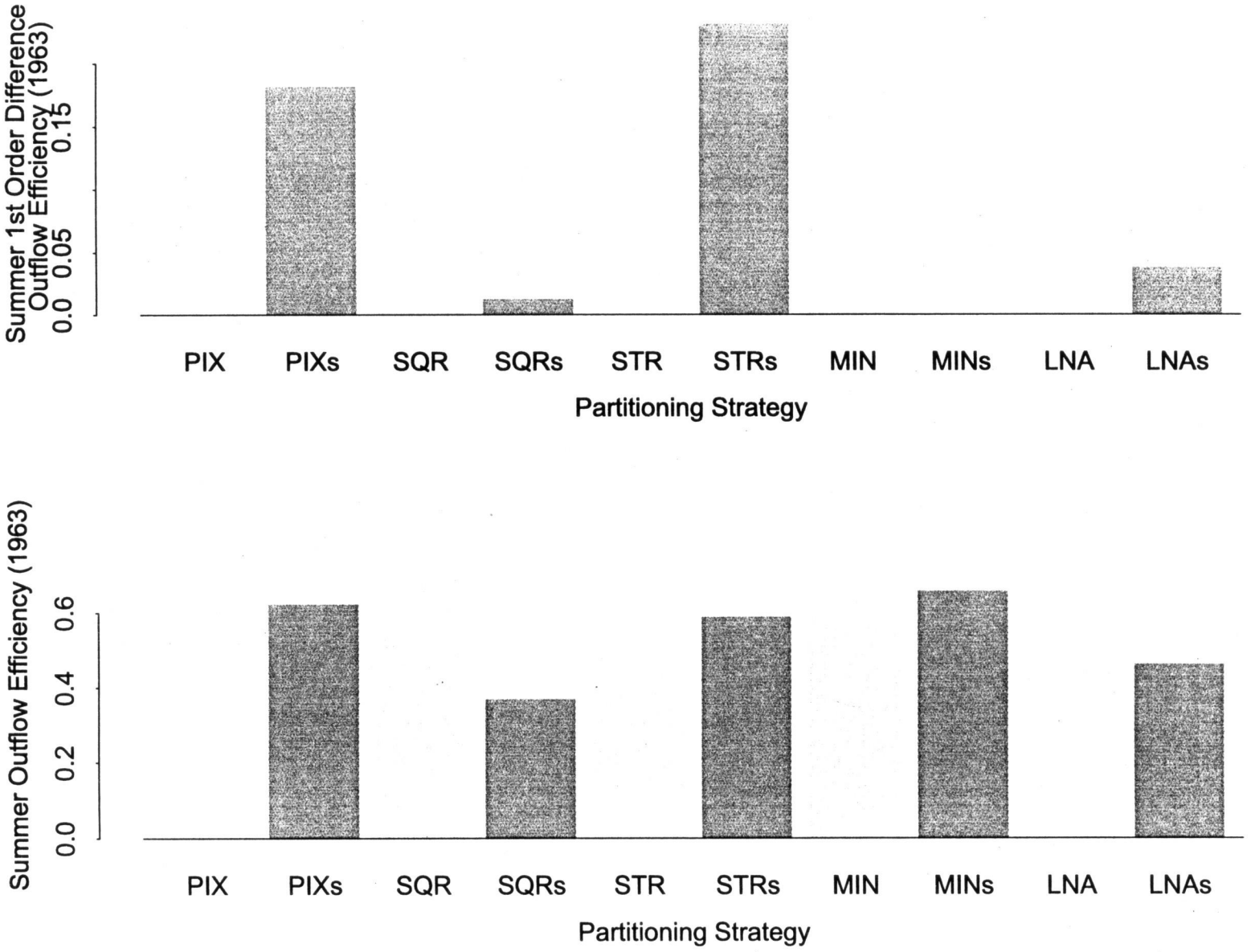

Figure 3.12: Nash-Sutcliffe Efficiency by partitioning strategy for a) 1st order difference time series and b) outflow time series

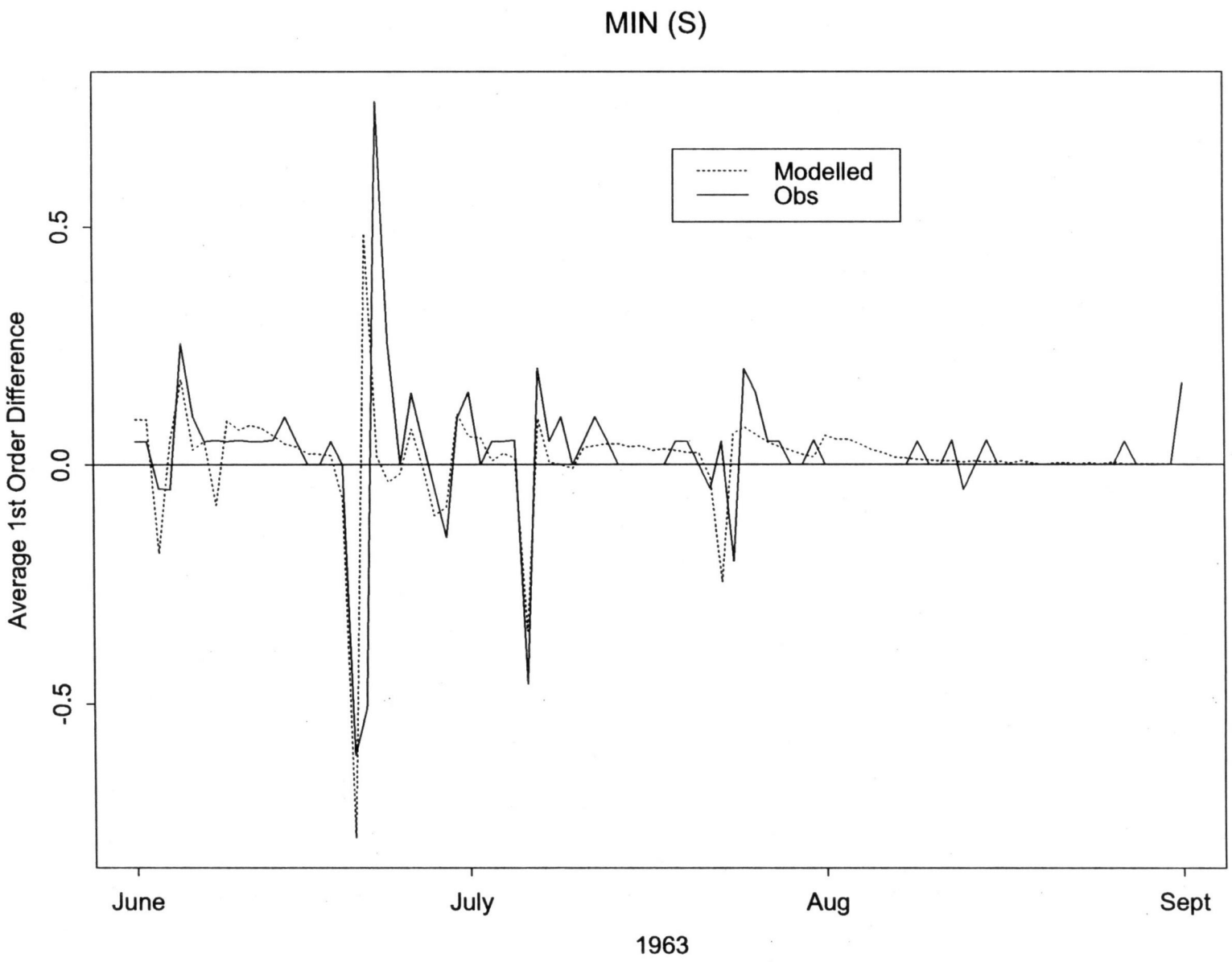

Figure 3.13: 1st order difference time series (summer 1963) for observed and MIN landscape representation

respectively, using calibrated m and K from Watershed 2. Recalibration using observed 1962 data from Watershed I does not significantly change the results. Figure 3.14 illustrates summer runoff results for Watershed I using summer calibrated values from Watershed 2. Results show a similar pattern to those observed for Watershed 2, such that use of variable slope in stream patch implementation is necessary to capture summer outflow dynamics.

Sensitivity to Local Stream Patch Information

The above results indicate the importance of including variability in stream patch slope implementation. To test the importance of including local information in modeling this variability, we test alternative implementations that use local patch slope or local flowpath gradient to represent the gradient to the stream. In coarser scale simulations, this information may not be available. We included it here to test the relative contribution of this information to simulation results. Table 3.4 records the calibration results for the MIN landscape representation for the different approaches to representing gradient to the stream. Results of including patch specific information are compared to those obtained by using a random distribution to incorporate variability in the stream patch gradient. Figure 3.15 illustrates the associated summer outflow response. For simulations using the local patch slope, calibrated values are similar to those obtained with a random variation in stream-side gradient and show a similar sensitivity to summer low flow dynamics, both in terms of outflow and 1^{st} order difference Nash-Sutcliffe efficiencies. Similarly, winter calibrated values and outflow results show a negligible difference between the random and local patch slope approaches. Use of the flow path gradient, however, degrades results and produces very poor Nash-Sutcliffe efficiency for 1^{st} order time series comparisons. Figure 3.15 shows that this corresponds with flashier hydrograph results, which may reflect the generally steeper gradients in flowpath direction upslope from the stream. These results suggest that, for this catchment, using a random distribution to include variance in sub-patch streamside gradient improves the model ability to capture summer low flow dynamics and performs as well as the use of local patch slope information and better than using upslope (flowpath) patch gradients. Although including variance does improve the results, Nash-Sutcliffe efficiencies are quite low for all approaches, particularly the 1^{st} order difference efficiencies. This may

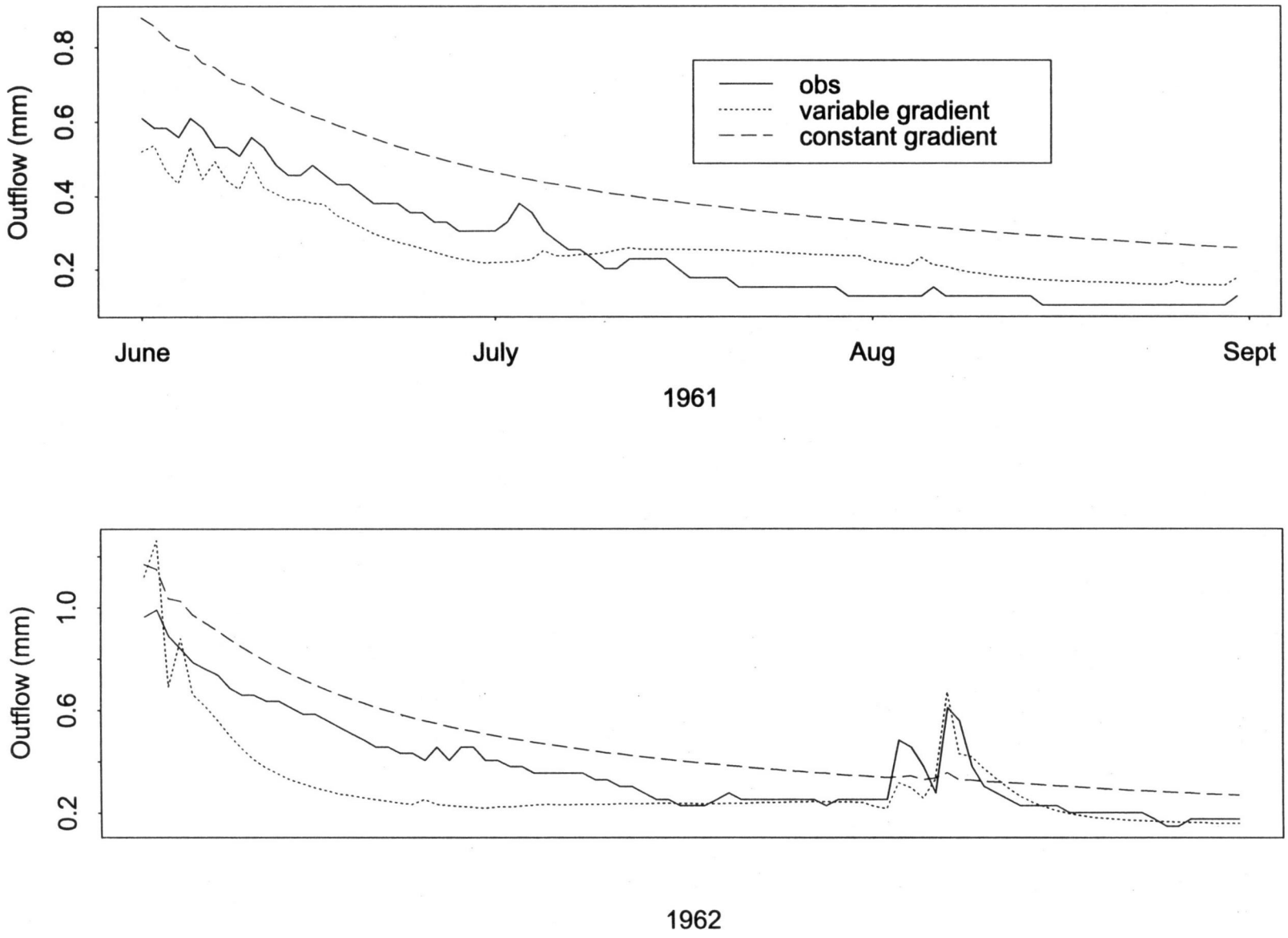

Figure 3.14: Summer outflow for Watershed 1, observed vs. simulated using MIN landscape representation with summer calibration from watershed 2 for 1963

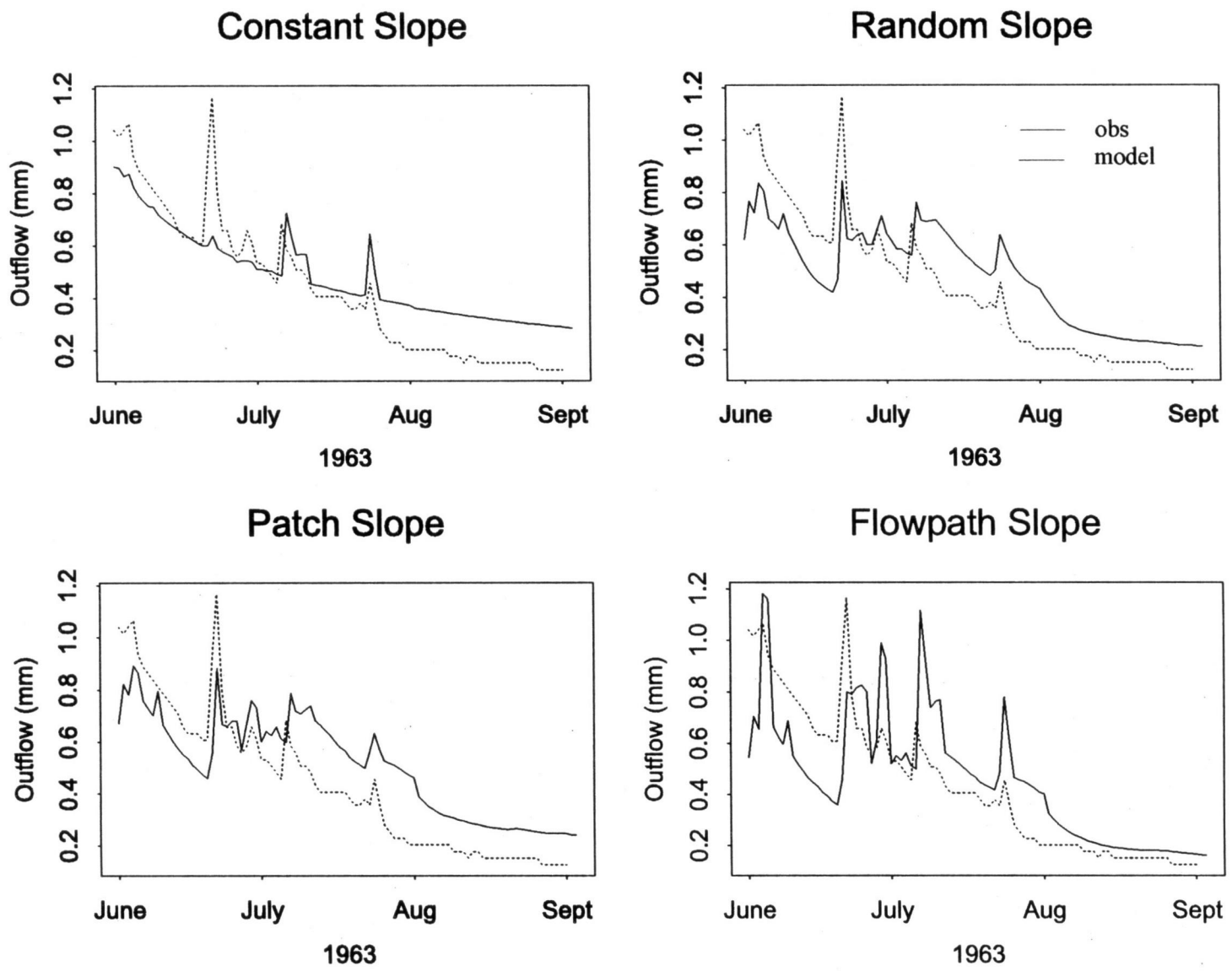

Figure 3.15: Summer outflow by streamside gradient implementation

suggest that the model requires additional information to capture summer flow dynamics. It may be that calibration of effective conductivity must account for local spatial variability of soil characteristics including the presence of macro-pores. Particularly during the drier summer, the effective conductivity in local streamside areas will control streamflow dynamics. These areas may, because of the their relative wetness, differ in effective conductivity in comparison with drier upland areas. The current model calibrates effective conductivity at the hillslope scale. Additional information would be required to calibrate the spatially variability of conductivity.

	Summer				***Annual***			
Streamside Gradient Estimation	**M**	**K**	**Outflow N.S. Eff.**	**1st order N.S. Eff**	**M**	**K**	**Outflow N.S. Eff.**	**1st order N.S. Eff**
Constant Gradient	0.87	8.6	0.68	0.11	0.96	10.0	0.72	0.62
Random Gradient	1.02	10.4	0.66	0.38	1.03	15.66	0.77	0.65
Local Patch Slope	0.97	9.7	0.69	0.44	1.03	15.13	0.77	0.66
Flowpath Gradient	1.02	9.8	0.65	0.12	1.03	15.24	0.77	0.52

Table 3.4: Alternative streamside slope estimation; calibration results

Conclusions

Results from this study highlight the particular sensitivity of summer low flow modeling to calibration and landscape representation. This study found that low flow or summer periods are particularly sensitive, since they reflect periods where areas able to make significant contributions to runoff production occur at a smaller scale. These findings are consistent field studies such as Woods et al (1997),Western et al (1999) and Grayson et al (1997) who found spatial variability of soil moisture to be greater during the drier periods and observe that the control of flow dynamics is dominated by local rather than hillslope processes during drier periods. In winter, wetter conditions, larger regions within the watershed make significant contributions to runoff production. The scaling and calibration issues discussed in this paper are particularly important in the modeling of low flow periods. Although summer flows represent only minor portions of the total annual flow, low flow dynamics have important implication for stream quality and ecosystem health issues. Further work will address whether summer calibration should also account for the potential spatial and within season temporal variability in effective conductivity, particularly in local, relatively wet areas. We hypothesize that further improvement in capturing low flow dynamics may be gained by examining local streamside effective conductivity. Higher effective conductivity in these wetter regions may reflect a distribution of macropores that is partially controlled by soil moisture conditions.

Examination of calibration results recommends that calibration be based on summer flow behavior since it is more likely to capture summer outflow dynamics and does not significantly degrade annual or winter results. For sensitive summer calibration, results here also note the limits of the Nash-Sutcliffe measure of outflow response for determining how well the resulting hydrographs are able to capture low flow dynamics. In addition to optimization based on the Nash-Sutcliffe, we propose a complementary use of the 1^{st} order difference time series. The Nash-Sutcliffe efficiency measure for 1^{st} order difference time series highlights flow dynamics, which are overwhelmed by mean values when using outflow time series comparisons. It should be noted, however that Nash-Sutcliffe efficiency values

for 1st order difference comparisons can be quite sensitive to small temporal shifts in the time series results. The use of the more sensitive 1st order difference and summer calibration period are therefore recommended as an approach to help to constrain the calibration procedure used in the model by restricting the range of acceptable parameters. Multiple metrics can be used to constrain the simulation by using an optimization function derived from a combination of the different measures. In this case, since summer calibration is more sensitive, it will control the selection of optimal parameters. Further constraint may be obtained by focusing on the pattern of soil moisture that controls this response. These simulations suggest a shift in drainage organization from a more local to hillslope spatial extent as the climate shifts from summer dry to winter wet periods. It is not feasible to measure soil moisture from the entire hillslope and point measurements cannot be used to calibrate a patch model. It may be possible however to use differences between soil moisture samples taken from ridge and streamside areas. Comparison between model and measured differences throughout the year will indicate how well the model is able to capture soil moisture dynamics.

In addition to the above recommendation on calibration procedure, this study also addresses the minimum representation necessary to accurately capture seasonal hydrologic response. Results suggest that the representation of stream side area is significant in the ability of the model to model summer low flow dynamics. Representation of stream side area as individual 30 m wide patches and a fine resolution partitioning of areas with high TOPMODEL wetness indices was necessary in order to capture summer response dynamics. Much coarser resolution representation of upland areas, on the other hand, was adequate. Thus a partitioning strategy based on 100m elevation intervals, a stream network and only two topographically defined wetness intervals, MIN, performed as well as the finer resolution pixel based approach, PIX. In some cases, the simpler MIN landscape representation actually performed somewhat better than finest resolution representation which suggest there may be some error reduction due to smoothing in the upslope areas by the coarser resolution partitioning strategy. Sensitivity to representation has implications for scaling, since it suggests that fine resolution information may only be necessary in particular areas, in this case, those areas adjacent to the stream. By using irregularly shaped patches, the explicit

routing approach provides a flexible and efficient method to address this spatially structured sensitivity to landscape representation.

The relatively small extent of the critical area in terms of near stream representation in this study may be a function of the steep, highly dissected hillslopes that comprise the H.J.Andrews watershed. Watersheds with more gently sloping or glaciated valleys will likely show a broader extent to the critical area. Additional study across a range of different watersheds and particularly for areas were fine resolution (i.e. < 30m) information is available for near stream areas would further clarify the role of calibration and landscape representation in modeling. The goal of such an approach would be to provide better and more systematic guidelines for modeling watersheds using across a range of available information, scales and surface variability.

This study also found that representing variability in stream pixel slope is important in representing low flow dynamics and less so for representing winter hydrologic response. Inclusion of variability in streamside gradient has similar scaling implications to patch representation. Increased sensitivity in the summer is again related to the more local behaviour of runoff dynamics occurring at that time. Results here suggest inflow areas surround the stream cannot be represented as a homogeneous patch, since variation in soil moisture characteristics along the stream length is important. Although this particular study focused on gradient, the use of soil transmissivity as another multiplier in (1) in the subsurface routing model, suggests that a similar sensitivity would be expected with soil transmissivity. In the actual catchment, in both slope and in transmissivity may act to control the pattern of outflow. These results reflect the potential in larger scale modeling to account for the role of fine scale variability in near stream controlling processes through the use of estimates of a parameter distribution i.e. without including explicit representation of the spatial organization of the stream side parameters which would require fine resolution information.

As noted in this study, results were not particularly sensitive to the distribution used to generate variability in streamside gradient. These results suggest that it is the variability in

hydrologic characteristics rather than spatial organization which is important within the stream side areas. Thus estimation of gradient distributions rather than explicit representation of these local areas can improve model representation of low flow dynamics. Although capturing exact time series pattern is difficult, as evidence by the low 1st order difference Nash Sutcliffe efficiencies, the use of variability in streamside gradient enables the model to capture summer streamflow variability. Capturing variability in low flow dynamics is important, since these dynamics may impact stream habitat and water quality. Where fine scale information to compute stream side gradients is not available, these results suggests that a hybrid model that combines the explicit routing approach with a distribution approach (similar to TOPMODEL) may be appropriate to represent sub-patch dynamics. In a hybrid model, the coarse resolution explicit routing approach preserves spatial connectivity between upland and bottomland areas while the within patch aspatial distributions within near stream areas or local hollows captures the role of high soil moisture variability in these areas during drier periods. The sub-patch aspatial component allows relevant spatially variability in soil moisture to be modeled without requiring detailed sub-resolution topographic and soils information. In modeling studies where fine resolution information is not available, incorporation of within patch distributions of specific hydrologic controls (i.e. slope or transmissivity) could provide a method to capture the significant variability in near stream behavior, while maintaining an overall explicit routing approach.

References

Barling, R., D., Moore, I.D., and Grayson, R.B. 1993 A quasi-dynamic wetness index for characterizing the spatial distribution of zones of surface saturation and soil water content, *Wat. Resour. Res* ,**30**, 1029-1044.

Band, L.E., Vertessy, R., Lammers, R., 1995. The effect of different terrain representations and resolution on simulated watershed processes, *Z.Geomorph N.F.* Suppl-Bd **101**, 187-199.

Band, L.E. Patterson, P., Nemani, R.R., and Running, S.W. 1993. Forest ecosystem processes at the watershed scale: incorporating hillslope hydrology. *Agriculture Forest Meteorology* **63**: 93-126.

Beven, K and Kirkby, M. 1979. A physically-based variable contributing area model of basin hydrology, *Hydrologic Science Bulletin* , **24**, 43-69.

Bruneau, P., Gascuel-Odoux, C., Robin, P., Merot, Ph., and Beven, K. (1995) "Sensitivity to space and time resolution of a hydrological model using digital elevation data", Hydrol. Proc., 10th Anniversary Issue, 55-69.

Clapp,R., Hornberger,G. 1978. Empirical equations for some soil hydraulic properties, *Wat. Resour. Res*, **14**, 601-604.

Duan, J. 1996. A coupled hydrologic-geomorphic model for evaluating effects of vegetation change on watersheds, Thesis, Department of Geography, University of Oregon.

Daly, C., Neilson, R.P., Phillips, D.L. 1994. A statistical-topographic model for mapping climatological precipitation over mountainous terrain, *Journal of Applied Meteorology*, **33**:2, 140-157.

Nelder, J. and Mead R. 1965. A simplex method for function minimization, *Comput. J.*, **7**, 308-313.

O'Loughlin, E.M.1990 'Modeling soil water status in complex terrain', *Agric. For. Meteorol.* **,50**, 23-38.

Ostendorf, B., Manderscheid, B. 1997. Seasonal modeling of catchment water balance: A two-level cascading modification of TOPMODEL to increase the realism of spatio-temporal processes, *Hydrol. Processes* , 11, 1231-1242.

Rosentrater, L. 1997. The thermal-climate of the H.J.Andrews Experimental Forest, Oregon, Thesis, Department of Geography, University of Oregon.

Running, S. 994.Testing Forest-BGC ecosystem process simulations across a climatic gradient in Oregon, *Ecological Applications*, **4**:2, 238-247.

Running, S., Nemani, R. and Hungerford, R. 1987. "Extrapolation of synoptic meteorological data in mountainous terrain and its use for simulating forest evapotranspiration and photosynthesis", *Can .J. For. Res* **17**:472-483.

Running, S. and Hunt, 1993. Generalization of a forest ecosystem process model for other biomes, BIOME-BGC and an application for global scale models, in *Scaling Physiological Processes: Leaf to Globe*, Academic Press.

Saulnier, G.M., Obled, C., and Beven, K., 1997. 'Analytical compensation between DTM grid resolution and effective values of saturated hydraulic conductivity within the TOPMODEL frameworks'. *Hydrol. Processes*, 11, 1331-1346.

Saulnier, G. M., Beven, K., Obled, C., 1997b. "Digital elevation analysis for distributed hydrological modeling: Reducing scale dependence in effective hydraulic conductivity values", *Wat. Resour. Res*, **33**, 2097-2101.

Saulnier, G. M., Beven, K., Obled, C., 1997c. 'Including spatially variable effective soil depths in TOPMODEL, *Journal of Hydrology*, **202**, 158-172.

Stednick, J. 1996. Monitoring the effects of timber harvest on annual water yield", *Journal of Hydrology*, **176**, 79-95.

Tani, M. 1997.'Runoff generation processes estimated from hydrological observations on a steep forested hillslope with a thin soil layer', *Journal of Hydrology*, **200**, 84-109.

Western , A., W., Grayson, R.B., Bloschl, G., Willgoose, G.R., McMahon, T.A. 1999. 'Observed spatial organization of soil moisture and its relation to terrain indices', *Wat. Resour. Res*, **35**, 797-810.

White, J. D. and S.W. Running 1994. 'Testing scale dependent assumptions in regional ecosystem simulations', *J. of Veg. Science*, **5**, 687-702.

Wigmosta, M., Vail, L., Lettenmaier, D. 1994. 'Distributed hydrology-vegetation model for complex terrain', *Wat. Resour. Res*, **30:6**, 1665-1679.

Woods, R. A., Sivapalan, M., Robinson, J.S. 1997. Modeling the spatial variability of subsurface runoff using a topographic index, *Wat. Resour. Res*, **33**, 1061-1074.

Zhang, W., Montgomery, D. 1994. 'Digital elevation model grid size, landscape representation and hydrologic simulations', *Wat. Resour. Res*, **30**, 1019-1028.

Chapter 4: Assessing the impact of road construction and forest harvesting on hydrologic response using RHESSys

Preface

This chapter illustrates the application of RHESSys and associated sub-models of drainage organization in the assessment of forest harvesting effects, particularly those due to roads. The need for hydro-ecological models such as RHESSys to integrate the findings from field research studies and apply them in a larger regional context across a population of hillslopes was discussed in the introduction. This background also illustrates the importance of drainage organization, and the potential for roads to modify drainage organization and subsequent hydrologic response. Earlier chapters have established the required model development, calibration and landscape representation that is necessary to represent topographic and soil controls on drainage organization. Incorporation of roads as objects into RHESSys requires dynamic modification of the drainage network and is described in this chapter. Results of this approach to modeling the effect of roads is presented and compared with field based studies on the effects of roads for a harvest watershed in the test study, H.J.Andrews catchment.

*submitted as Tague, C., Band, L.E, Assessing the impact of road construction and forest harvesting on hydrologic response using RHESSys, *Earth Surface Processes and Landforms*.

Abstract

In this paper, we incorporate a conceptual model of the effect of roads and forest harvesting on hillslope soil moisture and runoff production into a hydro-ecological modeling system, RHESSys and discuss the model results for a range of scenarios for a small catchment in the Western Oregon Cascades. We use the model to explore the implications of road cut depth and road drainage patterns, on seasonal hydrologic responses including runoff production, soil moisture and ecological processes such as evapotranspiration. By examining hydrologic response within a seasonal and hillslope context, we illustrate the complex role played by roads in terms of both the spatial and temporal persistence of the effects of an increase in local drainage efficiency associated with particular road segments. Model results are also compared with observed outflow responses for a paired catchment study using the test case watershed. Results show the potential for an ecologically significant change in soil moisture in the area downslope from the road. These changes are mediated by the drainage patterns associated with roads, specifically whether road culverts serve to concentrate or to diffuse flow. The modeled effects on seasonal outflow response are less significant but do show clear temporal patterns associated with climate pattern, hillslope drainage organization and road construction. Comparison between modeled and observed outflow response suggest that the model does not yet capture all of the processes involved in assessing the effects of forest road construction.

Introduction

Forest roads have been associated with increased peak flows for a number of monitored catchments in the Pacific Northwest. Plot-level studies have also illustrated the ability of forest roads to intercept and route both subsurface and saturated overland flow more efficiently to the stream (Wemple et al, 1996) as well as generate additional surface runoff as a result of reduced infiltration capacity of the road surface (Luce and Cundy, 1994). This paper uses an ecosystem model, RHESSys, Regional Hydro-Ecological Simulation System, to address the effects of forest roads on hydrologic response within both a catchment and a seasonal context. We use the model to generate hypotheses about the broader spatial and seasonal effect of roads, which include impacts on summer low flow and on peak flow responses. We compare these modeling results with available field data and propose additional field testing.

The connection between forest harvesting and hydrology continues to be an important scientific and forest management issue in the Pacific Northwest. Both field based and modeling approaches have explored changes in the magnitude, timing and inter-catchment variability of hydrologic response following harvest. Roads in themselves have the potential to alter hydrologic response and may also act synergistically with forest harvesting. Case studies, such as Jones and Grant (1996), Wright et al (1990), Harr et al. (1975), King and Tennyson (1984), Keppler et al. (1990), indicate that roads can have significant effects on peak flow; however, these results vary significantly across sites, different road construction patterns, storm events and seasonal precipitation. Spatially distributed modeling provides a technique to organize the interacting effects of these different controls on hydrologic response thereby helping to explain observed variability in watershed hydrologic responses to road construction.

In many field and modeling studies, the exploration of the effect of roads has centered on peak flow response (e.g. Storck et al., 1998). In this paper, we include consideration of the seasonal and spatially distributed effects of roads. Variability in peak flow response due to roads may in part be explained by examining this seasonal context. In the Pacific Northwest, there is a distinct seasonality to precipitation, with a significant percentage of precipitation

falling during winter months followed by a dry period during the summer. In addition, effects of forest harvest disturbance on summer low flow can have significant ecological consequences related to streamflow quality and quantity, which support aquatic habitat and human uses of streams (Johnson, 1998; Hicks et al, 1991). Disturbances may also affect soil moisture, which is a control on plant evapotranspiration, photosynthesis and species competition, especially in water limited environments.

To examine the role played by roads, we incorporate a conceptual model of road impacts into a spatially distributed hydro-ecological modeling system, RHESSys. Simulations are developed for a test case harvested watershed in the H.J.Andrews Experimental Forest in the western Oregon Cascades. A range of scenarios is used to generate hypotheses about the variability of hydrologic response to roads. Simulation results are also compared with results from an empirical study in the H.J.Andrews watershed in order to assess how well the model captures the processes of interest.

Conceptual Model

Wemple et al (1996) propose that connectivity of road ditches and culverts with stream networks increases the impact of roads on peak flow. Wemple et al (1996) suggest that road-stream connectivity effectively increases the drainage density of the watershed and consequently can increase peak flow. Our conceptual model also includes consideration of impacts where roads are not directly linked to a stream, but still route flow to particular downslope areas. In these cases roads may serve to concentrate flow in relatively wet areas or to diffuse flow into relatively drier downslope areas.

Thus, we are interested not only in increased outflow due to the increased hydrological connectivity to stream, but also in:

(1) hydrologic effects on areas below the road which receive less recharge due to the redirection of flow into ditches.

(2) outflow and soil moisture response in cases in which road culverts drain into areas not hydrologically connected to the stream.

The effects of road construction include both the direct effects due to water intercepted by the road and rerouted and the secondary effects in the area below the road, due to the reduction in subsurface and surface flow inputs. As shown in Figure 4.1, the reduction in recharge to areas below the road will result in a decrease in downslope soil moisture. It may also result in a decrease in saturated subsurface throughflow. From the perspective of catchment outflow, it is the combination of the effects from areas below the road and the increase in drainage efficiency due to redirection by the road that will create the net effect of streamflow. The relative timing and spatial distribution of these two effects will likely be different, since road-redirection effects are fast relative to effects on subsurface throughflow in the area below the road. The combined effects will create a temporally complex pattern and will create contrasting effects in different areas of the hillslope. We use the implementation in RHESSys to explore the interaction of these different processes.

The above discussion applies in the case where water is redirected by the road into culverts and gullies which are hydrologically connected to the stream, and thus they remove water from the road discharge area. In many cases, however, road culverts serve only to concentrate the flow in particular areas below the road. The effect of this concentration of flow will depend upon the characteristics of the receiving areas. In Figure 4.2 we illustrate two end member cases. In the first, flow is concentrated in a relatively wet area below the road. This would correspond with road culverts draining into downslope hollows, which may increase areas of saturated subsurface throughflow. The potential to increase peak flow effects is similar to the situation where culverts are hydrologically connected to the stream, although effects may be diminished since the flow is not channeled. Alternatively, road culverts may redirect the flow to relatively drier areas and act to essentially diffuse the flow, as shown in Figure 4.2. In this case, we would expect potentially greater evapotranspiration in the discharge area and an overall reduction in outflow as opposed to the preceding two

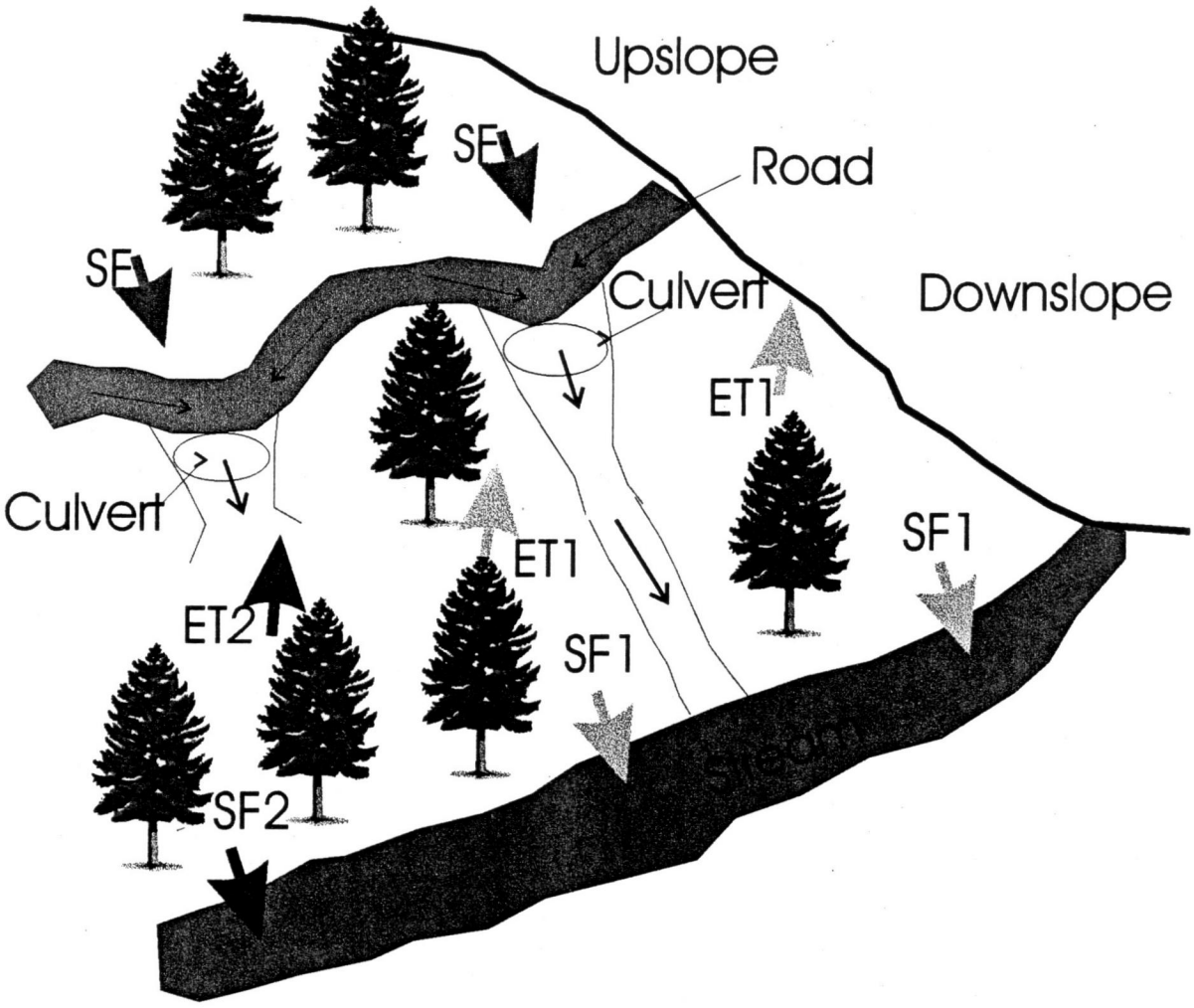

Figure 4.1: A conceptual model of the effects of roads on downslope saturated subsurface throughflow, evapotranspiration and runoff production

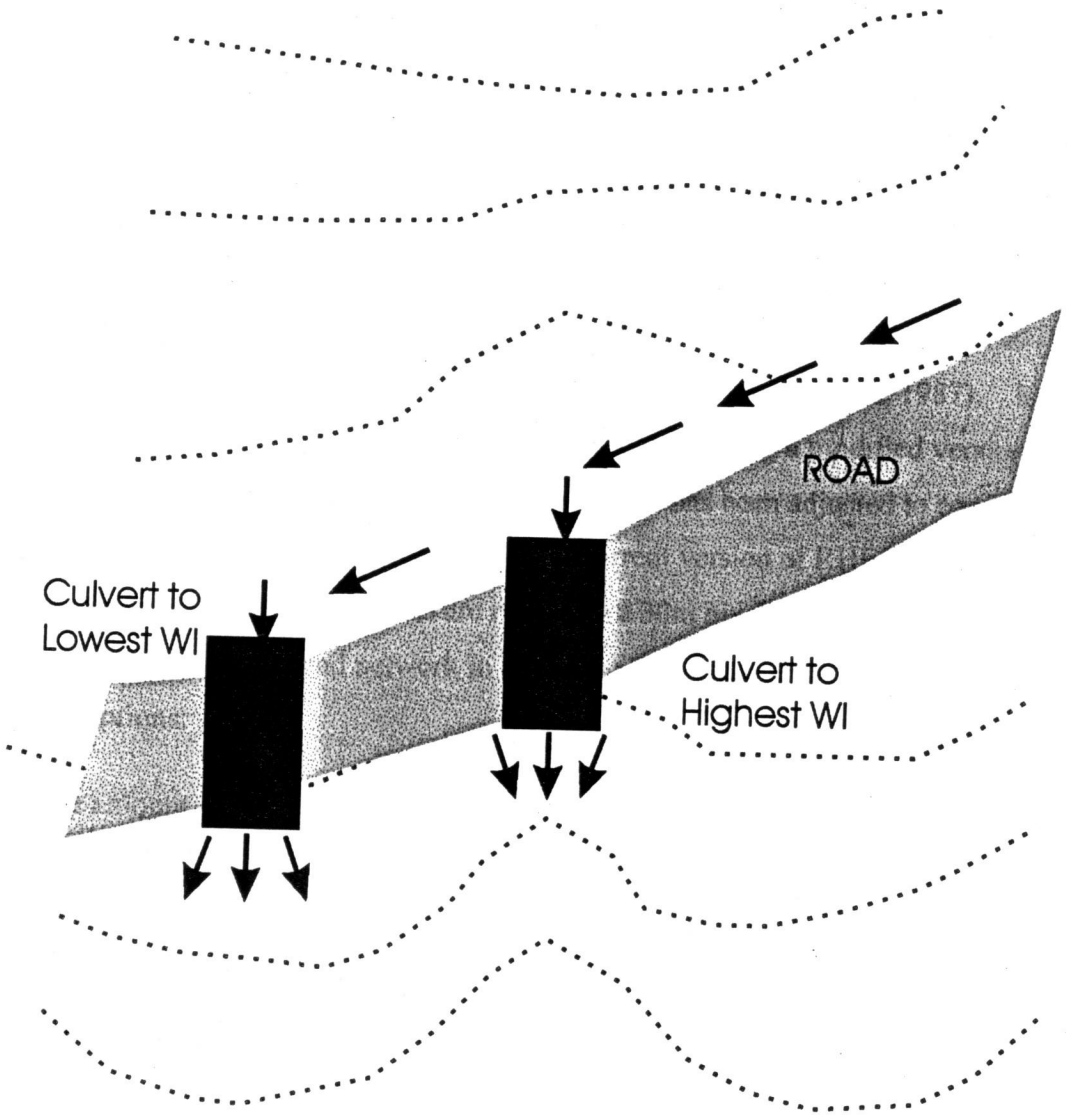

Figure 4.2: Road drainage pattern alternatives: Routing to highest wetness index; Routing to the lowest wetness index

cases where flow is concentrated or channeled directly to the stream. In addition to connectivity, road cut depth can vary depending upon local slope, and road width. Road cut depth directly impacts the amount of subsurface runoff that is intercepted by the road and therefore the magnitude of road effects.

The Simulation Model

To illustrate the various effects of roads on hydrologic response, we apply the above conceptual model to RHESSys: the Regional Hydro-Ecological Simulation System. RHESSys is modeling system which combines distributed flow modeling with an eco-physiological canopy model, based on BIOME_BGC (Running and Hunt, 1993) and a climate interpolation scheme based on MTN_CLIM (Running et al, 1987). In RHESSys simulations, explicit distributed routing is performed using a modified version of the DHSVM algorithm (Wigmosta et al, 1994) which has been adjusted to consider irregular patch areas. Process algorithms used in the current version of RHESSys are described in Tague et al. (1998). Simulations are run using a 30m pixel based partitioning strategy. Implementation of a road network in the RHESSys framework makes the following assumptions:

· The amount of subsurface throughflow intercepted by the road is a function of the road cut depth and the current saturation deficit of the area upslope from the road. Any saturated subsurface throughflow above the road cut and any overland flow are consider to be intercepted by the road.

· The intercepted flow is redirected to one of three downslope patches, specified by the user: the nearest stream, a relatively wet adjacent downslope or a relatively dry adjacent downslope patch. Relative wetness is determined by using the TOPMODEL wetness index (Beven and Kirkby, 1979).

Roads are implemented at the 30m patch scales. Thus all intercepted flow from a given 30m patch that contains a road, is redirected by the road culvert (i.e. the road culvert is assumed to be at the downslope corner of the patch). Redirected flow is sent to the nearest downslope

stream or to highest/lowest downslope adjacent patch, depending on apriori user specification. The nearest downslope stream is determined by the shortest flowpath length

The wetness index is calculated as:

$$w_i = \ln\{\frac{aT_i}{T_o \tan\beta}\} \qquad [1]$$

where Ti and To are local and mean hillslope saturated soil transmissivity, respectively, tan b is local slope and a is upslope contributing area. Note we are using TOPMODEL here only to derive an index of relative downslope patch wetness. Lateral hydrologic fluxes are modeled using the explicit routing approach as described above.

The model is applied using a map of the road network but without a detailed survey of individual road culvert characteristics. For this study, end member scenarios are examined where all roads redirect flow in the same manner (i.e. all roads redirect flow to the nearest downslope stream or all roads redirect flow to the adjacent downslope patch with the highest/lowest wetness index). This permits investigation of simplified scenarios at the ends of a continuum where roads can connect directly to the stream, concentrate flow in hollows below the road or diffuse flow to drier areas below the road. An algorithm for determining road connectivity will be implemented in later versions of the model. Wemple et al (1996) propose a relationship between road connectivity (to stream channels) and road and topographic characteristics including slope and the road length draining the culverts. Similarly for these exploratory simulations, road cut depth is assigned by the user. In subsequent simulations, road cut depth will be estimated based on a typical road width and local slope.

Method

We apply this model to Watershed 3 in the H.J.Andrews Forest in the western Oregon Cascades. Elevation within the 101 ha. watershed ranges from 400m to 1000m. Mean annual precipitation is greater than 2000 (mm) and shows a clear seasonal variation with most of the precipitation falling between October and April. Precipitation and temperature inputs are taken from a single base station within the catchment. Variation in incoming radiation with elevation and aspect is adjusted using MTN_CLIM logic (Running et al, 1987). Precipitation lapse rates with elevation are derived from PRISM (Daly et al, 1994) and temperature lapse rates estimated by Rosentrater (1997) for the H.J.Andrews basin.

Soils are gravelly clay loam with high infiltration capacities and high hydraulic conductivity (> 80 m/day). Vegetation is dominated by Douglas Fir (Pseudotsuga menziesii). Figure 4.3 illustrates the position of roads relative to the stream drainage pattern in the watershed. Road construction on Watershed 3 began in April 1959. In August 1962, 25 % of the forest was clearcut and then burned in February 1963.

The model was calibrated using data from a neighboring unharvested watershed, Watershed 2, using daily outflow from 1963. Lateral saturated hydraulic conductivity, Ksat, was used as the calibration parameter. Point measurements of hydraulic conductivity do not take into account the high within patch variability in conductivity and do not account for preferential flow through macro-pores etc. Calibration produces an effective conductivity which estimates a patch scale conductance to water flux. An initial set of spatially distributed Ksat values were assigned based on soil texture maps for the area. For calibration, all Ksat values were scaled by a single multiplier. Thus calibration alters the magnitude of basin effective conductivity but not the spatial distribution. The optimal multiplier was determined based

Road Network

Cut Block

Stream Network

Elevation Range: 400-1000m,
Annual Pcp: 2300mm
100 ha

Roads Constructed April, 1959,
Forest harvest 25% - Aug, 1962-Feb, 1963

Figure 4.3: Stream and road network for Watershed 3: H.J.Andrews Experimental Watershed.

upon outflow comparisons between observed and modeled outflow using the Nash-Sutcliffe efficiency measure (Nash and Sutcliffe, 1970). A maximum Nash-Sutcliffe efficiency measure of 0.77 was obtained for Watershed 2 outflow for 1963. Simulation results for the calibration year are shown in Figure 4.4.

The model calibration achieves a reasonable correspondence between observed and modeled outflow, although the model is less sensitive to early fall precipitation events. Soil and climate information are the main sources of error in the model. Local variations in climate, particularly temperature inversions and spatial variation in precipitation falling as rain versus snow are not well represented in the model. Spatial variation in soil parameters is also difficult to infer from available soil maps. Using the same calibration parameters that were used for Watershed 2, we compared observed and modeled outflow for Watershed 3 for a pre-disturbance year, 1959. Watershed 3 also exhibits a reasonable correspondence, i.e. a Nash Sutcliffe efficiency of 0.7, between observed and modeled outflow.

To illustrate the implications of the conceptual model, we test the effect of two road construction scenarios:

(1) road cut depths

We begin by exploring an extreme 'worst case' scenario in which a moderate road cut depth (5m) is used and all roads are assumed to be hydrologically connected to the stream. Simulations are repeated for a more moderate cut bank depth of 0.5m and differences in response noted.

(2) road -stream connectivity

We assess three scenarios with respect to road connectivity as discussed above. We consider a 'worst case' scenario where all roads are hydrologically connected to the stream. We also model two scenarios where intercepted flow is redirected to downslope areas through culverts that drain to high or low wetness index downslope patches.

The above scenarios are used to assess the implications of the proposed model on the spatial and temporal persistence of road construction effects on hydrologic response. We are also

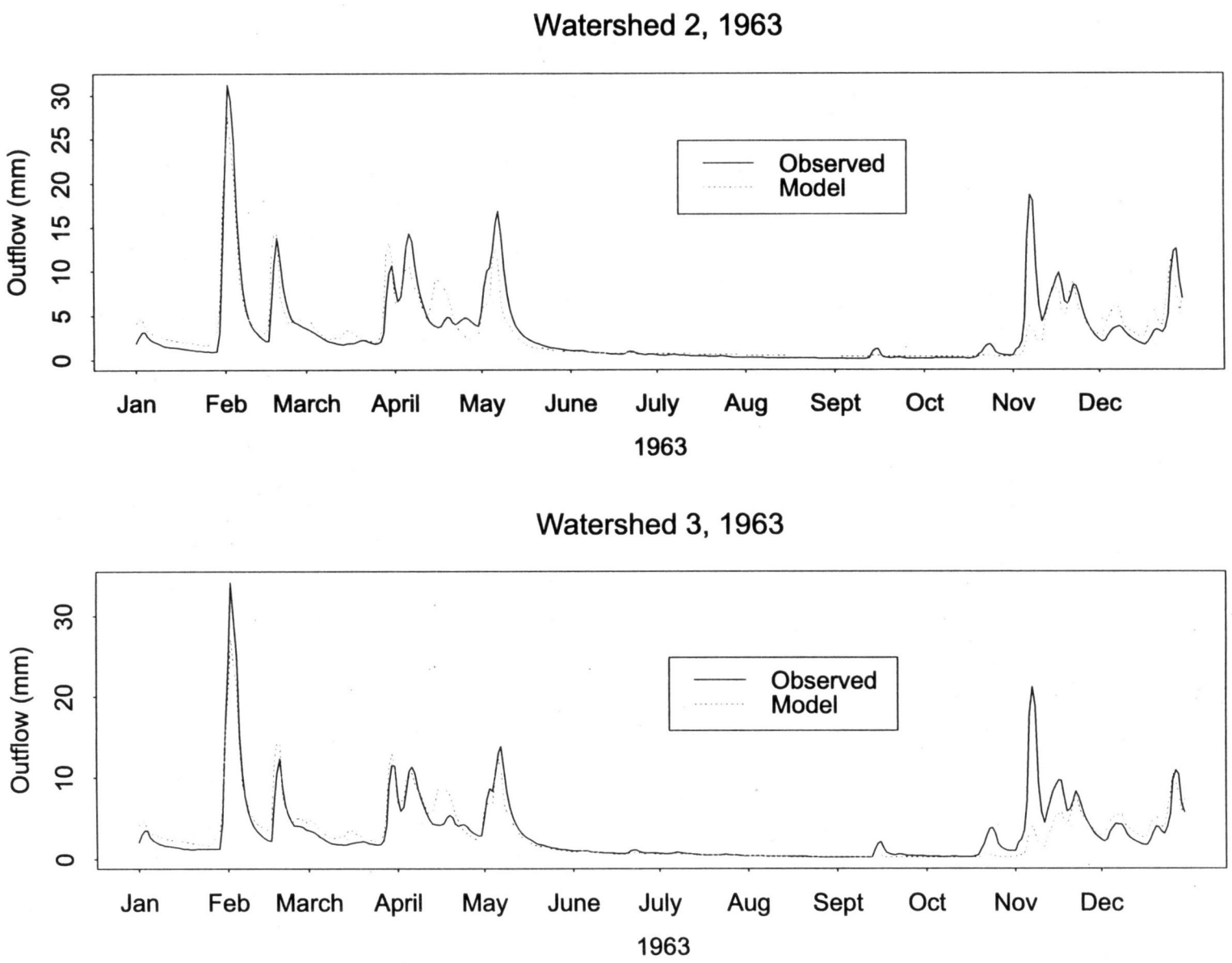

Figure 4.4: Daily Outflow for Watershed 2 and Watershed 3; Simulated vs. Observed

interested in comparing these results with empirical data. Paired catchment comparisons between Watershed 3 and the control unharvested Watershed 2 provide information on outflow differences between responses with and without both roads and forest harvesting. We compare these empirical differences with simulation results for scenarios with and without roads.

Results

Simulated Annual and Summer Outflow

Table 4.1 summarizes model predictions of the percent change in annual and summer flow due to disturbance for the various road construction scenarios.

	Percent Change in Annual Outflow			**Percent Change in Summer Outflow**		
Road Construction	Road effects during pre-harvest period	Road effects during harvested period	Combined disturbance effects	Road effects during pre-harvest period	Road effects during harvested period	Combined disturbance effects
0.5 m Cut Bank; Route to Stream	0.4	0.1	7.8	-1.2	-1.7	24.7
5 m Cut Bank; Route to Stream	1.9	1.5	9.2	33	26	59.0
5 m Cut Bank; Route to Highest WI	0.2	0.0	7.6	0.5	0.0	26.8
5 m Cut Bank; Route to Lowest WI	-0.1	-0.1	7.5	-1.8	-2.9	22.9

Table 4.1: Summer and annual outflow response to road construction by road cut depth and culvert routing characteristics.

Pre-Harvesting (Roads Only) Period

Three periods for comparison are considered. The first is the comparison between simulations with roads and without roads for the pre-harvest (1959-1962) period. For this period, changes in annual flow are small (< 2%) for all road construction alternatives. Changes in annual flow are balanced by a reduction in evapotranspiration. For summer flow periods, effects are more significant and more varied across road construction conditions. For the 5m road cut case, a consistent increase in flow is shown, averaging about 30% of total summer flow. Although not shown here, further simulation shows that the additional sensitivity to road cut depth diminishes beyond the 5m cut bank depth. For the smaller road cut, flow consistently decreases slightly during the summer. The increase in summer outflow associated with the moderate cut bank is due to the cut bank interception of deeper saturated throughflow in near stream areas which occurs even for small storms during the summer. In this case, roads are acting as extensions of the stream network and therefore increasing the local streamside area contributions to summer flow. The shallower 0.5m cut bank is not able to access this local deeper throughflow. The decrease in summer outflow associated with the shallower cut bank is therefore a result of the reduction in soil moisture recharge earlier in the season due to redirection of this recharge by upslope roads.

Post-Harvesting Period

We also examine the period in which both forest harvest and roads occur (1962-1969). We limit this period to the early response of forest harvesting before significant regrowth has occurred. Table 4.1 summarizes both the combined effects of roads and harvesting and a scenario that isolates the contribution of roads during this time period.

The model produces the greatest relative increases during the summer low flow periods. The effect of forest removal contributes an 8% increase in annual flows and a 25% increase in summer flows. The greater sensitivity of summer flows to forest removal is consistent with the greater role of evapotranspiration during the summer. The net effect of harvesting versus road construction dominates in all cases except for the summer outflow response generated

using a 5m cut bank. In this case, roads and harvest together produce a 59% increase in summer outflow response.

To disentangle the effect of roads from harvesting, we compare scenarios with roads and without roads during the harvested period. These scenarios illustrate the potential for any synergistic effects due to harvesting on the response due to roads. Results summarized in Table 4.1 suggest that the effects of roads on annual and summer outflow are similar for pre and post harvest periods. (Note that percentage effects diminish slightly due to the larger flow volumes in post-harvesting periods but the net effect of roads does not change).

Effect of Road-Stream Connectivity

Routing to the highest wetness index patch produces a negligible increase in both summer and annual flow as shown in Table 4.1. Although these results are not always significant in terms of magnitude, they are consistent with the conceptual model where roads routing directly to the stream produce the largest effects due to flow channelization and routing culverts to the highest wetness index follows but diminishes this effect.

Conversely, routing to the lowest wetness index produces a negligible decrease in annual flow and a small but consistent decrease in summer outflow and a corresponding increase in both summer and annual evapotranspiration. Although the magnitude of total effect is negligible, it is consistent with the interpretation of roads routing to the lowest wetness index as acting to diffuse subsurface flow by redirecting flow away from hollows. In drier local areas, these effects may be stronger.

Within-Season Outflow Dynamics

The within seasonal effects are also of interest, since they illustrate temporal dynamics. Figure 4.5 and Figure 4.6 illustrate cumulative outflow differences for simulations with roads and without roads for 1959, for the 5 and 0.5m cut bank, respectively. Superimposed on a net seasonal increase in outflow, both cut depths show a repeated pattern of increase and decrease in outflow differences during the spring and winter periods. For a given storm, a

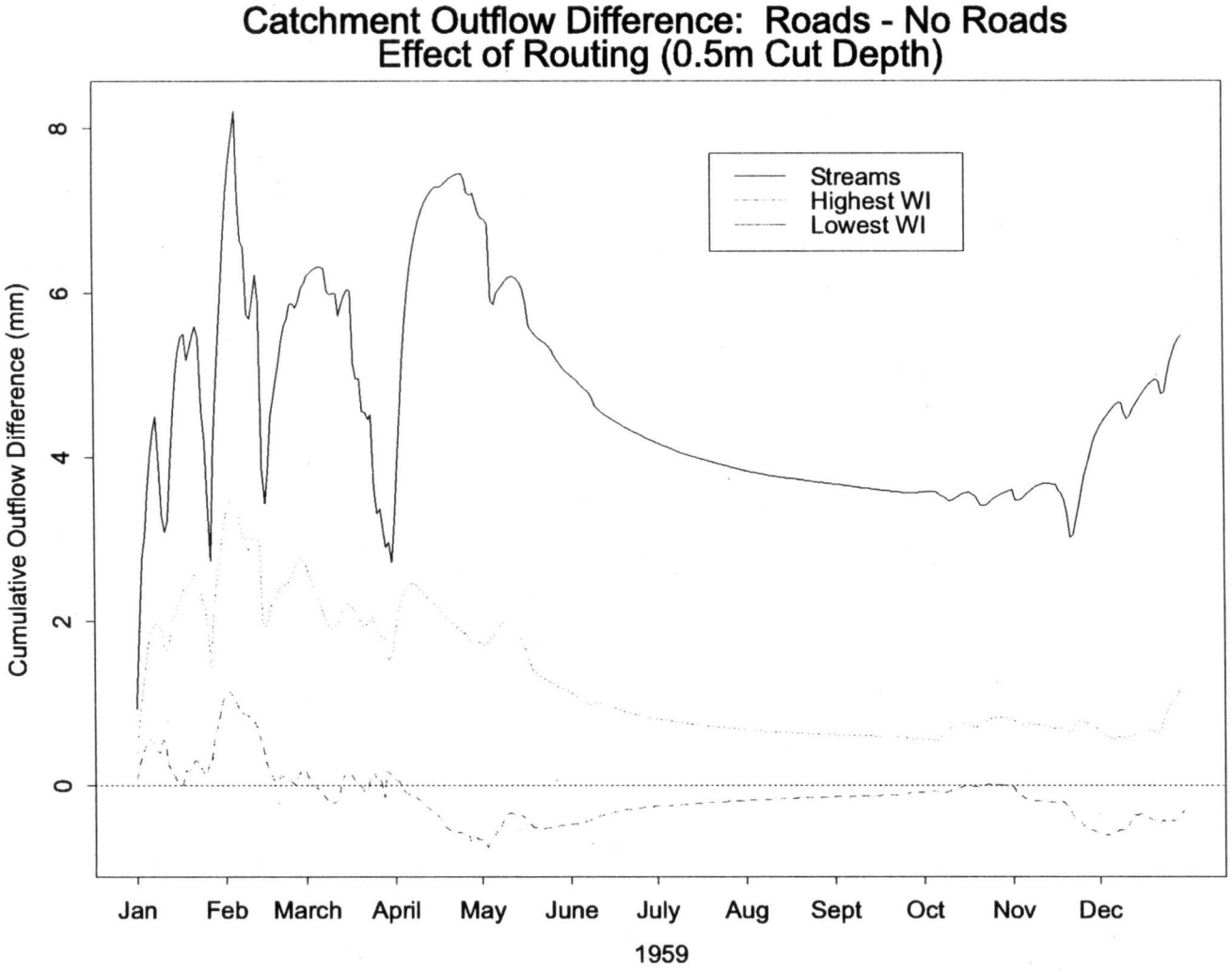

Figure 4.5: Cumulative outflow difference for simulations with roads and base line (no road) scenarios using a low 0.5 m road cut depth for three road - culvert drainage scenarios
a) road culverts route water directly to the stream
b) road culverts concentrate the flow in relatively wet areas i.e high wetness index, WI or
c) road culverts concentrate flow in relatively dry areas i.e low wetness index.

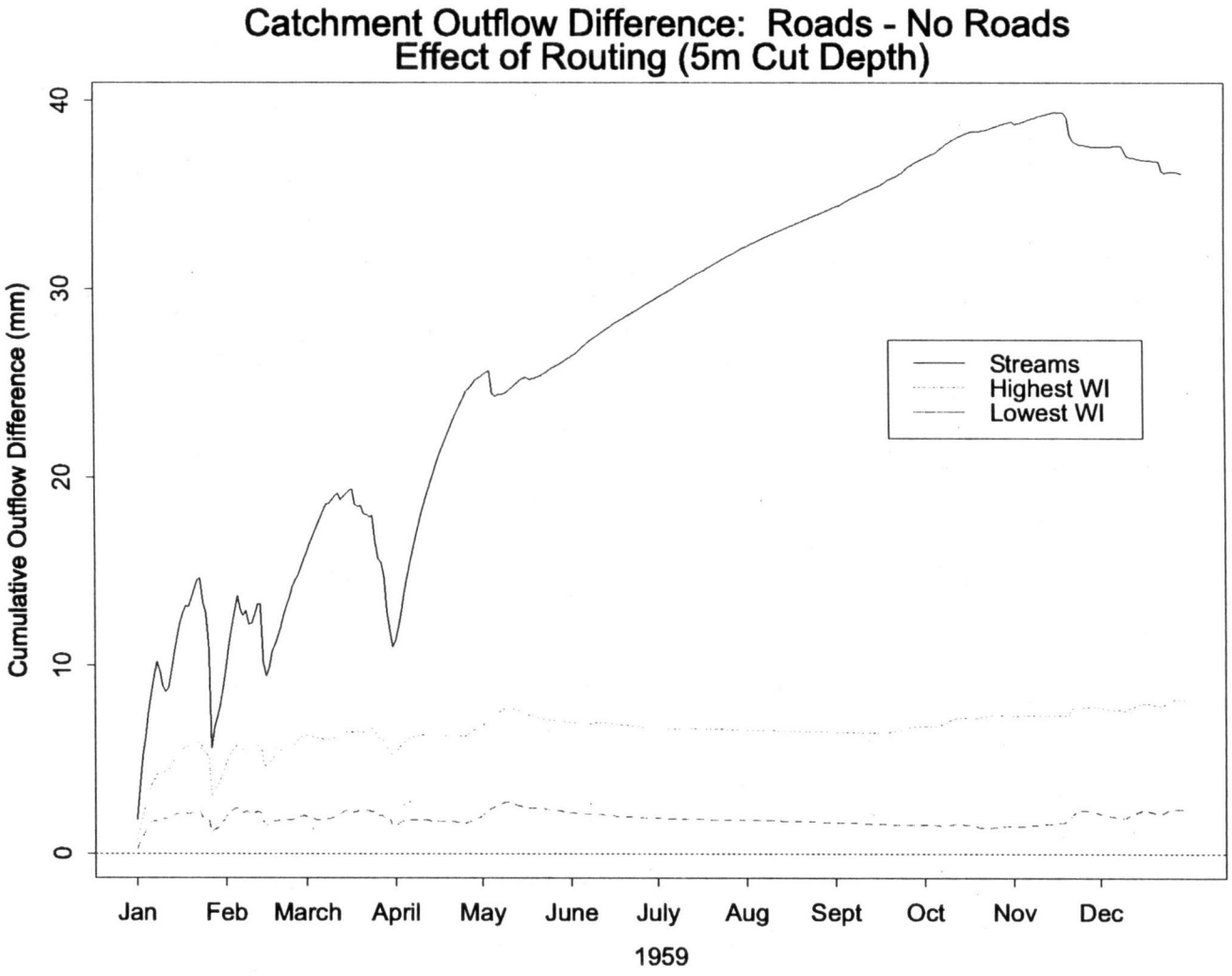

Figure 4.6: Cumulative outflow difference for simulations with roads and base line (no road) scenarios using a moderate 5 m road cut depth for three road - culvert drainage scenarios
a) road culverts route water directly to the stream
b) road culverts concentrate the flow in relatively wet areas i.e high wetness index, WI or
c) road culverts concentrate flow in relatively dry areas i.e low wetness index.

scenario with roads may produce more outflow as a result of subsurface throughflow interception by the road and more efficient routing of this flow to the stream. The consequence of this redirection, however, is a reduction in subsurface recharge to areas below the road. In inter storm and subsequent storm periods, these downslope areas may then contribute less outflow to adjacent streams. In this case, we see a partial recovery occurring. The timing of this recovery will depend upon the history of storm events and the hillslope characteristics. These simulation results show that for Watershed 3, the decrease in flow, following increases in peak flow, occurs within the winter season and with a similar frequency for moderate and low cut banks.

This pattern of recovery occurs, with diminished magnitude, when intercepted flow is routed to the highest wetness index. For routing to the lowest wetness index, effects are further diminished and, for the low cut bank, are the inverse of what is found with routing directly to the stream or to the highest wetness index. This inverse and diminished pattern associated with routing to the lowest wetness index supports the conceptual model that routing to the lowest wetness index acts to diffuse rather than to concentrate flow. In the 5m cut depth cases, the additional interception by the high cut bank overshadows these diffusive characteristics.

It should be noted that the scenarios tested here assume a single culvert for each 30-m pixel. Varying the concentration of culverts and therefore the magnitude of flow concentration/diffusion may produce more or less significant results. Figure 4.7 illustrates the impact of increasing culvert spacing to 120m in the model. Results show that the outflow difference associated with roads follows a similar seasonal pattern. For individual events, the increase in outflow associated with roads is slightly (< 1mm) more flashy with the larger culvert spacing. This reflects the larger contributing area (and therefore magnitude of intercepted flow) associated with a larger culvert spacing. The greater intercepted flow produces both higher increase in outflow followed by greater decreases in outflow for subsequent events. For one particular storm event, the 120m culvert spacing produces a change in the timing of response in comparison with the no road scenario (i.e. storm outflow occurs one day earlier, producing the two sequential spikes in the outflow difference). Use

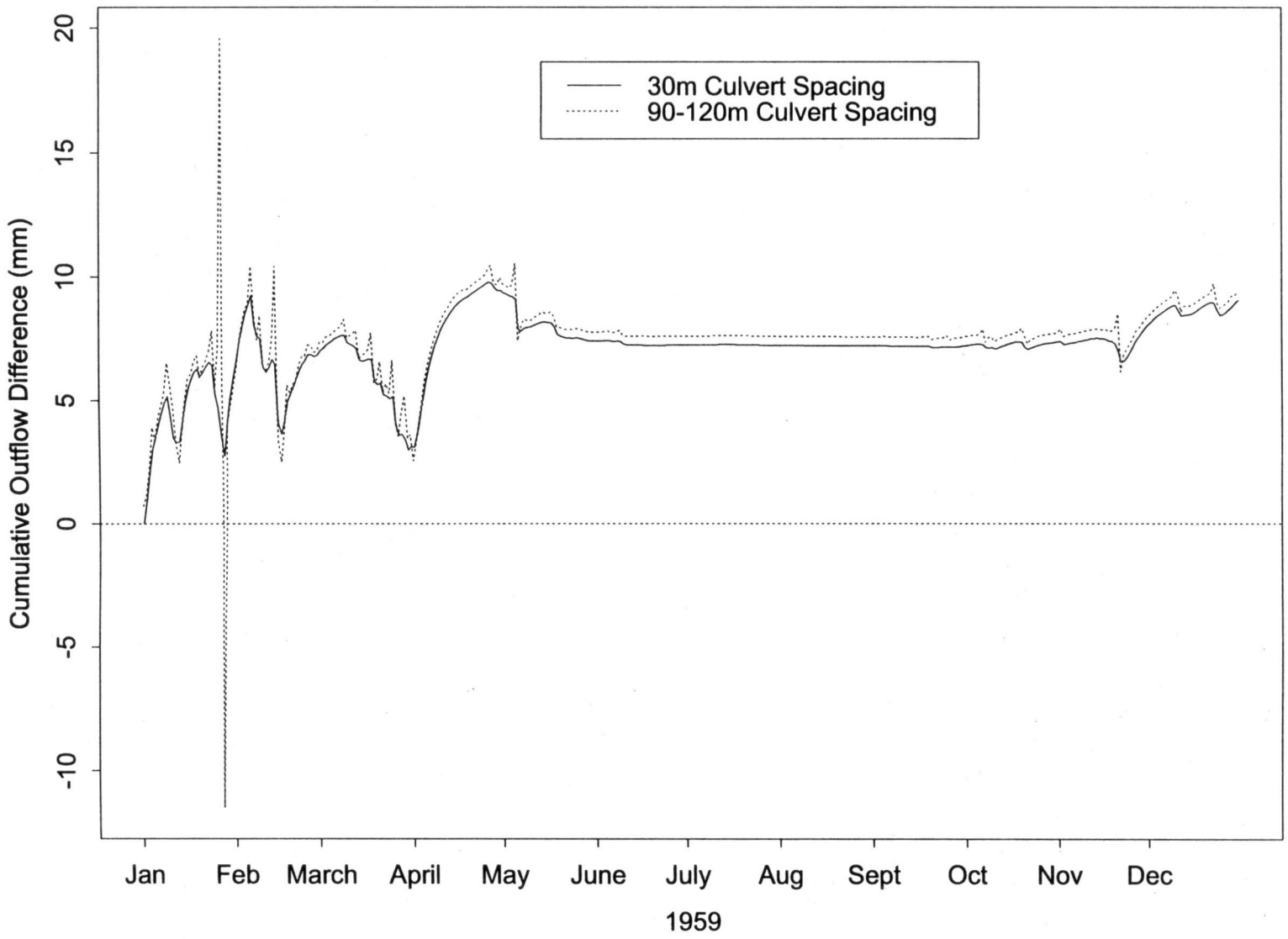

Figure 4.7: Cumulative outflow difference for simulations with roads and base line (no road) scenarios- 5 m road cut depth for fine (30m) and coarse (90-120m) culvert spacing.

of the daily time step in the model results in this apparent dramatic difference in outflow. To explore the effect of roads on timing in more detail, a sub-daily time step would be required.

Spatially Distributed Soil Moisture

The spatial extent of the reduction in recharge to areas below the road relative to the road and to the hillslope drainage features will have an impact on hydrologic response characteristics. To explore this, we examine the spatial pattern of the effect of roads on saturation deficit. Figure 4.8 maps the spatial distribution of the differences in saturation deficit and evapotranspiration for a representative summer day for scenarios with and without roads. Differences in saturation deficit are greatest immediately below the road but extend from the area immediately below the road to the stream network. This illustrates the spatial persistence of road effects to adjacent stream areas that control subsurface routing to the stream. The impact of a change in saturation deficit on subsurface throughflow (and eventually streamflow) is mediated by associated changes in evapotranspiration. In Figure 4.8, differences in evapotranspiration show a smaller spatial extent than differences in soil moisture. Evapotranspiration is a secondary effect and in lower elevation, wetter areas, it may not be limited by soil moisture. Significant differences (i.e. > 50% in local area) in evapotranspiration near to the road (i.e. within 200m) also illustrate the potential for ecologically significant consequences on downslope vegetation.

Figure 4.9 illustrates the generalization of these results through time. Figure 4.9a shows the mean and standard deviation of the daily increase in saturation deficit due to roads as a function of flowpath distance from the road for March to October 1959. This graph illustrates the pattern of spatial persistence of effects on saturation deficit, showing the greatest effects occur within the first 100m below the road and a continued increase in saturation deficit for a significant distance down slope. Figure 4.9c illustrates the corresponding pattern for the reduction in downslope evapotranspiration due to roads. A similar, although muted, reduction in the mean decrease in evapotranspiration with downslope distance is shown. The greater variance associated with evapotranspiration is due to the non-linear relationship between soil moisture and evapotranspiration i.e. a reduction of

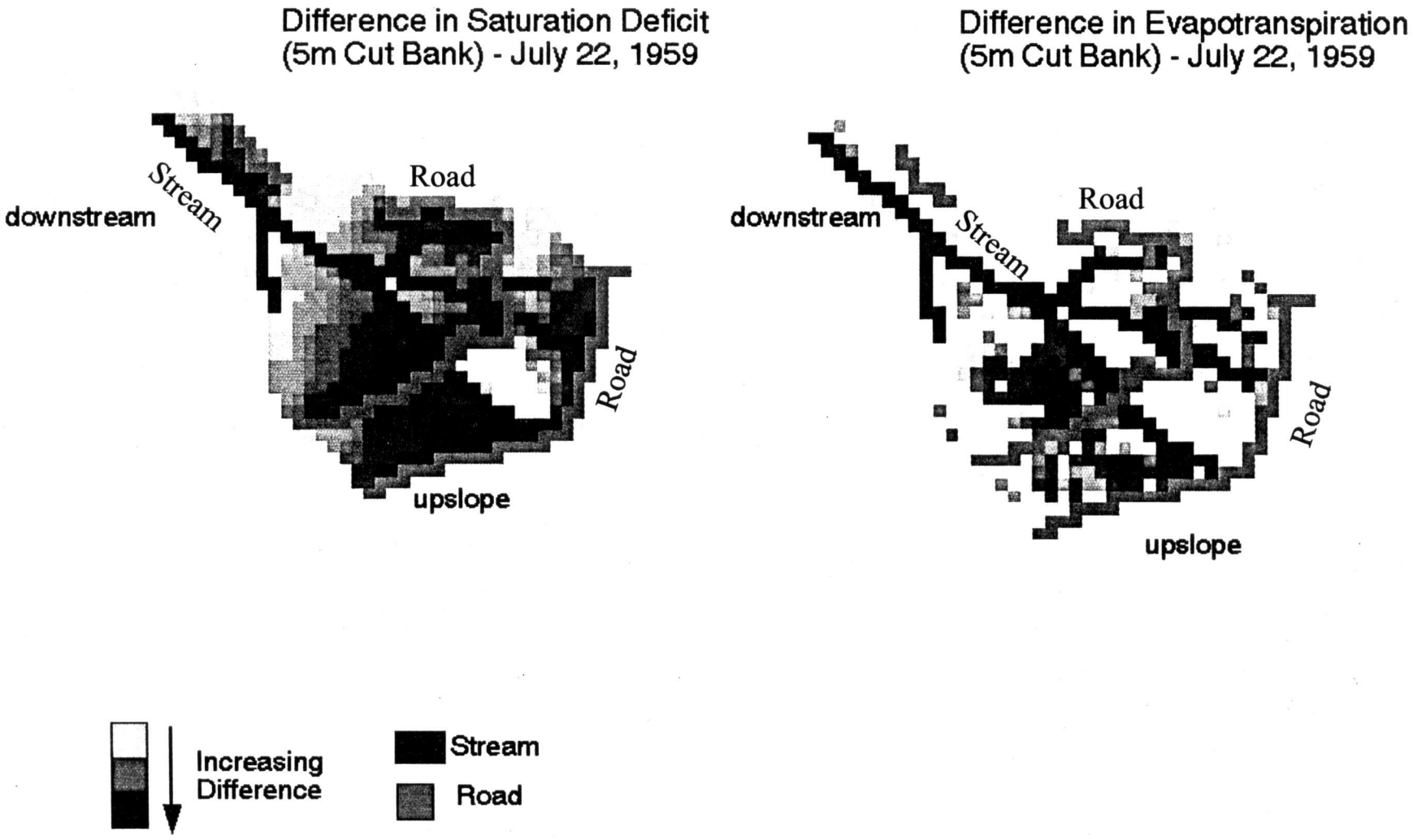

Figure 4.8: Spatial distribution of differences in saturation deficit and evapotranspiration below the road due to road construction effects; for July 22, 1959

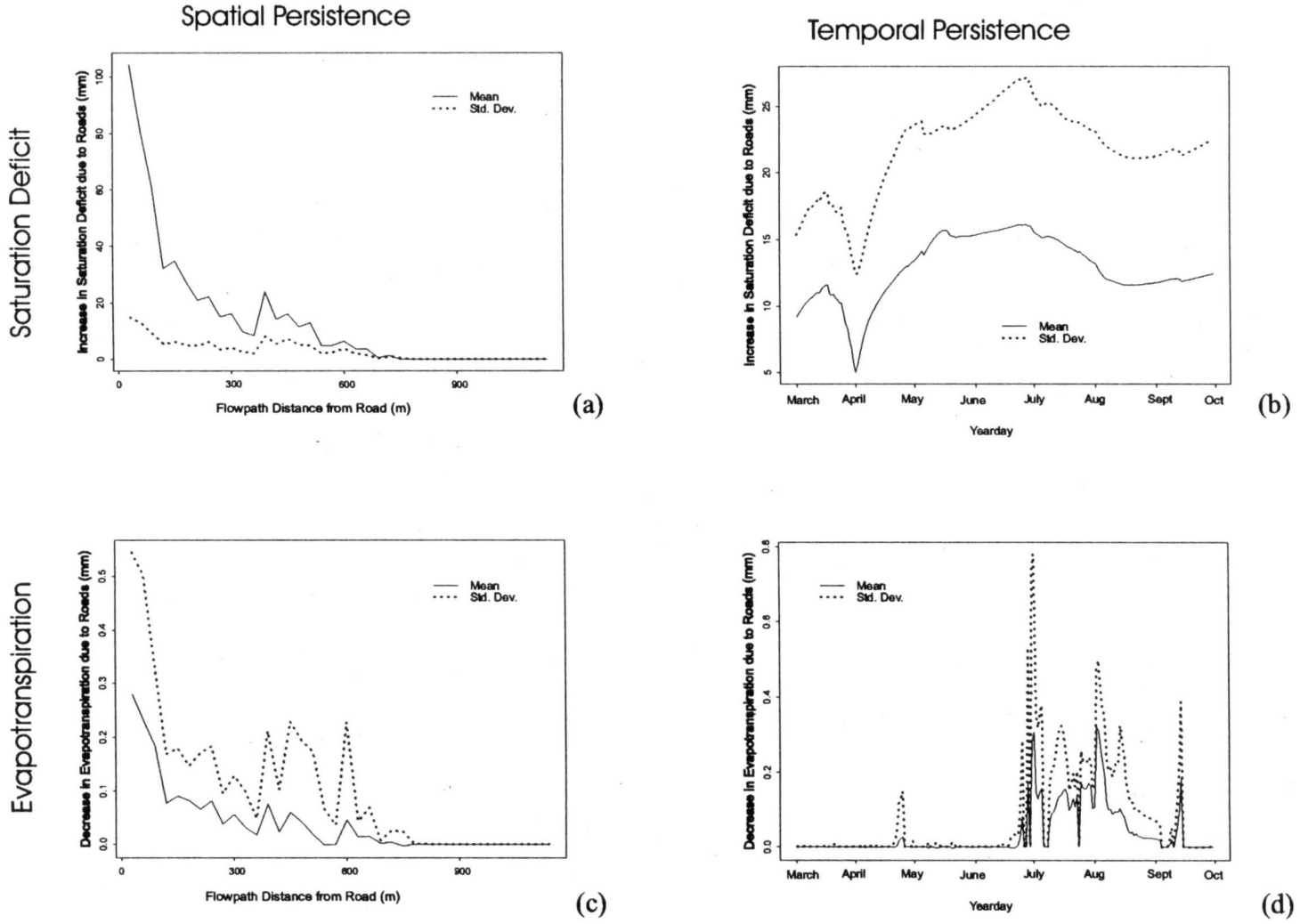

Figure 4.9: Spatial and temporal persistence of road construction effects on downslope soil moisture and evapotranspiration; mean and variance for 1959 a) saturation deficit difference by distance from road b) daily saturation difference c) evapotranspiration difference by distance from road d) daily evapotranspiration difference.

soil moisture in relatively dry periods will have significantly greater effects on evapotranspiration than a similar reduction during in wetter periods. In local areas, effects on evapotranspiration can be quite large with maximum difference in ET of greater than 3mm observed for areas near to the road and a difference of greater than 2mm for areas more than 500m downslope. Figures 4.9b and d illustrates the temporal persistence of road effects on downslope saturation deficit and evapotranspiration respectively. Effects on saturation deficit tend to increase from wet periods in March and April, where differences between road and non-road simulations are dominated by differences in outflow rather than soil moisture. Differences increase into mid-summer and then drop off as evapotranspiration differences, as shown in Figure 4.9d, begin to reduce soil moisture differences. Evapotranspiration differences due to road construction are most pronounced during dry late summer periods, again due to the greater sensitivity of evapotranspiration effects during dry periods.

Observed measures of spatially distributed soil moisture were not available for Watershed 3. Model results therefore are presented as hypothesis regarding significant impacts in areas below roads. In future work, we plan to compare model results with field investigations that contrast both soil moisture and productivity in areas above and below road cuts. The model will be used to determine areas where these effects are likely to be significant. Examining field evidence of the impact of roads in these areas will provide an opportunity to test the model representation of spatially distributed soil moisture.

Empirical Paired Catchment Comparisons

We now compare model results with empirical data. We analyze variation in observed daily and annual outflow from Watershed 3 against the neighboring undisturbed Watershed 2 and another neighboring Watershed 1 in the H.J.Andrews basin. Watershed 1 was 100% harvested in 1963 without any prior road construction. Hicks et al (1991) develop a least-squares regression relationship for summer and annual watershed yields for pre-harvesting periods for both Watershed 1 and Watershed 3 against the control watershed, Watershed 2. Using this regression relationship to examine post-harvesting differences in the relationship between the control and disturbed catchments, Hicks et al (1991) indicate a significant increase in summer low flow response immediately and for the first few years following harvesting for both watersheds. In their development of regression relationships, Hicks et al

(1991) include the road only period in Watershed 3, from April, 1959 to August 1962, in the pre-disturbance period.

Given our interest in the effects of roads on seasonal flow, we repeat this regression using only the pre-road period of record from 1955 to 1959. A least square regression relationship between Watershed 3 and the control watershed is also calculated for daily flows for the pre-harvested period. Although samples of daily outflow are highly correlated, we include this regression simply to offer additional insight into when within season differences between post and pre road construction periods may be occurring.

Table 4.2 summarizes results from a linear regression analysis that relates annual outflow from Watershed 3 with the control watershed for the pre-treatment period. A reasonable p-value was obtained, although the pre-treatment period for which data was available was relatively short (4 years; i.e. n=4). Regression results differed from those obtained by Hicks et al (1991), also shown in Table 4.2 and illustrate the contribution of the period of road construction as part of the pre-treatment period.

Annual Water Yield (mm)			
Scenario	*Regression Model*	*R2*	*p-value*
From Hicks et al. (1991) for Watershed 3 - (1953-1962)	W3 = 0.839*W2 + 110.53	0.94	<0.001
Watershed 3 (W3) (1954-1959)	W3 = 0.75*W2 + 275.99	0.96	0.017
Watershed 1 (W1) (1954-1959)	W1 = 1.11*W2 + 384.5	0.98	0.007
Summer Water Yield (mm) (July to September)			
From Hicks et al. (1991) for Watershed 3 - (1953-1962)	W3 = 0.861*W2 + 11.43	0.63	0.006
Watershed 3 (W3) (1954-1959)	W3 = 1.043*W2 + 5.59	0.77	0.1216
Watershed 1 (W1) (1954-1959)	W1 = 0.47*W2 + 4.95	0.62	0.28
Daily Water Yield (mm)			
Watershed 3 (W3) (1954-1959)	W3 = 1.04*W2 + 0.06	0.81	<0.001

Table 4.2: Least-Squares Linear Regression Results for outflow from Watershed 3 and Watershed 1 with control watershed, Watershed 2 in pre and post road construction periods

Figure 4.10a plots the residuals for Watershed 3 based on predictions of annual outflow from Watershed 2. Road construction begins in 1959 and harvesting in 1963. The residuals should indicate the impact of this disturbance. As expected following harvest, observed annual outflow was greater than predicted from the unlogged watershed. Increases of approximately 25% occurred with some inter-annual variability. This corresponds well with modeled results shown in Table 4.1 for 0.5 m cut bank road construction and forest harvest effects, which also show a 25% gain in annual outflow following harvest. Results for the road only years (1959-1963), however, were surprising. Residuals show a decrease in observed annual outflow relative to what was predicted from the control watershed. A decrease in outflow associated with road construction is unexpected given the conceptual model discussed above, which predicts increases or negligible changes in annual outflow for all road construction scenarios, as shown in Figure 4.10b. Summer outflow residuals were small (<5%) and show no consistent pattern during the road construction period prior to harvest. To assess whether the decrease in relative annual flow for the 1959-1963 period was due to climatic factors, we repeated the regression analysis for Watershed 1. Watershed 1 was harvested in 1963 with no prior road construction. Residuals for Watershed 1 do not show any significant changes during the 1959-1963 period.

Figure 4.11b also compares the regression results for Watershed 3 with model results, using a 5m cut depth and routing all roads to lowest wetness index area below the road. This road construction scenario serves as the lowest outflow end-member of our conceptual model. Even in this end-member case, the model does not capture reduced outflow effects shown in the road construction period using the observed data, but does reproduce a similar augmentation of outflow due to forest removal after 1963.

Further information about the timing of the observed decreases in outflow is gained by using a daily regression between Watershed 3 and the control watershed. Regression results for the daily time period are shown in Table 4.2. Figure 4.12 plots the cumulative outflow difference between observed Watershed 3 outflow and the predicted outflow based on the control watershed. Watershed 3 outflow is also shown on each graph to depict the seasonal context. The pattern of variability in the relationship between Watershed 2 and Watershed 3 changes significantly after road construction (i.e. 1956 and 1957 are pre-road construction years; 1960

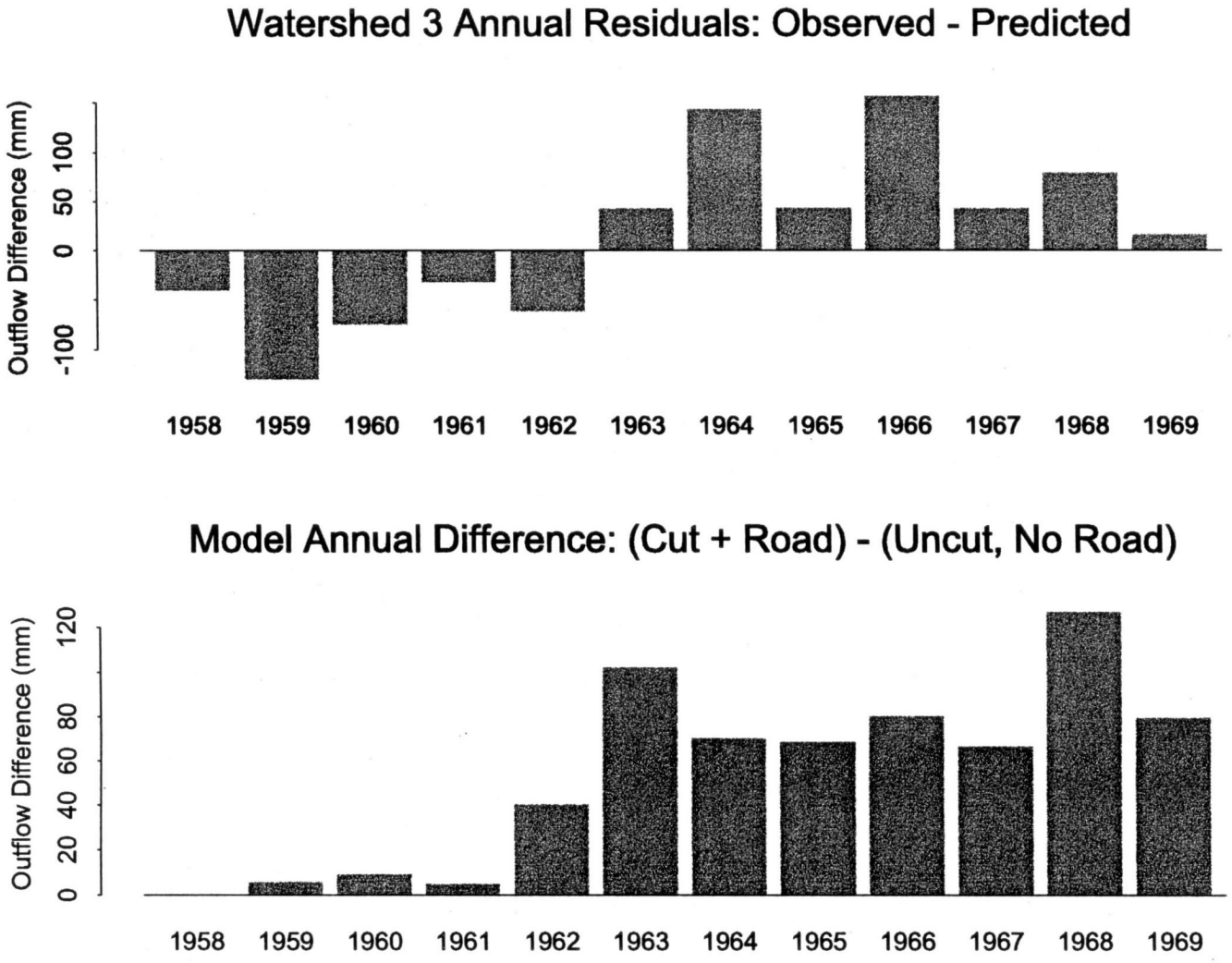

Figure 4.10: Annual outflow difference due to roads for Watershed 3
a) residuals (observed - predicted) for empirical relationship based on Watershed 2 and Watershed 3
b) simulated differences (simulations with roads (5m cut depth; routing to the stream) and forest harvesting - baseline unharvested simulation)

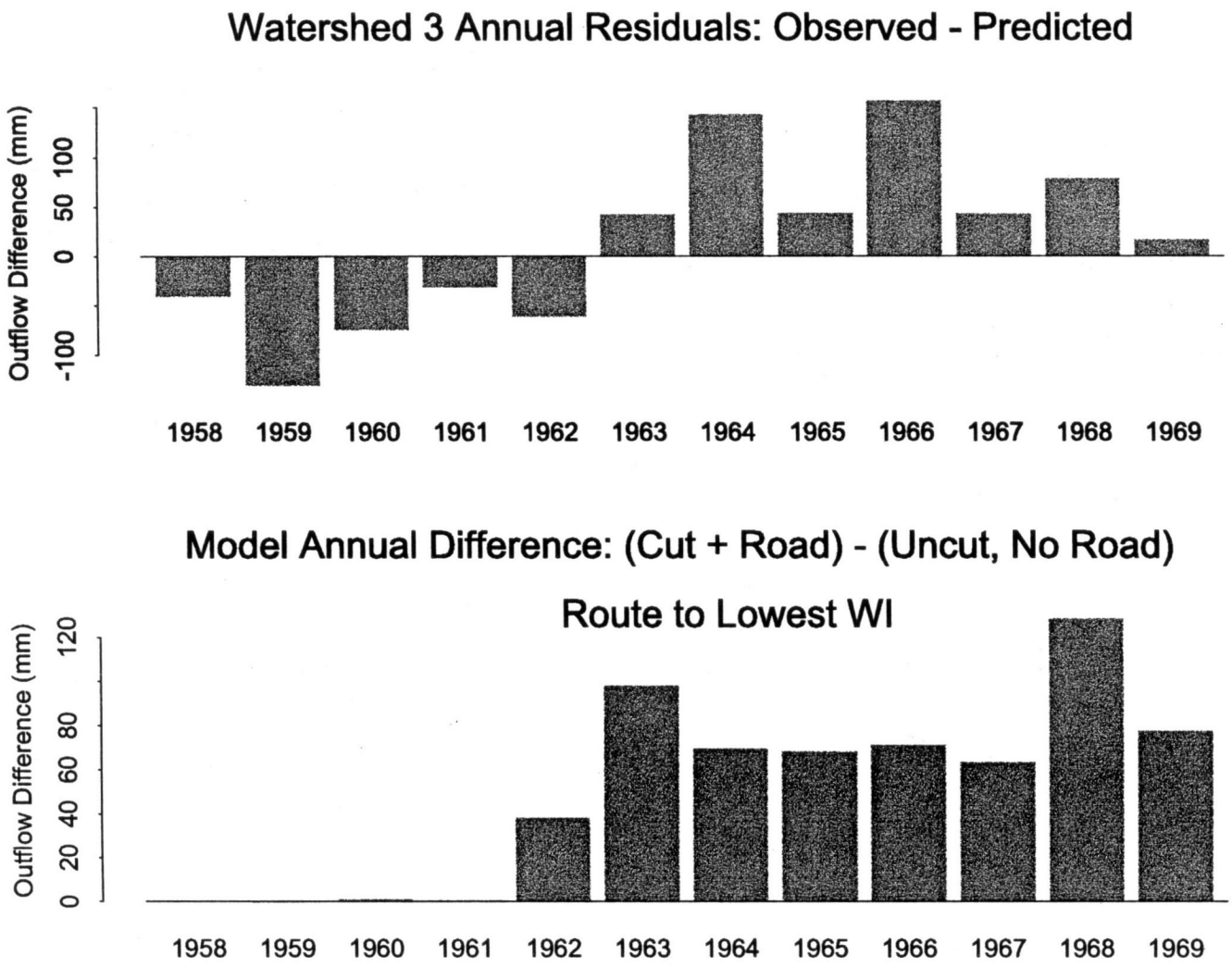

Figure 4.11: Annual outflow difference due to roads for Watershed 3
a) residuals (observed - predicted) for empirical relationship based on Watershed 2 and Watershed 3
b) simulated differences (simulations with roads (5m cut depth; routing to lowest wetness index) and forest harvesting - baseline unharvested simulation)

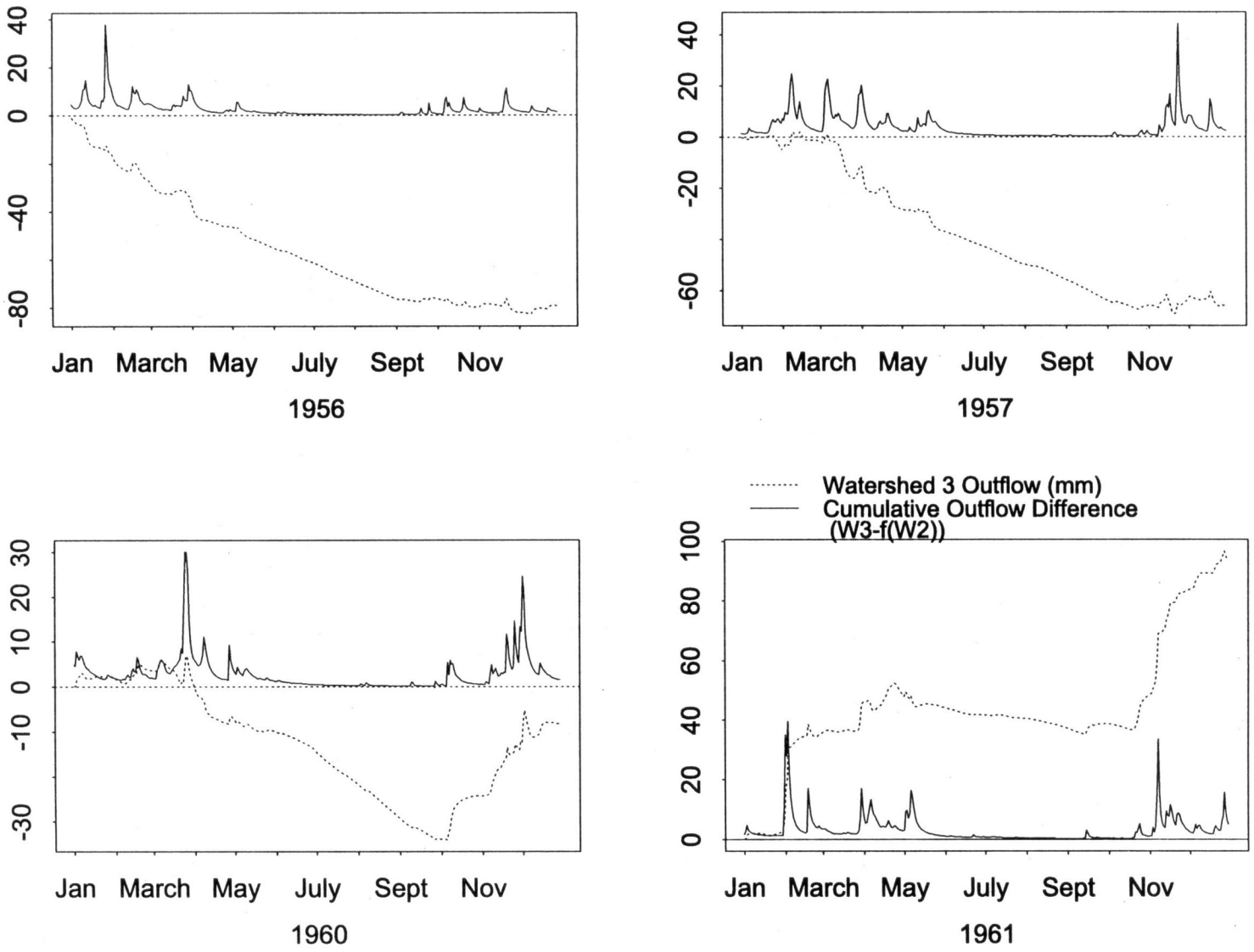

Figure 4.12: Empirically derived cumulative outflow residuals (observed - predicted) for pre-road construction years (1956-1957) and post road construction years (1960-1961).

and 1961 are post-road construction years). Figure 4.12 also illustrates that a reduction in outflow from Watershed 3 relative to Watershed 2 occurs during the spring and summer periods for both post and pre-construction years, which suggests that the relationship between Watershed 2 and Watershed 3 varies seasonally. Differences between the pre and post logging scenarios, however, are most significant in the late winter and spring. In the pre-road construction years, predictions based on Watershed 2 tend to under-estimate Watershed 3 response during the late winter to spring period. After road construction, predictions from the control watershed tend to over-estimate this response. This suggests that the reduction in annual outflow associated with roads is due to late wet season dynamics. During this period there is significant variability in soil moisture and soil moisture draw down from saturation begins to occur. Road construction will reduce recharge to downslope areas during this period. This reduction in recharge appears to more than compensate for the increase in runoff associated with efficient routing of upslope flow by roads to the stream. This response would only occur if recharge to lower slopes during this period tends to produce a non-linear response. A non-linear increase in runoff may occur if recharge tends to increase the presence of macro-pores in the downslope region and thus increases subsequent drainage efficiency in the downslope area.

Conclusions

Results from the modeling study of Watershed 3 illustrate the potentially complex interactions involved in watershed response to road construction as part of forest harvesting. Results from these simulations focus attention on the spatial and temporal persistence of changes in downslope soil moisture due to the re-routing, concentration and potential diffusion of flow intercepted by the road. This persistence means that the re-routing of water that occurs during particular winter storms has effects on the hillslope response to later storms and summer hydrologic response, including low flow and evapotranspiration.

The most significant effects were found for patterns of spatially distributed summer soil moisture. This study suggests that road construction can produce a significant reduction in downslope soil moisture and associated evapotranspiration in local areas. Reduction in

evapotranspiration can in turn have ecological effects on forest health and productivity. Reduction in regrowth and/or low flow both have forest management implications. These results offer impetus for a field-based investigation of road construction effects on harvested areas below roads and in more water-limited environments. In future work, we plan to use a combination of modeling and field survey techniques to assess the potential for reduced recovery in these areas which have received less attention in the current research on hydrologic effects of forest practices.

The spatial and temporal persistence of road construction effects on downslope soil moisture also has implications for runoff response, although these effects are less significant. In our modeling study, it appears that roads can increase daily peak flow for some storms, which is consistent with findings from field research (Jones and Grant, 1996; Wright et al, 1990) that show that increases in peak flow may occur only for specific storm events. Empirical comparisons between observed outflow from Watershed 3 and Watershed 2 also offer evidence of a winter recovery effect, where road effects on outflow vary for different winter storm events and during winter inter-storm periods.

From the perspective of both soil moisture and runoff production, the compensation by downslope areas distinguishes increased routing efficiency due to road construction from an increase in stream drainage density. Because streams are located at the bottom of hillslope drainage networks, they do not impact a downslope area. Roads, given their relative hillslope position, do have the potential to impact downslope areas. Simulations here suggest that these effects can have significant effects on the redistribution of soil moisture, flow paths and source areas for runoff. Simulation results also illustrate the importance of the timing of the processes involved in creating the overall effect of road construction. In the case of peak flows, variability may also occur due to differences in rainfall intensity. The daily time step of the current version of the model precludes investigation of these effects. Further model development will incorporate sub-daily rainfall intensity information to explore this potential control on the variability in road construction effects.

Model results illustrate the degree to which road construction effects are mediated by road cut depth and road routing characteristics. The hydrologic importance of cases where roads are hydrologically connected to the stream, either directly through culverts or through gullies,

has been noted by other researchers (Wemple et al., 1996). These simulations suggest that the concentration or diffusion of subsurface flow as controlled by the road system drainage pattern, may also have effects on soil moisture and runoff production, although the magnitude of effects are much smaller. These results may be more dramatic in drier more sensitive regions and suggest the need for field research study to collaborate simulation findings. Further study will examine soil moisture both immediately below road cuts and further downslope, for both different cut depths and for different road culvert drainage patterns (i.e. diffusion: culvert routing to low wetness index vs. concentration: culvert routing to high wetness index).

The comparison between the modeling response and observed paired catchment responses indicates that there are additional controlling processes that are not captured by our conceptual model. Although the statistical significance of the observed relationships was small, the observed relationship between the control watershed and the harvested watershed illustrate an annual reduction in outflow associated with roads. Seasonal comparisons further suggest that this reduction, relative to the pre-harvesting periods, occurred mainly during the late winter and spring. We suggest several possible explanations for this discrepancy between the model and paired catchment relationships. The simulations indicate the complex role played by the combination of increased drainage efficiency during a storm, and the delayed effect of a reduction in downslope recharge. Observed results may indicate a greater and disproportionate impact of the downslope reduction in recharge. Hysterisis effects in the downslope area could account for this effect, allowing more water in downslope areas to be lost due to evapotranspiration in the case where water is channeled by the road, particularly during the spring period when soil moisture drawdown from saturation tends to occur. In this case, the increased drainage efficiency associated with roads is more than compensated for by a decrease in drainage efficiency in the areas below the road. Alternatively, it may be that roads act as terraces, holding some of the intercepted flow in surface storage, which is then lost as evaporation. Further field investigation is necessary to examine these hypotheses.

Finally, results from this modeling study illustrate the importance of both complex spatial and temporal patterns in controlling the impact of road construction effects on distributed soil

moisture, runoff production and associated ecological responses such as evapotranspiration. These results highlight the importance of using models to situate road construction and harvesting within a hillslope drainage organization and the pattern of seasonal inputs. Model results suggest that these sources of variability must be taken into account in assessing the potential impact of different road construction scenarios. Thomas and Megahan (1996) similarly argue for a better understanding of controls on response variability in their critique of statistical approaches to assessing forest harvesting impacts. Model results are preliminary and require further field verification, however, they do offer a method for designing further field investigation and for understanding variability in observed response. Further work will be directed towards using the model to assess the relative sensitivity of different forest harvesting and road construction scenarios across a range of watersheds.

Acknowledgements: We gratefully acknowledge support in terms of database development from the staff at the H.J.Andrews LTER. We also acknowledge both G. Grant and B. Wemple for their contribution in discussions about the effects of roads in this catchment.

References

Beven, K and Kirkby, M. 1979. "A physically-based variable contributing area model of basin hydrology, *Hydrologic Science Bulletin*, **24**, 43-69.

Daly, C., Neilson, R.P., Phillips, D.L. 1994. A statistical-topographic model for mapping climatological precipitation over mountainous terrain, *Journal of Applied Meteorology*, **33**:2, 140-157.

Harr, R.D., Harper, W.C., Krygier, J.T, Hsieh, F.S. 1975. Changes in storm hydrographs after road building and clear-cutting in the Oregon Coast Range, *Wat. Res. Research* 11:3,436-444.

Hicks, B.J., Beschta, R. L., Harr, R.D., 1991. Long-term changes in streamflow following logging in Western Oregon and associated fisheries implications, *Wat. Res. Bull.*, 27, 217-225.

Johnson, R. 1998. The forest cycle and low river flows: a review of UK and international studies, *Forest Ecology and Management*, 109, 1-7.

Jones, J.A., and Grant, G.E. 1996. Peak flow responses to clear-cutting and roads in small and large basins, western Cascades, Oregon, *Wat. Res. Research*, 32:4, 959-974.

Keppler, E. T., Ziemer, R. R. 1990. Logging effects on streamflow: Water yield and summer low flows at Caspar Creek in Northwestern California, *Wat. Res. Research,* 26:7, 1669-1679.

King, J.G., Tennyson, L.C. 1984. Alteration of streamflow characteristics following road construction in north central Idaho, *Wat. Res. Research*, 26:7, 1159-1163.

Luce, C.H., Cundy, T.W. 1994. Parameter identification for a runoff model for forest roads, *Wat. Res. Research,* 30:4, 1057-1069.

Nash, J., and Sutcliffe, J. 1970. 'River flow forecasting through conceptual models: Part1 - a discussion of principles', *Journal of Hydrology*, **10**, 282-290.

Rosentrater, L. 1997 'The thermal climate of the H.J.Andrews Experimental Forest, Oregon", MSc Thesis, Department of Geography, University of Oregon.

Running, S., Hunt, E.R. 1993. Generalization of a forest ecosystem process model for other biomes, BIOME-BGC, and an application for global-scale models, *in Scaling processess between leaf and landscape levels*, ed. J.R. Ehleringer and C. Fields, Academic Press, 141-158.

Running, S., Nemani, R., Hungerfored, R. 1987.Extrapolation of synoptic meteorological data in mountainous terrain and its use for simulating forest evapotranspiration and photosynthesis, *Can.J.For.Res*, **17**;472-483.

Storck, P.A., Bowling, L., Wetherbee, P., Lettenmaier, D. P. 1998. Application of a GIS based distributed hydrologic model for the prediction of forest harvest effects of peak flow in the Pacific Northwest, *Hydrol. Process.*, 12, 889-904.

Tague, C. L., Fernandes, R. and Band, L.E., 1998. RHESSys 4.6: User Manual.

Thomas, R. B. and Megahan, W.F. 1998. Peak flow responses to clear-cutting and roads in small and large basins, western Cascades, Oregon: A second opinion, *Wat. Res. Research,* 34:12, 3393-3403.

Wemple, B. C., Jones, J.A., Grant, G.E. 1996. Channel network extension by logging roads in two basins, western Cascades, Oregon, *Wat. Res. Bulletin*, 32:6, 1195-1207.

Wigmosta, M., Vail, L., Lettenmaier, D. 1994. 'Distributed hydrology-vegetation model for complex terrain', *Wat. Resour. Res*, **30:6**, 1665-1679.

Wright, K.A., Sendek, K.H., Rice, R.M, Thomas, R.B. 1990. Logging effects on streamflow: Storm runoff at Caspar Creek in Northwestern California, *Wat. Res. Research* 26:7, 1657-1667.

Conclusions

This document has presented an analysis modeling of drainage organization and its modification due to disturbance as a key component of a hydro-ecological model. Analysis was done using the RHESSys simulation system and applied to modelling seasonal outflow for a number of small catchments in the Pacific Northwest.

Drainage organization provides both the context in which hydrologic response to disturbances such as forest harvesting occur and can be, in turn, modified by disturbances such as road construction. Adequate representation of drainage organization in modeling is, therefore, a prerequisite for using these models as tools in the assessment of watershed responses to different management scenarios. The results of this investigation into drainage representation in a hydro-ecological model offer several conclusions and recommendations both in term of the general use of this modeling tool and in terms of contributing to the understanding of how road construction may impact watershed hydrologic response.

The first chapter provides an overview of the RHESSys modeling system and the modifications that have been made in the development of the most recent version. This latest version of RHESSys provides a more object-oriented approach that facilitates the implementation of different landscape objects and associated processes at different scales. A key feature of RHESSys, as a spatially distributed hydro-ecological modeling system, is that it is a tool that combines together different processes and disturbance regimes within a spatial and temporally varying context. This allows the model to generalize finding from field research and intensive field study to a general population of catchments within a given region. The representation of drainage organization, both in terms of the algorithms used and the associated landscape representation, is a key component of this context.

The second chapter begins the investigation of how well drainage organization is represented in the model. Results from this chapter show that an explicit routing algorithm is necessary to capture seasonal changes in drainage organization which occur in regions like the Pacific

Northwest where wet winters are followed by much drier summers. This study found that the simpler TOPMODEL approach could not adequately capture the shift from hillslope to more local level drainage organization that occurred during the summer. Results, however, also illustrate the sensitivity of the explicit routing approach to noise or random variation in soil and topographic input information. Results show that sensitivity is greater during low flow periods for the explicit routing approach. Results also suggest that calibrated effective conductivity may vary with seasonal and storm driven activation of macropores at high moisture conditions in specific areas. Further work will explore the incorporation of a dynamic model of effective conductivity into the explicit routing model. The third chapter further emphasizes model sensitivity to low flow periods and shows that the sensitivity of the model to calibration and landscape representation is also greater during drier conditions. This is again related to the more local control of drainage organization that occurs during these periods. Calibration and field verification can take advantage of this sensitivity to better constrain model behaviour. This suggests that in applying RHESSys and other similar model in regions with significant seasonal variability in climate, model parameterization and testing should be focused on these drier periods, in spite of their smaller contribution to watershed outflow. These dynamics also present opportunities for field testing of the model representation of spatially distributed soil moisture. Examination of the relative changes in soil moisture measurements taken in upland and streamside areas from wet to dry periods is recommended.

In the third chapter I also address landscape representation. This is a central issue in an object-oriented system. Simulation results suggest that the scale of drainage organization varies spatially and that this should be reflected in the partitioning of the landscape. In particular, representation of areas near to the stream is critical and requires fine-resolution partitioning while upland areas may be treated as coarser units. Results from this study show that landscape partitioning strategies that did not include fine (i.e. 30m pixel) resolution near to the stream did not adequately capture low flow dynamics. These simulations show that variation in near stream hydrologic characteristics such as gradient or soil transmissivity are critical when local (streamside) drainage organization controls outflow response dynamics. This modeling study, however, suggest that simply including the variance, without explicit

spatial information, may be sufficient to capture the effect on outflow response. This offers the possibility of representing fine-resolution information in near stream areas as estimated distributions rather than explicit spatial information, which may be more difficult to obtain. Further research will endeavor to field studies where fine scale information is available to explore the shape of these distributions across watersheds with different topographic characteristics and associated stream order.

The final section of this document investigates drainage organization in the context of applying the model to assessing hydrologic response to forest harvesting. The drainage organization modeled in earlier chapters is based on topographic and soil control of flowpaths. This initial drainage organization provides the context in which harvesting effects occur. To assess the impact of both road construction and tree removal therefore requires an adequate representation of drainage organization. The above recommendations related to model calibration and landscape representations must be considered as prerequisites for using model as an approach to assessing the impacts of forest practices on hydrologic response. In addition, however, road networks can alter flow paths and thus models must also represent the potential for modifications to drainage organization. In the final chapter, I extend the investigation to examine how the RHESSys modeling system can be used to examine the effects of roads on drainage organization and the resulting seasonal hydrologic response.

Roads are modeled as a means to redirect subsurface and surface flow and therefore, require fine-resolution information, including information about road cut depth and local road culvert connectivity with the downslope area and the stream network. In this study, hypothetical scenarios were used, which illustrate the importance of local road connectivity information – where roads may serve to concentrate flow, diffuse flow or connect flow directly with the stream network. These simulations illustrate how roads behave similarly to stream networks because they increase drainage efficiency. In this sense roads act as local controls on drainage organization. Model results, however, also show that roads differ from streams in their relationship with overall hillslope drainage organization. Roads, unlike streams, are not necessarily located in areas of relative convergence. This placement of roads relative to hillslope drainage organization means that roads can have significant impacts on the

hydrologic response of the area below the road. In this study, the effects of roads on downslope soil moisture were shown to be significant due to the loss of recharge to these downslope areas. This change in soil moisture in turn can effect ecological response variables such as evapotranspiration and productivity and any subsequent streamflow response that is controlled by the downslope area. The impact of roads, therefore, depends upon their position relative to overall hillslope drainage organization and the sensitivity of the downslope area (i.e. in dry climates a reduction in soil moisture can have a more dramatic effect of evapotranspiration).

Further work will examine different configurations of road networks relative to hillslope drainage organization for a range of different watersheds and different climatic conditions. The model also offers the potential to be used to represent the combined effects of both roads and forest harvesting. In this study, the effect of vegetation removal is captured reasonably well. Future work will also consider the co-variation in the spatial organization of forest removal, the road network and hillslope drainage organization. Field testing of these model results will also be done by examining soil moisture and productivity in areas above and below road cuts. This will also indirectly serve as a means to assess model representation of spatially distributed soil moisture patterns. Finally, the methodology used in the implementation of roads within RHESSys can also be extended to explore other local flowpath modifications associated with land use change such as the construction of sewers in urbanizing watersheds. Further development and application of RHESSys will explore these broad land use change scenarios.

Finally, results from the model investigation lead to insight into our understanding of the role potentially played by roads in the watershed hydrologic response to disturbance. Comparison of model outflow with observed regression relationships from paired catchment experiments suggests that the model does not adequately represent all processes involved in road construction effects. It is difficult to determine the cause of these discrepancies, given the limited data provided by the paired catchment experiments i.e. outflow data for only 4 years with road construction only. Modeling in other catchments with associated paired catchment experiments may offer additional insight. Nonetheless, the current version of the

model can still be used to generate hypothesis about the potential effects of road construction and forest harvesting. A key finding is that the spatial and temporal persistence of the effect of roads, and their complex relationship with drainage organization means that variability in hydrologic response is to be expected. Models serve as a tool for investigating the controls on this variability. This illustrates one of the key roles that models can potentially play in the continuing concerns about land management of forested watershed. Models, such as RHESSys, are a means to generate hypothesis and contribute to understanding of responses across the range of different watersheds that must be addressed by land-use managers.

Appendix A: RHESSys Process Algorithms

The following section describes in detail many of the algorithms used within RHESSys to model climate, vegetation and hydrologic processes. The description of these algorithms is organized by the RHESSys spatial hierarchy, described in Chapter 1 of this document. In general, climate processing is done at the zone spatial level. Sub-surface and surface hydrologic transport is done at the hillslope and basin level. Vertical soil moisture processing is done at the patch level and vegetation processes are modeled at the canopy stratum level.

Zone Algorithms

Potential, above atmosphere, radiation is computed following MTN_Clim logic (Running et al., 1987) derived from Garnier and Ohmura (1968) and is based upon latitude, slope, and aspect. Day length is truncated by east and west horizons for the study site.

Potential radiation is adjusted by atmospheric transmissivity using MTN_Clim approach based upon Bristow and Campbell (1984), unless cloud cover data is available. If cloud cover input data is available, cloud transmissivity is used to adjust incoming radiation directly such that:

$$K_{direct} = K_{clear\_sky\_direct} * (1.0 - cf) * co \quad [1]$$

$$K_{diffuse} = K_{clear\_sky\_diffuse} * (1.0 - cf) \quad [2]$$

Where co is cloud_opacity and is assumed to be 0.8 (Linacre,1992); cf is cloud fraction; K_{direct} and $K_{diffuse}$ are shortwave direct and diffuse radiation at the top of the canopy, respectively and $K_{clear\_sky\_direct}$ and $K_{clear\_sky\_diffuse}$ are direct and diffuse radiation without reduction due to atmospheric conditions.

Minimum and maximum temperatures are required inputs and are adjusted based on zone topography following MTN_CLIM (Running et al., 1987). Dewpoint temperature, if it is included with base station data, is similarly adjusted by a dewpoint_lapse rate. If it is not included, it is assumed to be minimum temperature value, after the elevation adjustment. Soil temperature is computed as a running average of average air temperature similar to (Zheng et al., 1993).

$$T_{soil}(t) = 0.9*(T_{soil}(t-1)) + 0.1*(T_{avg}) \quad [3]$$

The buffering effect of snow cover is not taken into account.

Precipitation adjustment with elevation differs from the earlier implementation based upon MTN_CLIM. MTN_CLIM assumes a linear scaling of precipitation with elevation. This applies well in areas dominated by orographic precipitation. In other areas where more synoptic climate patterns dominate precipitation, this approach may not be valid. In the current version of RHESSys, an input map of precipitation lapse rates is used. This map of precipitation fields can be determined using available models such as PRISM (Daly et al., 1994) or Daymet (Thornten et al., 1997). Daily rain duration is used in the calculation of evaporative fluxes. If this information is not available as input, rain duration is assumed to be the full day on days with precipitation.

Saturation vapor pressure is estimated from air temperature (Jones, 1992) as:

$$E_{sat} = 613.75 * \exp\frac{(17.502 * T_{avg})}{(240.97 + T_{avg})} \quad [4]$$

Patch Algorithms

Vertical soil moisture processes are modeled at the patch layer, which consists of both an unsaturated and saturated soil moisture zone as well as a surface detention storage or snowpack.

Daily saturation deficit (s) is modeled as:

$$\Delta s = -q_{drain} + q_{cap} + T_{sat} \qquad [5]$$

And daily storage in the unsaturated zone (Θ) is modeled as:

$$\Delta\Theta_{unsat} = -q_{drain} + q_{cap} - T_{unsat} \qquad [6]$$

where q_{drain} and q_{cap} are drainage from the unsaturated zone and capillary rise, respectively. T_{sat} and T_{unsat} are transpiration from the saturated and unsaturated zone, respectively.

Any rainfall on patch areas whose soil moisture is in excess of capacity produces return flow. Infiltration is modeled using a Phillip's equation (Phillip, 1957). Infiltration excess must also satisfy a surface detention storage before any return flow is produced.

RHESSys maintains both a depth to saturation given in meters (z) and a saturation deficit (s) given in meters of water. Conversion from saturation deficit to depth to the water table must take into account varying porosity with depth. Porosity is assumed to vary exponentially with depth as:

$$\phi(z) = \phi_0 * \exp^{(-\frac{z}{p})} \text{ for } (z >= 0); \qquad \phi(z) = 1 \text{ for } (z < 0) \qquad [7]$$

where ϕ is porosity, z is depth, ϕ_0 is porosity at the surface and p is the porosity decay rate. The user, however, may specify a constant porosity .

Drainage from the unsaturated zone to the saturated zone is limited by the field capacity of the unsaturated zone and by a vertical hydraulic conductivity in the unsaturated zone.

$$q_{drain} = \min\left\{K_{unsat}(z_s), q_{potential\_drainage}\right\} \quad [8]$$

$$q_{potential\_drainage} = \Theta_{unsat} - \Theta_{fc} \quad [9]$$

where $\Theta_{fc.}$ is soil moisture storage at field capacity, K_{sat} and K_{unsat} are saturated and unsaturated hydraulic conductivity, respectively.

Unsaturated hydraulic conductivity K_{unsat} is derived from a user selected soil moisture characteristic curve. Currently implemented curves include:

a) Clapp and Hornberger (1978):

$$K(s) = K_{sat} * S^{(2b+3)} \quad [10]$$

where S is relative soil moisture storage computed as (Θ_{unsat}/s) and s is the saturation deficit and b is a pore size index, described by Clapp and Hornberger (1978).

Or b) vanGenuchten and Nielsen (1985):

$$K(s) = K_{sat} S^{0.5}[1-(1-S^{\frac{1}{c}})^{c}]^2 \quad [11]$$

where c is a soil parameter.

Saturated hydraulic conductivity, $K_{sat.}$ is assumed to be the saturated hydraulic conductivity at the water table depth computed from:

$$K_{sat} = K_{sat_0} * \exp^{(\frac{-z_s}{m_z})} \quad [12]$$

where K_{sat0} is saturated hydraulic conductivity at the surface and m is the associated decay rate with depth. z_s is depth to saturation.

Unsaturated zone soil moisture at field capacity, $\Theta_{fc.}$ is determined by numerically integrating relative soil moisture storage at field capacity for depth z, $S_{fc}(z)$, * porosity over the depth to saturation. Porosity is assumed to vary with depth as noted above. Step size in numerical integration is currently set at 0.01 meters.

$$\Theta_{fc} = \sum_{z=z_s}^{z=0} \phi(z) * S_{fc}(z) * \Delta z \quad [13]$$

where Δz is step size.

Soil moisture characteristics curves ,Ψ-S, are derived from either Clapp and Hornberger (1978) or van Genuchten and Nielsen (1985) parameters. For relative soil moisture at field capacity for depth z, $S_{fc}(z)$, is estimated by assuming that Ψ=z and using moisture characteristic curves.

a) Clapp and Hornberger (1978)

$$S_{fc}(z) = \left(\frac{\Psi_{ae}}{(z_s - z)} \right)^b \quad [14]$$

Or b) for van Genuchten and Nielsen (1985)

$$S_{fc}(z) = \left(1 - \left(\frac{(z_s - z)}{\Psi_{ae}} \right)^c \right)^{-b} \quad [15]$$

where b is pore size index and c is a soil parameter and Ψ_{ae} is soil air entry pressure.

If porosity does not vary with depth, unsaturated zone soil moisture at field capacity can be computed analytically as:

$$\Theta_{fc} = \frac{1}{(1-b)} * \phi_0 * \Psi_{ae}{}^b * z_s{}^{(1-b)} \quad [16]$$

Leaf-Water Potential and Potential Exfiltration

Transpiration is computed from a Penman-Monteith equation, described in the discussion of canopy processes below. Feedback from soil-moisture to transpiration process occurs through the predawn leaf-water-potential ($LWP_{predawn}$) modification of canopy conductance. Leaf water potential is assumed to be a function of soil moisture tension, Ψ, and is computed using either

a) Clapp and Hornberger (1978):

$$LWP_{predawn} = \min (LWP_{min\_spring}, -0.01 * \Psi_{ae} (S^{-b})) \quad [17]$$

where LWP_{min_spring} is the minimum leaf water potential, and S is current relative soil moisture content computed as (Θ_{unsat}/s)

or b) Van Genuchten relationships:

$$LWP_{predawn} = \min (LWP_{min\_spring}, -0.01 * \Psi_{ae} (S^{\frac{1}{(1-1/b)}} - 1)^{\frac{1}{b}}) \quad [18]$$

Stomata are considered completely closed at a maximum leaf water potential, LWPsc, , which is a stratum default.

For bare soil evaporation, or transpiration from a canopy stratum with zero rooting depth and zero height (i.e. certain moss canopy types), feedback from soil moisture is set by a potential exfiltration rate. Potential exfiltration is computed from a modification of Eagleson (1978) by Wigmosta et al. (1994):

$$q_{pot\_exfil} = \left(S^{\frac{1}{2b}} + 2 \right) * \sqrt{\frac{8\phi_{avg} K_{sat} \Psi_{ae}}{3 * (1+3b)(1+4b)}} \quad [19]$$

where porosity (φ_{avg}) and saturated hydraulic conductivity (K_{sat}) are averaged over depth to saturation (z_s) using (7) and (12) respectively. S is relative soil moisture content computed as (Θ_{unsat}/s) with an added restriction on the maximum active soil depth over which the exfiltration process applies. Thus, if saturation deficit is greater than an active soil depth, specified as a patch parameter, then the relative soil moisture, S, is computed as ($\Theta_{unsat}/s_{active\_soil\_depth}$).

Capillary Rise

Potential capillary rise is computed based upon Gardiner's (1958) approximation to the Richard's equation.

$$q_{cap} = K_{sat}(z) * (1 + \frac{1.5}{(c-1)}) * (\frac{\Psi_{ae}}{(z_s - \Psi_{ae})})^c \quad [20]$$

where K_{sat} is calculated from (12). c = 2+3*b, where b is pore size index, z_s is depth to saturation. Capillary rise is limited to filling unsaturated zone to field capacity. To correct for sub-daily plant responses, 1/2 of the potential capillary rise is allocated to the unsaturated zone at the start of the day. The remaining potential is available later in the day to fill plant demands in the unsaturated zone (i.e. transpiration demands for plants with roots in the unsaturated zone).

Snowmelt

The snowmelt sub-model is a quasi energy budget approach. Melt from the snowpack is computed as the addition of three energy terms, radiation melt, $M_{rad.}$ temperature melt, M_T, and melt due to advected energy from precipitation, M_v. A snowpack energy deficit, Q_{snow}, is computed as an accumulative degree-day model.

$$Q_{snow} = \max((Q_{snow} + T_{air}), Q_{snow\max}) \quad [21]$$

Melt from temperature and advection occur only when the snowpack is ripe or the energy deficit is greater than zero. (Q_{snow} > = 0). Radiation melt, as sublimation, can occur when Q_{snow} is less than 0.

Melt due to radiation is computed as:

$$M_{rad} = \frac{(K_{direct} + K_{diffuse} + L)}{\lambda_f \rho_{water}} \quad [22]$$

where λ_f is the latent heat of fusion and ρ_{water} is the density of water, Kdirect and Kdiffuse are direct and diffuse shortwave radiation absorbed by the snowpack. L is longwave

radiation. λ_f is replaced by λ_s, latent heat of sublimation, when $Q_{snow} < 0$. Direct and diffuse shortwave radiation absorption by the snowpack (K_{direct} and $K_{diffuse}$) are computed based on a Beer's Law extinction . This approach is used to maintain consistency with radiation attenuation through vertical canopy layers.

$$K = (1-\alpha) * K_{down} * (1-\exp^{-k}) \quad [23]$$

where K is the absorbed radiation. Incoming direct and diffuse radiation, K_{down}, on the snowpack refer to radiative fluxes transmitted through any higher canopy layers as described in the discussion below on canopy stratum algorithms. The extinction coefficient, k, is input as a patch parameter. Setting k to an arbitrary large value will insure that all non-reflected radiation will be absorbed by the snowpack. Snowpack reflectance or albedo ,α, is estimated based upon a snowpack surface age following Laramie and Schaake (1972):

$$\alpha = 0.85 * 0.82^{Age_{snow}^{0.46}} \; if(Qsnow >= 0) \quad [24]$$

$$\alpha = 0.85 * 0.94^{Age_{snow}^{0.58}} \; if(Qsnow < 0) \quad [25]$$

where Age_{snow} is the number of days since last snowfall.

Long wave radiation into the snowpack is estimated from air temperature following Croley (1989).

$$L = 41.868 * (ess_{atm} * \sigma * (T_{air} + 273)^4 - 663) \quad [26] \quad \text{for } (T_{air} > 0 \text{ and } Q_{snow} > 0)$$

$$L = 41.868 * ((ess_{atm} - 1) * \sigma * (T_{air} + 273)^4) \quad [27] \quad \text{otherwise}$$

where σ is the Stefan-Boltzmann constant. Atmospheric emissivity, ess_{atm}, is adjusted for overstory canopy (Dingman, 1994) and cloud fraction (Croley, 1989). If cloud fraction data

is not available cloud fraction is assumed to be 1.0 for days with precipitation and 0.0 for dry days.

$$ess_{atm} = (1 - F) * (0.53 + 0.065 * \frac{e_a}{100}^{0.5}) * (1 + 4.0 * cf) + F \quad [28]$$

where F is the fractional canopy cover over the snowpack, e_a is atmospheric vapor pressure.

Temperature melt, M_T, estimates latent and sensible heat flux contributions to snowmelt using a temperature index. (Coughlan and Running, 1997) and adjusted for the effects of variation in wind speed due to forest cover over a snowpack (Dunne and Leopold, 1978).

$$M_T = MT_{coef} * T_{air} * (1 - 0.8 * F) \quad [29]$$

where MT_{coef} is the temperature melt coefficient, which is input as a patch default parameter.

Melt due to incoming precipitation, M_v, is calculated as:

$$M_v = \rho_{water} * T_{air} * precip * c_{water} \quad [30]$$

where precip is the precipitation falling on the snowpack, c_{water} and ρ_{water} are the heat capacity and density of water, respectively.

Hillslope Algorithms

Computation of soil moisture redistribution occurs at the hillslope level. Soil moisture redistribution includes calculation of saturation sub-surface throughflow and saturation or Hortonian overland flow. Two separate algorithms have been implemented: TOPMODEL, which is a quasi-distributed approach and a fully explicit spatial routing model, based on the DHSVM routing approach. The user selects which of the two approaches to use at run-time.

TOPMODEL

TOPMODEL (Beven and Kirkby, 1979) is a statistically based approach that redistributes water based on an index of hydrologic similarity. As a statistically based approach, TOPMODEL represents a simplified approach that has been applied and tested to numerous catchments as reviewed by Beven (1997). TOPMODEL relationships are based on the assumption that saturated hydraulic conductivity varies exponentially with depth; that water table gradients can be approximated by local topographic slope and that steady state flux is achieved within the modeling time step.

TOPMODEL distributes a mean soil moisture deficit (s) based on a local wetness index

$$w_i = \ln\{\frac{aT_e}{T_o \tan\beta}\} \quad [31]$$

where T_e and T_o are mean and local hillslope saturated transmissivity, respectively, tan β is the local slope and a is upslope contributing area.

Local saturation deficit, for each patch, is computed as:

$$s_i = \bar{s} + m_s\{\lambda - w_i\} \quad [32]$$

where λ is mean hillslope wetness index value, s is the mean hillslope saturation deficit and m_s is a decay rate of hydraulic conductivity with saturation deficit. Transmissivity is assumed to be

$$T = \int_{z_s}^{\infty} K_{sat0} e^{(-\frac{s}{m_s})} dz \quad [33]$$

where K_{sat0} is saturated hydraulic conductivity at surface and z_s is current saturation deficit.

Saturation overland flow (return flow) is produced for patches if ($s_i < 0$). Baseflow for the hillslope is calculated as:

$$q_{base} = \exp^{(-\lambda)} * \exp^{(-\bar{s}')} \quad [34]$$

where ś is the mean hillslope saturation deficit adjusted to include a portion of the capillary fringe as follows:

$$\bar{s}' = \sum_{\substack{a=all \\ patches}} s_a - 0.5 * (\Psi_{ae_a} * \phi_{0_a}) \quad [35]$$

where ϕ_0 is porosity at the surface, Ψ_{ae} is air entry pressure and s_a is saturation deficit for patch a.

Explicit Routing

As an alternative to the TOPMODEL approach, the explicit routing model, modified from DHSVM (Wigmosta *et al.*, 1994) is used. This method depends on assumptions similar to those used in TOPMODEL. The DHSVM routing approach also requires an imposed stream

network in addition to the definition of spatially explicit patches and their connectivity. Explicit routing is performed using a pseudo-hourly time step such that all vertical fluxes including rainfall infiltration are done at the beginning of the day and the routing algorithm is subsequently repeated for each of 24 hours.

The routing scheme assumes that saturated throughflow from patch a to patch b can be estimated as:

$$q(t)_{a,b} = \{ T(t)_{a,b} \tan\beta_{a,b} w_{a,b} \} \quad [36]$$

where w is flow width, tan β is local slope, and T is transmissivity as defined in (28).

For grids, flow widths are assumed to be 0.5 * grid size for cardinal directions and 0.354 * grid size for diagonal directions after Quinn *et al.* (1991). For irregular elements flow widths are summed along the shared boundary between patches a and b.

Following Wigmosta et al. (1994) , the DHSVM algorithms can be arranged as follows to facilitate implementation:

$$q_{a,b} = \frac{\gamma_{a,b}}{\Gamma_a} Q_{out_a} \quad [37] \qquad Q_{out_a} = h_a \Gamma_a \quad [38]$$

$$h_a = \exp(\frac{-s_a}{m_{s\,a}}) - \exp(\frac{-D_a}{m_{s\,a}}) \quad [39]$$

where D_a is water equivalent depth at the maximum soil depth for patch a and s_a is saturation deficit and

$$\gamma_{a,b} = \omega_{a,b} K_{sat\,a} m_{s\,a} \tan\beta_{a,b} \quad [40] \text{ and } \Gamma_a = \sum_{\substack{all \\ b}} \gamma_{ab} \quad [41]$$

Following the calculation of subsurface throughflow, any surface flow (i.e. saturation overland flow or Hortonian overland flow) produced by the patch is routed following the same patch connectivity. All surface flow produced by a patch is assumed to exit from the patch within a single time step. If the receiving patch is not saturated, surface flow is assumed to infiltrate and is added to unsaturated soil moisture storage (Θ_{unsat}). Note that the algorithm permits multiple flow paths. This is consistent with Quinn et al. (1991) who observe that multiple flow methods yield more realistic hillslope drainage patterns.

Patch flow gradient, Γ, and associated γ for each downslope neighbouring patch are automatically derived by using a preprocessing routing, CREATE_FLOWPATHS, which outputs these values to a, flow_table, which is then input into RHESSys. In creating the set of neighbors for each patch, CREATE_FLOWPATHS also checks for potential pits. Pits are patches or groups of patches that do not point to any downstream patch. In a single basin, pits should occur only for the outlet patch. The elimination of pits is a reasonable assumption in areas where flow is dominated by the topography of the modeled landscape. Many pits found in modeling drainage networks are the result of landscape representation, including DEM accuracy and resolution rather than actual flow characteristics. This is particularly true in flatter areas (O'Callaghan and Mark, 1984). In landscapes with large regions of relatively flat terrain where flow routing is more diffuse and significantly depends upon micro (or sub-scale) topography, the assumptions used in the DHSVM explicit routing model are no longer valid and explicit routing should not be applied.

In CREATE_FLOWPATHS, a pit is defined as all patches that point to the patch with no immediate downstream neighbor. CREATE_FLOWPATHS eliminates pits by recursively climbing from the pit to the minimum elevation upslope patch which points to a receiving patch lower than the bottom patch in the pit. In the current version of RHESSys, subsurface throughflow and saturation or Hortonian overland flow are all routed along the same drainage network. The current approach ignores the possibility of surface water accumulation in topographic hollows. RHESSys does allow detention storage to occur on individual patches. Some modification to both RHESSys and

CREATE_FLOWPATHS would be necessary, however, to incorporate hillslope level (multiple patch) surface storage.

Stream and Road Processing

Patches containing streams and road are require special processing when using the explicit routing routine. Calculation of the gradient associated with stream patches, as done by the CREATE_FLOWPATHS preprocessing routing offers 4 different options for the user:

- A constant value for all stream patches
- The local patch gradient
- A value taken from a random distribution
- The flowpath gradient upslope from the stream

This gradient is then used in (36) to determine flow from the stream containing patch.

Patches containing roads are processed as regular patches unless the road_flag has been activated. When the road flag is activated, subsurface throughflow from roads is partitioned into flow directed to the usual set of downslope patches and flow directed to an alternative patch as specified in the *flow table* , output from CREATE_FLOWPATHS, as shown in Figure A.1

Use of an alternative receiving patch allows flow intercepted by a road to be routed directly to a stream or to a particular downslope patch. Alternate patches are specified in CREATE_FLOWPATHS, prior to RHESSys execution. Setting the alternative patch to a stream patch for all roads can be used to illustrate the maximum increase in effective drainage density associated with the road network. This simulates the case where roads re-direct water directly to the stream either directly or through a system of gullies. Alternatively, CREATE_FLOWPATHS can route flow such that roads serve to concentrate flow in relatively wet or dry areas below the road. Wemple et al. (1996) discussed factors that influence road-stream connectivity through associated gully formation.

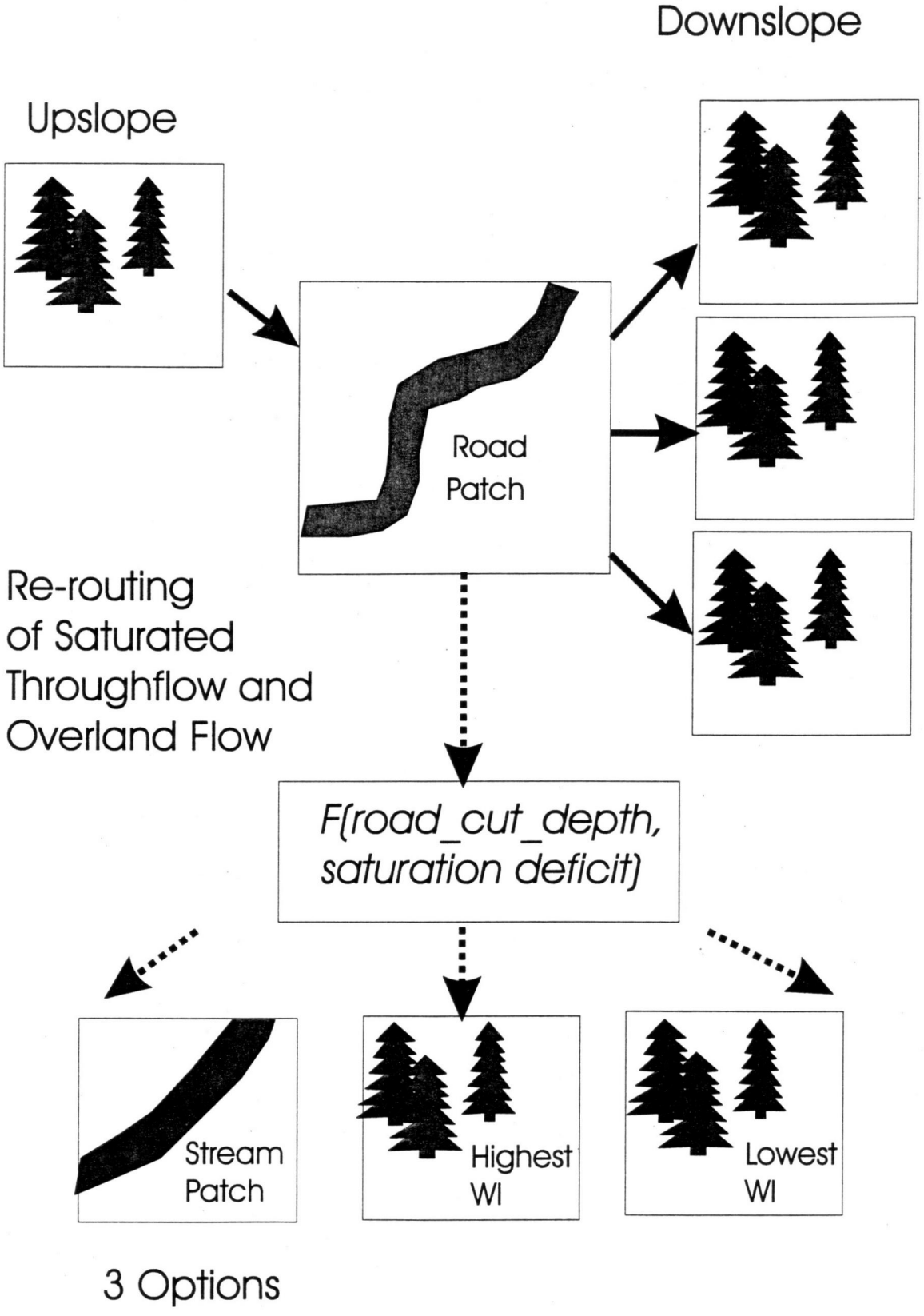

Figure A.1: Alternative routing for patches containing roads where patches containing roads route water to a stream patch, a relatively wet patch or a relatively dry patch.

The amount of saturated subsurface flow intercepted by the road is a function of the road cut depth and the current saturation deficit. If the road cut bank depth is less than depth to saturation, the road intercepts none of the saturated throughflow. If road cut depth is greater than depth to saturation, all subsurface throughflow produced above the road cut depth is routed to the alternate receiving patch such that:

$$q_{road} = \Gamma * \left[\exp^{(\frac{-s_{road\_cut}}{m_s})} - \exp^{(\frac{-D}{m_s})} \right] \quad [42]$$

and

$$q_{patches} = \Gamma * \left[\exp^{(\frac{-s}{m_s})} - \exp^{(\frac{-D}{m_s})} \right] - q_{road} \quad [43]$$

where q_{road} is flow routed to the alternate downslope patch and $q_{patches}$ is flow routed to the usual set of downslope patches. s_{road_cut} is the water equivalent depth of road cut, s is patch saturation deficit, m_s is decay of conductivity with saturation deficit; D is water equivalent depth at the maximum soil depth and * is defined as in (41). Further details on the processing associated with road networks can be found in Tague and Band (submitted c).

Canopy Strata Algorithms

Canopy strata are processes as a set of layers of different heights. All strata in a given layer (i.e. with equal height) share the same environment. Canopy layers at the same height must have a combined fractional coverage equal to 1. Layers are processes from highest to lowest so that fluxes such as radiation and rain throughfall can be attenuated by each successive canopy layer.

Most canopy processes are executed at the end of the daily time step, with the exception of the computation of leaf water potential, described above, and leaf on/off computations. Additional description and testing of many canopy processes are described in Fernandes (1999).

The current implementation maintains a maximum summer canopy leaf area index and plant area index throughout the simulation. Leaf drop in the fall and leaf out in the spring are modeled as a linear decay or expansion of this maximum leaf area. Year-days for the beginning of fall leaf drop and spring leaf out are specified as canopy defaults . The lengths of the decay and expansion periods are assumed to be equal and are also specified as defaults. Full leaf drop results in an LAI of 0.001 and a corresponding reduction of PAI such that:

$$\text{PAI (after leaf drop)} = \text{PAI}_{\text{max}} - \text{LAI}_{\text{max}} \qquad [44]$$

Radiation Interception

Canopy radiation absorption and reflection is modeled separately for diffuse and direct radiative fluxes and for PAR fluxes. Direct radiation absorption is a modification of Beer's Law with a correction for the effect of low sun angles in sparse canopies (Chen et al. 1997). The effect of a random distribution of leaves is assumed to be incorporated into the stratum extinction coefficient, k, which is a stratum parameter.

$$K_{direct} = (1 - \alpha_{direct}) * K_{down\,direct} * (1 - \exp^{(ext_{coef})}) \quad [45]$$

$$ext_{coef} = 1.1 * k * \frac{(1 - gap) * PAI_{proj}}{\cos(\Theta_{noon})} \quad [46]$$

where K_{direct} is direct radiation absorption for a particular stratum, K_{down} is the direct radiation at the top of the canopy layer, PAI_{proj} is projected plant area index, gap is the gap fraction. For sparse canopies, this value will be less than 1. k is the Beer's Law extinction coefficient, α_{direct} is direct radiation canopy reflectance (albedo), Θnoon is solar angle at noon.

If ext_{coef} is less than 0.3, i.e. a sparse canopy, a correction factor, c_{sparse} is applied such that:

$$K_{direct} = (1-\alpha_{direct}) * K_{down\,direct} * (1 - correction * \exp^{(ext_{coef})}) \quad [47]$$

$$correction = (1-\alpha_{background}) * \frac{(\Theta_{noon} - \frac{\Pi}{2}) * \sin(\Theta_{noon}) + \cos(\Theta_{noon})}{(\frac{\Pi}{2} - \Theta_{noon}) * (1 - \sin(\Theta_{noon}))} \quad [48]$$

where $\alpha_{background}$ is background canopy reflectance.

Diffuse radiation absorption is modeled based upon Norman(1981) such that

$$K_{diffuse} = (1-\alpha_{diffuse}) * K_{down} * (1 - \exp^{-((1-gap)*PAI)^{0.7}} + S) \quad [49]$$

where S is the back scattering component calculated as

$$S = 0.07 * \frac{K_{down\,direct}}{K_{down\,diffuse}} * (1.1 - 0.1 * (1-gap) * PAI) * \exp^{(-\cos(\Theta_{noon})} \quad [50]$$

Absorbed radiation for PAR fluxes are calculated using (36) and (38) above for direct and diffuse PAR respectively. Reflectance coefficients and direct radiation extinction coefficients are replaced by PAR specific coefficients included in the canopy default file.

Aerodynamic Conductance

Aerodynamic conductance is computed separately for overstory, understory and surface stratum following the model of Heddeland and Lettenmaier (1995). A patch level stability correction is included based upon Oke (1987). Understory and surface aerodynamic resistance assume a logarithmic windspeed decay profile to the top of the canopy and an exponential decay profile within the canopy.

Stratum Canopy Conductance

Stratum canopy conductance is computed separately for vascular and non-vascular water flux from the stratum . For non-vascular strata, stratum conductance represents the inverse of the additional resistance to surface vapor flux beyond aerodynamic conductance provided by that layer. Vascular stratum conductance represents the inverse of additional resistance provided by stomata control. Vascular stratum conductance is based upon the Jarvis multiplicative model of stratum conductance (Jarvis, 1976) where the maximum (plant specific) conductance is scaled by the environmental factors as follows:

$$gs = f(APAR) * f(CO2) * f(LWP) * f(T_{avg}) * f(T_{\min}) * f(vpd) * gs_{\max} * LAI * f_{stm} \quad [51]$$

where APAR is absorbed PAR. gs is stratum conductance. gs_{max} is maximum stomata conductance and f_{stm} is stomatal fraction. Both are input as stratum parameters. Stratum conductance, gs, is also limited by a default cuticular conductance (scaled by LAI) for that stratum. Different environmental scaling factors can be readily substituted. All multipliers range from 0 to 1. In the current implementation, environmental scaling factors for the Jarvis model are taken from Running and Coughlan (1988).

Non-vascular stratum conductance or surface conductance (gsurf) computations apply particularly for surface covers such as mosses and are used in the calculation of bare soil evaporation. In this case, surface conductance (g_{surf}) is calculated using an empirical relationship with soil moisture storage described by Kelliher et al. (1986) based on sandy loam soils. This may not be valid for other soil types. Further details of this approach can be found in Fernandes et al. (submitted) and Williams and Flanagan (1997). Note also that surface conductance here refers to patch surface conductance rather than stratum surface conductance, as defined above, since it reflects sub-surface soil characteristics. In calculating soil surface conductance, soil moisture dynamics are restricted to the active soil layer, defined in the patch default file. (i.e. Similar to the exfiltration calculation in (16), soil moisture content, S, is calculated as ($\Theta_{unsat}/s_{active\_soil\_depth}$) if saturation deficit (s_z) is greater than active soil depth and (Θ_{unsat}/s_z) for saturation deficit less than active soil depth).

Interception

Snow and rain interception are limited both by a static snow/rain water holding capacity of the canopy cover and by the snow or rainfall rate such that

$$\Delta\Theta_{int} = \min\{ pcp*(1\text{-}gap), PAI*\Theta_{cap} - \Theta_{int}) \quad [52]$$

where Θ_{int} is interception storage, pcp is incoming precipitation (rain or snow), PAI is plant area index, Θ_{cap} is specific storage capacity (i.e. per lai). Specific storage capacity is given for both rain and snow in the canopy default file.

Sublimation of snow storage is a function of available radiation at that canopy layer:

$$Q_{sublimation} = \min\{\frac{(K_{direct} + K_{diffuse})}{(latent\_heat)} * \rho_{snow}, \Theta_{int}\} \quad [53]$$

K_{direct} and $K_{diffuse}$ are direct and diffuse radiation available at that canopy layer, ρ_{snow} is the density of snow. Note in the current implementation this value is a constant and the effect of variation in snow density is ignored. For Tair < 0, latent heat is latent heat of fusion + latent heat of vaporization. For Tair > 0, latent heat is latent heat of fusion and $Q_{sublimation}$ refers to melting of intercepted snow.

Evaporation

Potential evaporation of rain stored on the canopy is computed using a Penman Monteith equation

$$E_{pot} = \frac{s(T)(R_{net}) + \rho * cp * vpd * g_a}{s(T) + \gamma * (1 + \frac{g_a}{g_{surf}})} \quad [54]$$

where s(T) is slope of saturation vapor pressure curve, computed as a function of air temperature (T). γ is the psychrometric constant calculated as a function of air pressure and temperature. Vpd is the vapor pressure deficit; g_a and g_{surf} are aerodynamic and surface conductance as described earlier. R_{net} is net radiation, with the addition of a heat flux term, computed as:

$$R_{net} = K_{direct} + K_{diffuse} + L + G_{surf} \quad [55]$$

where K_{direct} and $K_{diffuse}$ are absorbed radiation as calculated in (36) and (38). L is longwave radiation, which is estimated at the patch level using air temperature and standard emissivities for vegetation, soil and *snow.* Longwave radiation should be stratum specific and will be modified in the future RHESSys versions. Surface heat flux, G_{surf}, is computed for surface strata, such as moss, lichen or bare soil. Surface heat flux is a function of rain

interception storage and heat capacity limits specified as stratum parameters. Surface heat capacities for strata other than surface strata should be set to zero.

$$G_{surf} = (C_{\min} + (C_{\max} - C_{\min}) * \frac{\Theta_{\text{int}}}{\Theta_{cap}}) * \frac{(\Delta T_{soil})}{\Delta_z} \quad [56]$$

where C_{min} and C_{max} are minimum and maximum soil/stratum heat capacities; Δz is soil depth over which heat flux is computed. ΔT_{soil} is estimated from current soil temperature and night-time air temperature range, assuming an exponential decay of temperature with depth (Oke, 1987).

$$\Delta T_{soil} = \frac{(1 - \frac{T_{soil}}{T_{\min}})}{\log(\frac{T_{soil}}{T_{\min}})} * T_{\min} - \frac{(1 - \frac{T_{soil}}{T_{night\,\max}})}{\log(\frac{T_{soil}}{T_{night\,\max}})} * T_{night\,\max} \quad [57]$$

where T_{min} is minimum daily temperature, $T_{nightmax}$ is maximum night-time air temperature.

To address sub-daily variability in vapor pressure deficit, we compute a separate evaporation term using (41) for rainy and dry periods during the day, using appropriate vpd terms for each period. Unless rain duration data is available as input, however, rain duration is assumed to be entire day. Thus, potential evaporation of surface water storage is :

$$E_{pot} = E_{rain} * t_{rain} + E_{dry}(t_{day\_length} - t_{rain}) \quad [58]$$

where E_{rain} and E_{dry} are calculated from (41) where vpd is set to 0.0 for rainy periods; t_{rain} is rain duration, t_{day_length} is daylength.

Radiation used for evaporation or sublimation of interception storage is subtracted from radiation balance for the corresponding canopy layer.

Transpiration

For the purposes of the canopy process routines in RHESSys, transpiration refers to water vapor flux from water stored in the soil. This includes transpiration from vascular plants which access soil water through roots and water flux from strata such as a litter layer where water is drawn to the surface via capillary rise or soil evaporation.

For stratum with stomata fraction > 0 and height > 0, transpiration is computed using the Penman Monteith equation (41) by substituting surface conductance with canopy conductance (gs) as computed using (39). Transpiration for these stratum only occurs during non-rainy periods and once any water intercepted by the canopy has been evaporated. Partitioning of transpiration requirements into unsaturated and saturated zone soil moisture storage is determined based upon rooting depth i.e.

$$Tr_{sat} = Tr^*(1-z_s/z_{root}) \qquad [59]$$

$$Tr_{unsat} = Tr-Tr_{sat} \qquad [60]$$

where Tr is total transpiration, Tr_{sat} is transpiration from the saturated zone, Tr_{unsat} is transpiration from unsat zone, z_s and z_{root} are depth to saturation and rooting depth, respectively. If unsaturated zone storage is less than Tr_{unsat}, capillary rise can be used to meet the demand. Any unmet demand after capillary rise has been exhausted is subtracted from final unsaturated zone transpiration (Tr_{unsat}) flux. Note that extraction of transpiration from soil moisture storage occurs at the patch level.

For surface stratum (i.e. height = 0) that have a non-zero rooting depth i.e. mosses with roots, transpiration is assumed to be the minimum of capillary rise and potential evaporation as calculated in (41).

For surface stratum with no roots, i.e. bare soil or litter layers, transpiration is essentially soil evaporation. For these stratum, transpiration is limited by radiation remaining after evaporation of any intercepted surface water as calculated in (41). Soil evaporation is also limited by potential exfiltration, as calculated at the patch level using (16). Thus transpiration for surface stratum with no roots is the minimum of potential exfiltration and potential soil evaporation.

Potential soil evaporation is calculated for both rainy and dry periods following the methodology described above for computing potential evaporation of intercepted water. In this case, surface conductance (g_{surf}) as discussed above is used.

Respiration and Photosynthesis

Canopy maintenance respiration and photosynthesis routines are taken directly from BIOME_BGC model (Peter Thornten's version). Maintenance respiration is computed separately for leaf, sapwood, fine and coarse root components and summed to give a total daily respiration value following Ryan et al. (1991). Photosynthesis is computed using the Farquhar model (Farquhar et al., 1982). Further details of the carbon budget are not included here since carbon fluxes are not specifically discussed in this document. Further information about carbon cycling will be discussed in documentation associated with the next version of RHESSys, which will include carbon, nitrogen cycling and dynamic allocation to vegetation.

References

Beven, K.J. 1997. TOPMODEL: A Critique, *Hydrol. Proc.*, **11**, 1069-1085.

Beven, K and Kirkby, M. 1979. "A physically-based variable contributing area model of basin hydrology, *Hydrologic Science Bulletin*, **24**, 43-69

Bristow, K.L. and Campbell, G.S. 1984. On the relationship between incoming solar radiation and daily maximum and minimum temperature, *Agric. For. Meteorol.* **31**:159-166.

Chen, J.M., Rich, P., M., Gower, S.T., Norman, J.M., Plummer, S. 1997. Leaf area index of boreal forests: Theory, techniques, and measurements, *J of Geophysical Res.*, **102**, 29,429-29,444.

Clapp,R., Hornberger,G. 1978. 'Empirical equations for some soil hydraulic properties', *Wat. Resour. Res*, **14**, 601-604.

Coughlan, J.C. and Running, S.W. 1997. 'Regional ecosystem simulation: A general model for simulating snow accumulation and melt in mountainous terrain', *Landscape Ecology* **12**, 119-136.

Croley, T.E., II, 1989. 'Verifiable evaporation modeling on the Laurentian Great Lakes', *Wat. Res. Research*, **25**,781-792.

Daly, C., Neilson, R.P., Phillips, D.L. 1994. A statistical-topographic model for mapping climatological precipitation over mountainous terrain, *Journal of Applied Meteorology*, **33**:2, 140-157.

Dingman, S.L. 1994. *Physical Hydrology*, Prentice Hall, New Jersy.

Dunne, T., Leopold, L.B. 1979. *Water in Environmental Planning*, Freeman and Co..

Eagleson, P.S. 1978.Climate, Soil and Vegetation 3. A simplified model of soil moisture movement in the liquid phase, *Wat.Res.Reseach*, **14**:5.

Farquhar, G.D. and vonCaemmerer, S. 1982. Modeling photosynthetic response to environmental conditions in *Encyclopedia of Plant Physiology, New Series, Vol 12B, Physiological Plant Ecology II*, eds. O.L. Lange, P.S. Nobel, C.B.Osmond and H..Ziegler, Springer-Verlag, Berlin, 549-587.

Fernandes, R., Tague, C., and Band, L. (submitted) "A spatially distributed model of overstory and moss water budgets in boreal conifer stands", *J of Geophysical* .

Fernandes, R. 1999. Scale Influences of Surface Parameterization on Modelled Boreal Carbon and Water Budgets, Phd. Dissertation, University of Toronto.

Francini, M., Wendling, J., Obled, Ch., and Todini, E. 1996. Some note about the TOPMODEL sensitivity to basin topography, *J. of Hydrol.*, 1975, 293-338.

Gardiner, W.R. 1958. Some steady-state solutions of the unsaturated moisture flow equation with application to evaporation from a water table, *Soil Sci.* **85**:4, 228-232.

Garnier, B.J. and Ohmura, A. 1968. A method of calculating the direct shortwave radiation income of slopes. *J of Appl. Meteorol.* 7:5, 796-800.

Heddeland, I. and Lettenmaier, D 1995. Hydrological modeling of boreal forest ecosystems, *Water Resource Series #14*, Dept of Civil Engineering, U of Washington, p38.

Kelliher, F.M., Black, T.A. and Price, D.T. 1986. Estimating the effects of understory removal from a douglas fir forest using a two-layer canopy evapotranspiration model, *Wat. Resour. Res.* **22**:13, 1891-1899.

Kirkby, M. 1997. TOPMODEL:a personal view, *Hydrol. Proc.*, 11:9, 1087-1099.

Jarvis, P.G. 1976. The interpretations of the variations in leaf water potential and stomatal conductance found in canopies in the field. *Philosophical Transactions Series B*, 273, 593-610.

Jones, H.G. 1992., *Plants and microclimate*, Cambridge University Press.

Linacre, E. 1992. *Climate data and resources : a reference and guide*, Routledge Press.

Luce, C.H., and Cundy, T.W. 1994. Parameter identification for a runoff model for forest roads, *Water. Res. Research*, **4**:1057-1069.

Norman, J.M., 1981. *Simulation of microclimates, in Biometeorology in integrated pest management*. Eds J.L. Hatfield and I.J.Thomson, pp65-99, Academic Press, New York.

O'Callaghan, J., Mark, D. 1984. 'The extraction of drainage networks form digital elevation data', *Computer Vision Graphics and Image Processing*, **23**, 323-344.

Oke. T., 1987, *Boundary Layer Climates*, 2nd ed., University Press, Cambridge, 435pp.

Phillip. J.R. 1957, The theory of infiltration: 4. Sorptivity and algebraic infiltration equation, *Soil Science*, **84**:257-264.

Quinn, P., Beven, K., Chevallier, P., and Planchon, O. 1991. 'The prediction of hillslope flow paths for distributed hydrological modeling using digital terrain models', *Hydrol. Proc.*, **5**, 59-79.

Running, S., Coughlan, J. 1988. A general model of forest ecosystem processes for regional applications: Hydrologic balance, canopy gas exchange and primary production processes, *Ecological Modeling*, **42**, 125-154.

Running, S., Nemani, R., Hungerfored, R. 1987.Extrapolation of synoptic meteorological data in mountainous terrain and its use for simulating forest evapotranspiration and photosynthesis, *Can.J.For.Res*, **17**;472-483.

Ryan, M. 1991. Effects of climate change on plant respiration, *Ecol. Appl.*, **1**:2, 157-167.

Tague, C. L., Fernandes, R. and Band, L.E., 1998. RHESSys 4.6: User Manual.

Tague, C. L. and Band, L.E., (submitted a). Evaluating Explicit and Implicit Routing for Catchment Scale Models of Forest Hydrology, *Journal of Hydrology*.

Tague, C. L. and Band, L.E. (submitted b). Modeling seasonal hydrologic response: Sensitivity to landscape representation and stream channel parameterization, *Hydrological Processes.*

Tague, C. L. and Band, L.E. (to be submitted c). Assessing the impact of road construction on seasonal hydrologic response using a spatially distributed hydro-ecological model, *Earth Surface Processes and Landforms*.

Thornten, P.E., Running, S.W. and White, M.A., 1997. Generating surfaces of daily meteorological variables over large regions of complex terrain. *Journal of Hydrology*, 190:214-251.

VanGenuchten, M.T. and Nielsen, D.R., 1985. On describing and predicting the hydraulic properties of unsaturated soils, *Annal Geophys*., 3: 615-628.

Wemple, B.C., Jones, J.A., Grant, G.E. 1996. Channel network extension by logging roads in two basins, Western Cascades, Oregon, *Wat. Resour. Bull.*, **32**:6, 1195-1207.

Wigmosta, M., Vail, L., Lettenmaier, D. 1994. 'Distributed hydrology-vegetation model for complex terrain', *Wat. Resour. Res*, **30:6**, 1665-1679.

Williams, T.G. and Flanagan, L.B. 1997. 'Effect of changes in water content on photosynthesis, transpiration and discrimination against $^{13}C0_2$ and $C^{18}O^{16}O$ in *Pleurozium* and *Sphagnum*, *Oecologica*, **108**:34-46.

Zheng, D., Hunt, E.R, Running, S.W. 1993 A daily soil temperature model based on air temperature and precipitation for continental applications, *Clim Res.* ***2***, 183-191.